

Jordan Journal of Mechanical and Industrial Engineering (JJMIE)

JJMIE is a high-quality scientific journal devoted to fields of Mechanical and Industrial Engineering. It is published by Hashemite University in cooperation with the Jordanian Scientific Research and Innovation Support Fund, Ministry of Higher Education and Scientific Research.

EDITORIAL BOARD

Editor-in-Chief

Prof. Moh'd Sami Ashhab

Assistant Editors

Dr. Ahmad AlMigdady

Dr. Mohannad Jreissat

Editorial Board

Prof. Tariq A. ALAzab

Al Balqa Applied University

Prof. Jamal Jaber

Al- Balqa Applied University

Prof. Mohamad Al-Widyan

Jordan University of Science and Technology

Prof. Mohammed Taiseer Hayajneh

Jordan University of Science and Technology

Prof. Mohammad Al-Tahat

The University of Jordan

Dr. Ali M. Jawarneh

The Hashemite University

THE INTERNATIONAL ADVISORY BOARD

Abu-Qudais, Mohammad

Jordan University of Science & Technology, Jordan

Tzou, Gow-Yi

Yung-Ta Institute of Technology and Commerce, Taiwan

Abu-Mulaweh, Hosni

Purdue University at Fort Wayne, USA

Jubran, Bassam

Ryerson University, Canada

Afaneh Abdul-Hafiz

Robert Bosch Corporation, USA

Kakac, Sadik

University of Miami, USA

Afonso, Maria Dina

Institute Superior Tecnico, Portugal

Khalil, Essam-Eddin

Cairo University, Egypt

Badiru, Adedji B.

The University of Tennessee, USA

Mutoh, Yoshiharu

Nagaoka University of Technology, Japan

Bejan, Adrian

Duke University, USA

Pant, Durbin

Iowa State University, USA

Chalhoub, Nabil G.

Wayne State University, USA

Riffat, Saffa

The University of Nottingham, U. K

Cho, Kyu-Kab

Pusan National University, South Korea

Saghir, Ziad

Ryerson University, Canada

Dincer, Ibrahim

University of Ontario Institute of Technology,
Canada

Sarkar, MD. Abdur Rashid

Bangladesh University of Engineering &
Technology, Bangladesh

Douglas, Roy

Queen's University, U. K

Siginer, Dennis

Wichita State University, USA

El Bassam, Nasir

International Research Center for Renewable
Energy, Germany

Sopian, Kamaruzzaman

University Kebangsaan Malaysia, Malaysia

Haik, Yousef

United Arab Emirates University, UAE

EDITORIAL BOARD SUPPORT TEAM

Language Editor

Dr. Baker M. Bani-khair

Publishing Layout

Eng. Ali Abu Salimeh

SUBMISSION ADDRESS:

Prof. Moh'd Sami Ashhab, Editor-in-Chief
Jordan Journal of Mechanical & Industrial Engineering,
Hashemite University,
PO Box 330127, Zarqa, 13133 , Jordan
E-mail: jjmie@hu.edu.jo



Hashemite Kingdom of Jordan



Hashemite University

Jordan Journal of
Mechanical and Industrial Engineering

JJMIE

An International Peer-Reviewed Scientific Journal
Financed by Scientific Research Support Fund

<http://jjmie.hu.edu.jo/>

ISSN 1995-6665

Jordan Journal of Mechanical and Industrial Engineering (JJMIE)

JJMIE is a high-quality scientific journal devoted to fields of Mechanical and Industrial Engineering. It is published by Hashemite University in cooperation with the Jordanian Scientific Research and Innovation Support Fund, Ministry of Higher Education and Scientific Research.

Introduction: The Editorial Board is very committed to build the Journal as one of the leading international journals in mechanical and industrial engineering sciences in the next few years. With the support of the Ministry of Higher Education and Scientific Research and Jordanian Universities, it is expected that a heavy resource to be channeled into the Journal to establish its international reputation. The Journal's reputation will be enhanced from arrangements with several organizers of international conferences in publishing selected best papers of the conference proceedings.

Aims and Scope: *Jordan Journal of Mechanical and Industrial Engineering* (JJMIE) is a refereed international journal to be of interest and use to all those concerned with research in various fields of, or closely related to, mechanical and industrial engineering disciplines. *Jordan Journal of Mechanical and Industrial Engineering* aims to provide a highly readable and valuable addition to the literature which will serve as an indispensable reference tool for years to come. The coverage of the journal includes all new theoretical and experimental findings in the fields of mechanical and industrial engineering or any closely related fields (Materials, Manufacturing, Management, Design, Thermal, Fluid, Energy, Control, Mechatronics, and Biomedical). The journal also encourages the submission of critical review articles covering advances in recent research of such fields as well as technical notes.

Guide for Authors

Manuscript Submission:

High-quality submissions to this new journal are welcome now and manuscripts may be either submitted online or email.

Online: For online and email submission upload one copy of the full paper including graphics and all figures at the online, submission site, accessed via <http://jjmie.hu.edu.jo>. The manuscript must be written in MS Word Format. All correspondence including notification of the Editor's decision and requests for revision, takes place by e-mail and via the Author's homepage, removing the need for a hard-copy paper trail

Submission address and contact :

Prof. Moh'd Sami Ashhab

Editor-in-Chief

Jordan Journal of Mechanical & Industrial

Engineering, Hashemite University

PO Box 330127, Zarqa, 13115, Jordan

E-mail: jjmie@hu.edu.jo

Types of contributions: Original research papers and Technical reports

Corresponding author: Clearly indicate who is responsible for correspondence at all stages of refereeing and publication, including post-publication. Ensure that telephone and fax numbers (with country and area code) are provided in addition to the e-mail address and the complete postal address. Full postal addresses must be given for all co-authors.

Original material: Submission of an article implies that the work described has not been published previously (except in the form of itstan abstract or as part of a published lecture or academic thesis), that it is not under consideration for publication elsewhere, the publication is approved by all authors and that, if accepted, it will not be published elsewhere in the same form, in English or in any other language, without the written consent of the Publisher. Authors found to be deliberately contravening the submission guidelines on originality and exclusivity shall not be considered for future publication in this journal.

Withdrawing: If the author chooses to withdraw his article after it has been assessed, he shall reimburse JJMIE with the cost of reviewing the paper.

Manuscript Preparation:

General: Editors reserve the right to adjust style to certain standards of uniformity. Original manuscripts are discarded after publication unless the Publisher is asked to return original material after use. Please use MS Word for the text of your manuscript

Structure: Follow this order when typing manuscripts: Title, Authors, Authors title, Affiliations, Abstract, Keywords, Introduction, Main text, Conclusions, Acknowledgements, Appendix, References, Figure Captions, Figures and then Tables. Please supply figures imported into the text AND also separately as original graphics files. Collate acknowledgements in a separate section at the end of the article and do not include them on the title page, as a footnote to the title or otherwise.

Text Layout: Use 1.5 line spacing and wide (3 cm) margins. Ensure that each new paragraph is clearly indicated. Present tables and figure legends on separate pages at the end of the manuscript. If possible, consult a recent issue of the journal to become familiar with layout and conventions. All footnotes (except for table and corresponding author footnotes) should be identified with superscript Arabic numbers. To conserve space, authors are requested to mark the less important parts of the paper (such as records of experimental results) for printing in smaller type. For long papers (more than 4000 words) sections which could be deleted without destroying either the sense or the continuity of the paper should be indicated as a guide for the editor. Nomenclature should conform to that most frequently used in the scientific field concerned. Number all pages consecutively; use 12 or 10 pt font size and standard fonts.

Corresponding author: Clearly indicate who is responsible for correspondence at all stages of refereeing and publication, including post-publication. The corresponding author should be identified with an asterisk and footnote. Ensure that telephone and fax numbers (with country and area code) are provided in addition to the e-mail address and the complete postal address. Full postal addresses must be given for all co-authors. Please consult a recent journal paper for style if possible.

Abstract: A self-contained abstract outlining in a single paragraph the aims, scope and conclusions of the paper must be supplied.

Keywords: Immediately after the abstract, provide a maximum of six keywords (avoid, for example, 'and', 'of'). Be sparing with abbreviations: only abbreviations firmly established in the field may be eligible.

Symbols: All Greek letters and unusual symbols should be identified by name in the margin, the first time they are used.

Units: Follow internationally accepted rules and conventions: use the international system of units (SI). If other quantities are mentioned, give their equivalent quantities in SI

Maths: Number consecutively any equations that have to be displayed separately from the text (if referred to explicitly in the text).

References: All publications cited in the text should be presented in a list of references following the text of the manuscript.

Text: Indicate references by number(s) in square brackets in line with the text. The actual authors can be referred to, but the reference number(s) must always be given.

List: Number the references (numbers in square brackets) in the list in the order in which they appear in the text.

Examples:

Reference to a journal publication:

[1] M.S. Mohsen, B.A. Akash, "Evaluation of domestic solar water heating system in Jordan using analytic hierarchy process". Energy Conversion & Management, Vol. 38 (1997) No. 9, 1815-1822.

Reference to a book:

[2] Strunk Jr W, White EB. The elements of style. 3rd ed. New York: Macmillan; 1979.

Reference to a conference proceeding:

[3] B. Akash, S. Odeh, S. Nijmeh, "Modeling of solar-assisted double-tube evaporator heat pump system under local climate conditions". 5th Jordanian International Mechanical Engineering Conference, Amman, Jordan, 2004.

Reference to a chapter in an edited book:

[4] Mettam GR, Adams LB. How to prepare an electronic version of your article. In: Jones BS, Smith RZ, editors. Introduction to the electronic age, New York: E-Publishing Inc; 1999, p. 281-304

Free Online Color : If, together with your accepted article, you submit usable color and black/white figures then the journal will ensure that these figures will appear in color on the journal website electronic version.

Tables: Tables should be numbered consecutively and given suitable captions and each table should begin on a new page. No vertical rules should be used. Tables should not unnecessarily duplicate results presented elsewhere in the manuscript (for example, in graphs). Footnotes to tables should be typed below the table and should be referred to by superscript lowercase letters.

Notification: Authors will be notified of the acceptance of their paper by the editor. The Publisher will also send a notification of receipt of the paper in production.

Copyright: All authors must sign the Transfer of Copyright agreement before the article can be published. This transfer agreement enables Jordan Journal of Mechanical and Industrial Engineering to protect the copyrighted material for the authors, but does not relinquish the authors' proprietary rights. The copyright transfer covers the exclusive rights to reproduce and distribute the article, including reprints, photographic reproductions, microfilm or any other reproductions of similar nature and translations.

Proof Reading: One set of page proofs in MS Word format will be sent by e-mail to the corresponding author, to be checked for typesetting/editing. The corrections should be returned within **48 hours**. No changes in, or additions to, the accepted (and subsequently edited) manuscript will be allowed at this stage. Proofreading is solely the author's responsibility. Any queries should be answered in full. Please correct factual errors only, or errors introduced by typesetting. Please note that once your paper has been proofed we publish the identical paper online as in print.

Author Benefits:

No page charges: Publication in this journal is free of charge.

Free offprints: One journal issues of which the article appears will be supplied free of charge to the corresponding author and additional offprint for each co-author. Corresponding authors will be given the choice to buy extra offprints before printing of the article.

PAGES	PAPERS
69 - 74	A New Analytical Approach for Crack Modeling in Spur Gears <i>Ehsan Rezaei, Mehrdad Poursina, Mohsen Rezaei, Alireza Ariaei</i>
75 - 82	Estimation of Fuel Consumption in a Hypothesized Spoke-hub Airline Networks for the Transportation of Passengers <i>Mohammad D. AL-Tahat, Dr. Mohammad Al Janaideh, Yousef Al-Abdallat, Mowafaq E. Jabri</i>
83– 89	Prediction Performance of End-Milling Process by Gene Expression Programming <i>Mohammed T. Hayajneh, Majid Abdellahia</i>
91– 103	Ergonomic Computer Workstation Design for University Teachers in Bangladesh <i>Md. Golam Kibria, Md. Rafiqzaman</i>
105– 115	Production and Distribution Decisions for a Multi-product System with Component Commonality, Postponement Strategy and Quality Assurance Using a Two-machine Scheme <i>Singa Wang Chiu , Jyun-Sian Kuo , Yuan-Shyi Peter Chiu , Huei-Hsin Chang</i>
117– 124	Optimal Off-Grid Hybrid Renewable Energy System for Residential Applications Using Particle Swarm Optimization <i>Osama Abuzeid , Amjad Daoud, Mahmoud Barghash</i>
125– 130	Using Renewable Energy Criteria for Construction Method Selection in Syrian Buildings <i>Bassam Hassan , Madonna Beshara</i>
131– 140	Impact of Decentralized PV Systems Installation on Transmission Lines During Peak Load Situations – Case Study Amman, Jordan <i>Daniel Christ, Martin Kaltschmitt</i>

A New Analytical Approach for Crack Modeling in Spur Gears

Ehsan Rezaei, Mehrdad Poursina^{*}, Mohsen Rezaei, Alireza Ariaei

Department of Mechanical Engineering, Faculty of Engineering, University of Isfahan, Isfahan, 81744-73441, Iran

Received 10 April, 2019

Abstract

Spur gear systems are widely used in power transmission systems in the industry. One of the common defects of the gears is tooth crack. Tooth crack increases the vibration and also generates noise. Previous studies have shown that tooth stiffness will decrease due to any crack and it is important to estimate the magnitude of reduction of tooth stiffness. This research suggests a new analytical approach for crack modeling and determining the reduction of time-varying gear mesh stiffness by Elastic Spring Method (ESM). Based on this approach, two or more cracks can be considered in one tooth. However, previous studies have primarily concentrated on one crack. In addition, it should be noted that each crack is replaced by one linear and one torsional spring in the present study. The results that were obtained from this method are validated through a comparison with Limit Line Method (LLM) and Finite Element Method (FEM).

© 2019 Jordan Journal of Mechanical and Industrial Engineering. All rights reserved

Keywords: Spur Gear - Tooth Crack – Mesh Stiffness –Analytical Approach- Finite Element Method;

1. Introduction

Like other components in the industry, gears which are made of teeth are subject to certain damages. Tooth crack is an unwanted phenomenon, and can cause serious and costly damages. Time-varying mesh stiffness is the main reason of vibration in gears [1]. There exist some studies on assessing mesh stiffness. The FEM [2, 3] and Analytical Method (AM) have been and are being applied for computing mesh stiffness. Wang and Howard [4] applied FEM to compute the torsional stiffness of a spur gear pair. Weber [5] and Cornell [6] applied AM to calculate the gear mesh stiffness, while Kasuba and Evans [7] computed the same through a digitization approach. Yang and Lin [8] calculated the mesh stiffness of spur gears through the potential energy method by considering bending, axial compressive and Hertzian energy.

The existence of the cracks in the gear teeth is considered as stiffness reduction. The most common method applied in reducing modulus of elasticity at crack location [9]. The effect of the crack propagation size on the mesh stiffness is studied by Tian [10]. Wu et al. [11] assessed this effect on the dynamic response of a gearbox. Pandya and Parey [12, 13] assessed the effect of the crack path on mesh stiffness subject to different gear parameters, such as pressure angle, fillet radius, contact ratio, and backup ratio.

An analytical approach is presented by Chaari [14] to evaluate reduction in total gear mesh stiffness due to crack propagation, and a FEM model is used to verify the results obtained in an analytic manner. A modified mathematical model is proposed by Zhou [15] on crack growth in the

tooth root. Two additional scenarios of (a constant crack depth with a varying crack length and a constant crack length with a varying crack depth) for cracks are presented by Chen & Shao [16]. An analytical approach to calculate the mesh stiffness and model the crack propagation with a non-uniform parabolic path depth is proposed by Mohammad [17].

Liming and Yimin [18] studied the effect of tooth root crack on the mesh stiffness and dynamic response of spur gear pair considering a half-sinusoidal function for crack propagation path based on the real crack profile. Zaigang et al. [19] assessed the effect of crack on the fillet-foundation stiffness of gear and by comparison with FEM result proved that the load carrying zone depends on the tooth root crack depth in calculating the fillet-foundation stiffness. Wu et al. [20] studied the effect of tooth root crack on the mesh stiffness and dynamic response of spur gear system by LLM and FEM and compared their results with the experimental signals.

In the most available studies, the LLM is applied to reduce tooth thickness and calculating the total mesh stiffness, where considering two or more cracks in one tooth is impossible. In the method presented here, by defining torsional and linear springs instead of the cracks, two or more cracks with constant or variable crack depths through the whole tooth width or any length at any location of the tooth can be modeled.

2. Mathematical Model

This section contains two subsections, the first is the mesh stiffness analytical calculation and the latter is a new approach for the crack modeling in the mesh stiffness.

^{*} Corresponding author e-mail: poursina@eng.ui.ac.ir.

2.1. Analytical Calculation of Mesh stiffness

The mesh stiffness analytical calculation is the most known and repeatedly explained method, but it is necessary to mention it here before proposing the new crack modeling approach. Mesh stiffness is a parameter subject to gear parameters such as module, number of teeth, pressure angle, face width, hub bore radius and material properties. The stiffness of a pair of teeth (single mesh) is obtained by calculating bending (k_b), shear (k_s), axial (k_a), fillet-foundation stiffness (k_f) of each tooth and contact stiffness (k_h) of the teeth as Eqs. (1) to (5) [21]:

$$\frac{1}{K_h} = \frac{4(1-\nu^2)}{\pi EL} \quad (1)$$

$$\frac{1}{k_b} = \int_0^d \frac{((d-x) \cos(\alpha_m) - h \sin(\alpha_m))^2}{E I_x} dx \quad (2)$$

$$\frac{1}{k_s} = \int_0^d \frac{1.2 \cos^2(\alpha_m)}{G A_x} dx \quad (3)$$

$$\frac{1}{k_a} = \int_0^d \frac{\sin^2(\alpha_m)}{E A_x} dx \quad (4)$$

$$\frac{1}{K_f} = \frac{\cos^2(\alpha_m)}{L \cdot E} \left[L^* \left(\frac{u_f}{S_f} \right)^2 + M^* \left(\frac{u_f}{S_f} \right) + P^* (1 + Q^* \tan^2(\alpha_m)) \right] \quad (5)$$

where, h , α_m , x , dx and d are defined in Fig. 1; E , G , and ν are the Young's modulus, shear modulus and Poisson's ratio of gear material respectively. L is the gear face width; A_x is the tooth section area at point x measured from $A_x = (2h_x)L$; and I_x is the moment inertia of tooth section area at point x measured through $I_x = \frac{1}{12}(2h_x)^3L = \frac{2}{3}h_x^3L$; the definition of u_f and S_f , L^* , M^* , P^* and Q^* are presented in [22].

After calculating the stiffness for pinion and gear, total single stiffness (K_e) is calculated as Eq.(6) [21]:

$$K_e = \frac{1}{\frac{1}{K_{ap}} + \frac{1}{K_{bp}} + \frac{1}{K_{sp}} + \frac{1}{K_{fp}} + \frac{1}{K_h} + \frac{1}{K_{ag}} + \frac{1}{K_{bg}} + \frac{1}{K_{sg}} + \frac{1}{K_{fg}}} \quad (6)$$

where the first four terms relate to pinion and the last four terms related to gear.

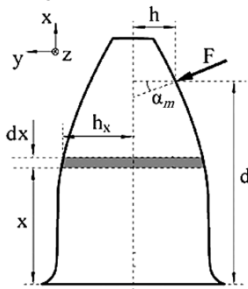


Figure 1. Tooth parameters

2.2. Analytical Crack Model

The issue of crack in the tooth root is the focus of many studies. The crack originates from freedom circle and extends to the center of the tooth on the root and then extends to other side of the tooth in a symmetric manner.

In general, the types of cracks in the root are of two categories (Fig. 2):

1. Overall crack with constant depth
2. Non-overall crack with varying depth

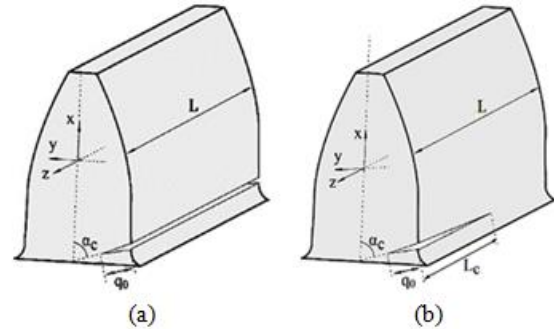


Figure 2. Cracked tooth (a) Overall crack with constant depth (b) Non-overall crack with varying depth

For modeling and calculating stiffness reduction of the cracked tooth, equivalent springs are applied. In this application the subject tooth is divided into two parts at the crack location, and the crack is replaced by linear and torsional springs, Fig. 3, subjected to a specified force and torque respectively. The stiffness of the springs are related to the depth of the crack and the thickness of the tooth in the crack region. In this model, the linear spring undergoes the shear force and torsional spring becomes subject to flexural torque. To assemble the linear and torsional springs, it is necessary to convert the angular deflection of the torsional spring to linear deflection by multiply it in the corresponding arm. After calculating the deflection due to rotation of torsional spring (δ_t) and the deflection of linear spring (δ_l) by Eqs. (7) and (8), their stiffness can be calculated as Eq. (9):

$$\delta_t = \frac{2 h_c}{E A_c} q_t(\lambda) (F \cdot u^2 \cos \alpha_m - F \cdot h^2 \sin \alpha_m) \quad (7)$$

$$\delta_l = \frac{2 F h_c}{E I_c} q_l(\lambda) \cos \alpha_m \quad (8)$$

$$k_t = \frac{F}{\delta_t}, \quad k_l = \frac{F}{\delta_l} \quad (9)$$

where, h , u and F are defined in Fig. 3; k_l and k_t are the linear and torsional spring stiffness respectively, h_c is the width of the tooth; A_c and I_c are area and area moment of inertia in the crack section respectively.

$q_t(\lambda)$ and $q_l(\lambda)$ are the functions related to the crack depth ratio that for the tooth with a rectangular section are expressed by Eq.(10) and (11) [23]:

$$q_t(\lambda) = \left(\frac{\lambda}{1-\lambda} \right)^2 (0.99 - \lambda(1-\lambda)(1.3 - 1.2\lambda + 0.7\lambda^2)) \quad (10)$$

$$q_l(\lambda) = \left(\frac{\lambda}{1-\lambda} \right)^2 (5.93 - 19.69 \lambda + 37.14 \lambda^2 - 35.84 \lambda^3 + 13.12 \lambda^4) \quad (11)$$

where, λ is the crack depth ratio and calculated by Eq.(12):

$$\lambda = \frac{q_c \sin \alpha_c}{h_c} \quad (12)$$

After calculating k_l and k_t the total mesh stiffness is expressed by Eq(13):

$$K_e = \frac{1}{\frac{1}{K_{ap}} + \frac{1}{K_{bp}} + \frac{1}{K_{sp}} + \frac{1}{K_{fp}} + \frac{1}{K_h} + \frac{1}{K_{ag}} + \frac{1}{K_{bg}} + \frac{1}{K_{sg}} + \frac{1}{\frac{1}{K_{fg}} + \frac{1}{K_{tp}} + \frac{1}{K_{lp}}}} \quad (13)$$

where, k_{tp} and k_{lp} are the stiffness of the equivalent torsional and linear springs on the pinion.

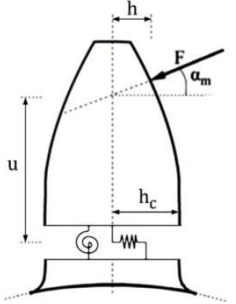


Figure 3. Cracked tooth model with torsional and linear spring

2.2.1. Tooth with two cracks

A tooth with two cracks is modeled in Fig. 4 where the mentioned springs are applied. The first crack is in tooth root, and the other is in pitch circle. At pitch location, when load position is below the crack location, no stiffness reduction takes place, while, when load position is above the crack location, the tooth is divided into three slices and the same calculation for stiffness reduction is made. After calculating K_t and K_l for the first and second cracks using Eqs. (14) and (15), the total mesh stiffness is calculated through Eq. (16):

$$\frac{1}{K_t} = \frac{1}{K_{t1}} + \frac{1}{K_{t2}} \quad (14)$$

$$\frac{1}{K_l} = \frac{1}{K_{l1}} + \frac{1}{K_{l2}} \quad (15)$$

$$K_{e1} = \frac{1}{\frac{1}{K_{ap}} + \frac{1}{K_{bp}} + \frac{1}{K_{sp}} + \frac{1}{K_{fp}} + \frac{1}{K_h} + \frac{1}{K_{ag}} + \frac{1}{K_{bg}} + \frac{1}{\frac{1}{K_{sg}} + \frac{1}{K_{fg}} + \frac{1}{K_{tp}} + \frac{1}{K_{lp}}}} \quad (16)$$

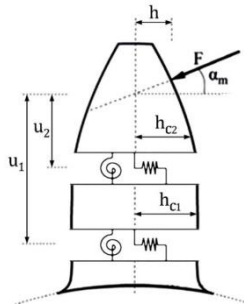


Figure 2. Modeling of the tooth with two cracks

2.2.2. Tooth with varying crack depths

A tooth with one crack that its depth ($q(z)$) follows a parabolic function along the tooth width shown in Fig. 5. When the crack length is less than the whole tooth width the following holds true (Eq.(17)) [21]:

$$\begin{cases} q(z) = q_0 \sqrt{\frac{w_c - z}{w_c}} & 0 < z < w_c \\ q(z) = 0 & z \geq w_c \end{cases} \quad (17)$$

where, w is the tooth width, w_c is the crack length, and q_0 is the maximum crack depth (Fig. 5). When the crack

length extends through the tooth width the following holds true (Eq. (18)):

$$q(z) = \sqrt{\frac{q_0^2 - q_2^2}{L} z + q_2^2} \quad (18)$$

To obtain the stiffness reduction for tooth with varying crack depths, the tooth face is divided into many slices and the previous equation are applied to calculate the crack depth in each slice. Then, the equivalent springs are modeled in each slice and whole stiffness of springs in all slices is obtained by adding all of them.

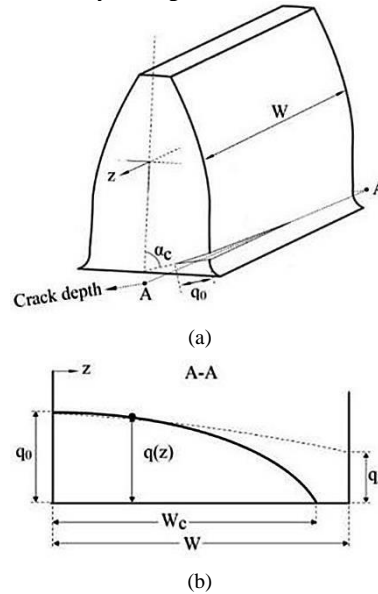


Figure 5. Modeling of gear tooth crack with non-uniform distribution. (a) Modeling of the cracked tooth, (b) crack depth distribution along the tooth width [21]

3. Result and discussion

To verify this proposed approach, a single stage gearbox is considered like that of [21]. The gear parameters are presented in Table 1, through which three examples are solved.

Table 1. Gear parameters [21]

Parameters	pinion	gear
Number of teeth	30	25
Module (mm)	2	2
Tooth width (mm)	20	20
Contact ratio	1.63	1.63
Pressure angle (deg.)	20	20
Young's modulus (GPa)	200	200
Poisson's ratio	0.3	0.3

The mesh stiffness results for different crack sizes that are mentioned in Table 2, drawn by Mohammed [21] are shown in Fig. 6-a, and the present results are shown in Fig. 6-b. It is obvious that the change patterns in both diagrams are similar and the values are the same approximately. The maximum difference is in 1.8 mm crack size with about 3 % difference.

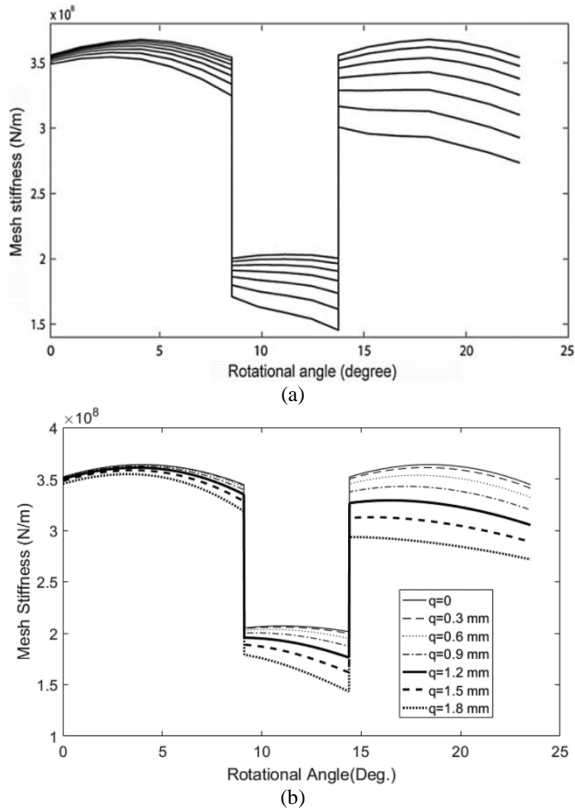


Figure 3. Time-varying gear-mesh stiffness for crack with constant depth (a) obtained by Mohammed [21] and (b) obtained in this study

Table 2. Data for crack with constant depth [21]

Case	q_0 (mm)	CL %	$\alpha_c = 70^\circ$
1	0	0	
2	0.3	8.06	
3	0.6	16.12	
4	0.9	24.19	
5	1.2	32.25	
6	1.5	40.32	
7	1.8	48.38	

In the second example, the results of the crack with non-uniform depth are compared with the results of Mohammed [24]. The result presented in Fig. 7 indicates a good agreement and validates the approach developed in this study. Crack properties of the driven gear are tabulated in Table 3.

Table 3. Data for crack with non-uniform depth [24]

Case	q_0 (mm)	w_c (mm)	q_2 (mm)	$\alpha_c = 70^\circ$
1	0	0	0	
2	0.2	5	0	
3	0.4	10	0	
4	0.6	15	0	
5	0.8	20	0	
6	1.0	20	0.45	
7	1.2	20	0.7	
8	1.4	20	0.925	
9	1.6	20	1.14	

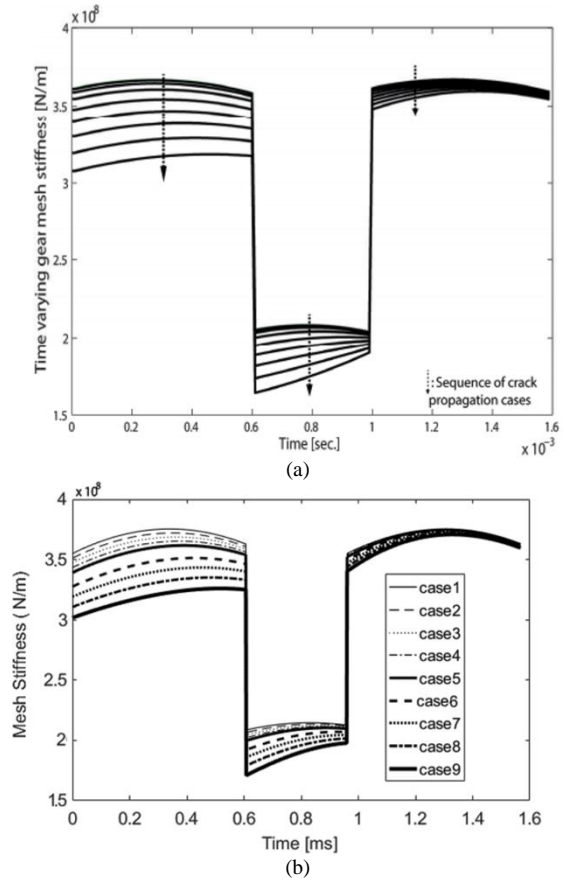


Figure 7. Time-varying mesh stiffness for non-uniform depth cracks (a) LLM used by Mohammed [24] and (b) ESM

In the third example, a tooth with two cracks as shown in Fig. 4 is of concern. The first crack is at tooth root and the second is at the pitch circle. Crack properties are tabulated in Table 4. The limit line method is unable to model two cracks in one tooth. So, the result of the proposed method is compared with the FEM. This example is modeled and simulated in Abaqus software by dynamic implicit solution method in plain stress condition and the cracks are modeled by the contour integral method. The element shapes and the meshing method that is used in the gears whole body is mesh quad free, except the cracks tip regions in the pinion tooth that mesh quad-dominated sweep is used. The numbers of elements in pinion and gear are 3211 and 5974 respectively. The element type was standard - Linear and contact defined as surface to surface with frictionless tangential behavior. The stress contour of modeled gears with only one tooth in contact is shown in Fig.8.

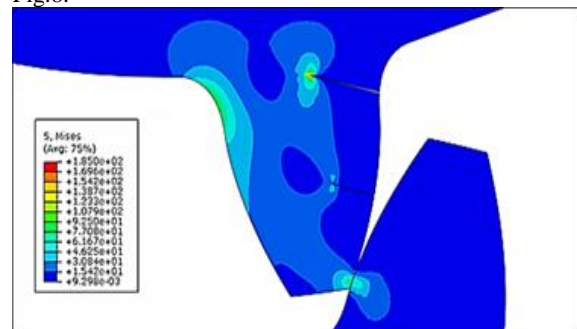
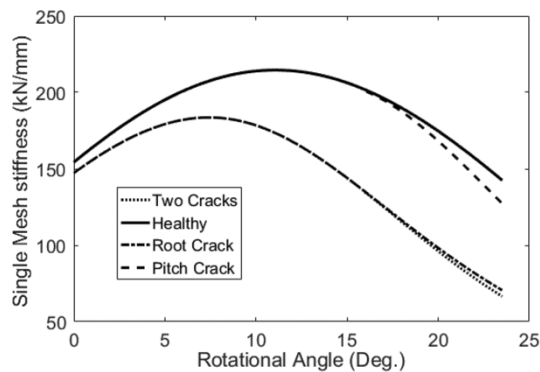


Figure 8. FEM Model

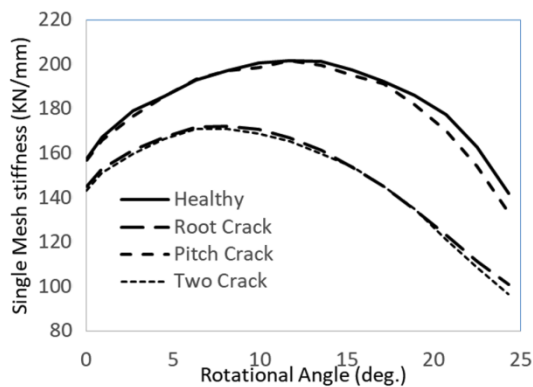
When the contact point is below the second crack zone, no reduction takes place. When the crack length in tooth root increases, the influence of the second crack will be decreased, a careful observation of Fig. 9 will prove this claim.

Table 4. data for two cracks

Case	Root Crack	Pitch Crack	$\alpha_c = 70^\circ$
	q_1 (mm)	q_2 (mm)	
1	0	0	
2	0	1	
3	1.8	0	
4	1.8	1	



(a)



(b)

Figure 9. Single mesh stiffness for a tooth with two cracks (a) AM result (b) FEM result

4. Conclusions

The results of this investigation show that the modeling two cracks in one tooth are obtainable by this newly proposed approach (ESM). In contrast, it was impossible according to previous studies. When the cracked tooth is in mesh, the influence of the crack decreases the gear mesh stiffness. Furthermore, the effect of a tooth crack on its stiffness is modeled by adding torsional and linear springs at the crack location. The recent approach results of single mesh stiffness in the case of two cracks in one tooth at the root and the pitch circles are compared with the FEM and showed the good agreement. The evidence from this study suggests that the obtained time-varying gear mesh stiffness can be applied in checking the dynamic behavior of the gear in the presence of the crack.

References

- [1] Lin, Jian, and Robert G. Parker. "Mesh stiffness variation instabilities in two-stage gear systems." *Journal of vibration and acoustics* 124, no. 1 (2002): 68-76.
- [2] Sirichai, Seney. "Torsional properties of spur gears in mesh using nonlinear finite element analysis." PhD diss., Curtin University, 1999.
- [3] Pimsarn, Monsak, and Kazem Kazerounian. "Efficient evaluation of spur gear tooth mesh load using pseudo-interference stiffness estimation method." *Mechanism and machine theory* 37, no. 8 (2002): 769-786.
- [4] Wang, Jiande, and Ian Howard. "The torsional stiffness of involute spur gears." *Proceedings of the Institution of Mechanical Engineers, Part C: Journal of Mechanical Engineering Science* 218, no. 1 (2004): 131-142.
- [5] Cornell, R. W. "Compliance and stress sensitivity of spur gear teeth." *Journal of Mechanical Design* 103, no. 2 (1981): 447-459. Cornell, R. W. "Compliance and stress sensitivity of spur gear teeth." *Journal of Mechanical Design* 103, no. 2 (1981): 447-459.
- [6] Kasuba, R., and Jt W. Evans. "An extended model for determining dynamic loads in spur gearing." *Journal of mechanical design* 103, no. 2 (1981): 398-409.
- [7] Yang, D. C. H., and J. Y. Lin. "Hertzian damping, tooth friction and bending elasticity in gear impact dynamics." *Journal of mechanisms, transmissions, and automation in design* 109, no. 2 (1987): 189-196.
- [8] Agosto, Frederick A. Just. "Damage detection based on the geometric interpretation of the eigenvalue problem." PhD diss., Ph. D. Thesis, 1997.
- [9] Tian, Xinhao. "Dynamic simulation for system response of gearbox including localized gear faults." PhD diss., University of Alberta, 2004.
- [10] Wu, Siyan, Ming J. Zuo, and Anand Parey. "Simulation of spur gear dynamics and estimation of fault growth." *Journal of Sound and Vibration* 317, no. 3-5 (2008): 608-624.
- [11] Pandya, Yogesh, and Anand Parey. "Simulation of crack propagation in spur gear tooth for different gear parameter and its influence on mesh stiffness." *Engineering Failure Analysis* 30 (2013): 124-137.
- [12] Pandya, Yogesh, and Anand Parey. "Failure path based modified gear mesh stiffness for spur gear pair with tooth root crack." *Engineering Failure Analysis* 27 (2013): 286-296.
- [13] Chaari, Fagher, Tahar Fakhfakh, and Mohamed Haddar. "Analytical modelling of spur gear tooth crack and influence on gearmesh stiffness." *European Journal of Mechanics-A/Solids* 28, no. 3 (2009): 461-468.
- [14] Zhou, Xiaojun, Yimin Shao, Yaguo Lei, and Mingjian Zuo. "Time-varying meshing stiffness calculation and vibration analysis for a 16DOF dynamic model with linear crack growth in a pinion." *Journal of Vibration and Acoustics* 134, no. 1 (2012): 011011.
- [15] Chen, Zaigang, and Yimin Shao. "Dynamic simulation of spur gear with tooth root crack propagating along tooth width and crack depth." *Engineering Failure Analysis* 18, no. 8 (2011): 2149-2164.
- [16] Mohammed, Omar D., Matti Rantatalo, and Jan-Olov Aidanpää. "Improving mesh stiffness calculation of cracked gears for the purpose of vibration-based fault analysis." *Engineering Failure Analysis* 34 (2013): 235-251.
- [17] Wang, Liming, and Yimin Shao. "Fault mode analysis and detection for gear tooth crack during its propagating process based on dynamic simulation method." *Engineering Failure Analysis* 71 (2017): 166-178.
- [18] Chen, Zaigang, Jie Zhang, Wanming Zhai, Yawen Wang, and Jianxin Liu. "Improved analytical methods for calculation of

- gear tooth fillet-foundation stiffness with tooth root crack." *Engineering Failure Analysis* 82 (2017): 72-81.
- [19] Wu, Jiateng, Yu Yang, Xingkai Yang, and Junsheng Cheng. "Fault feature analysis of cracked gear based on LOD and analytical-FE method." *Mechanical Systems and Signal Processing* 98 (2018): 951-967.
- [20] Mohammed, Omar D., and Matti Rantatalo. "Gear tooth crack detection using dynamic response analysis." *Insight (Northampton)* 55, no. 8 (2013): 417-421.
- [21] Sainsot, Philippe, Philippe Velez, and Olivier Duverger. "Contribution of gear body to tooth deflections—a new bidimensional analytical formula." *Journal of mechanical design* 126, no. 4 (2004): 748-752.
- [22] Tada, Hiroshi, Paul C. Paris, and George R. Irwin. "The stress analysis of cracks." *Handbook*, Del Research Corporation(1973).
- [23] Mohammed, Omar D., Matti Rantatalo, and Uday Kumar. "Analytical crack propagation scenario for gear teeth and time-varying gear mesh stiffness." *vol 6* (2012): 1106-1111.

Estimation of Fuel Consumption in a Hypothesized Spoke-hub Airline Networks for the Transportation of Passengers

Mohammad D. AL-Tahat^{*a}, Dr. Mohammad Al Janaideh^b, Yousef Al-Abdallat^c,
Mowafaq E. Jabri^c

^aIndustrial Engineering Department, The University of Jordan, Amman 11942 – Jordan

^bThe University of Jordan, Mechatronics Engineering Department, School of Engineering, Amman 11942, Jordan.

^cThe University of Jordan, Industrial Engineering Department, School of Engineering, Amman 11942, Jordan.

Received 13 May, 2019

Abstract

Transportation industry expands rapidly, fuel is a main cost element in air transportation industry. Worldwide airline networks strive to adopt a method, which enables them, to schedule their flights, with the minimum quantity of fuel to transport passengers through hub and spoke airlines networks. Therefore, fuel consumption should be investigated as economically as possible. To minimize the voyage fuel consumption for a set of aircraft routes, merging airfreight transportation routes through the hub and spoke networks plays a significant value in reducing the redundancy of long flights. A transshipment network of various numbers of international airports is developed; the developed transshipment network is then converted into a transportation network that is assumed to transfer passengers from their source airport to their intended destination airport directly. The methodology has been applied to three different real-life cases. Obtained solutions are tested and validated. Rationality of solutions are decided. A scientific methodology for the analysis and for the scheduling of passengers' transportation is presented. The methodology generated valid solutions that have been found workable which can improve transportation economics.

© 2019 Jordan Journal of Mechanical and Industrial Engineering. All rights reserved

Keywords: Spoke-hub modelling; Transportation; Transshipment; Airlines Fuel consumption; Passengers scheduling; Airline routing;

1. Introduction

Fuel costs are an airline's second largest expense. Only labor costs exceed fuel's cost. In 2000, airlines paid about \$5.4-billion in fuel costs, (Air Transport Association (ATA)). Any increase in fuel costs is usually passed onto passengers in the ticket price. Fuel price fluctuations and variations in the total operational cost of passenger transportation show that an increase (decrease) in fuel price leads to rise (fall) in total operation cost. Most of the passenger airlines in operation use a hub-and-spoke network to route their plane traffic. As shown by Figure 1, a hub is a central airport that flights are routed through, and spokes are the routes that planes take out of the hub airport. Most major airlines have multiple hubs. They claim that hubs allow them to offer more flights for passengers. Today, most airlines have at least one central airport that their flights must go through. From that hub, the spoke flights take passengers to select destinations. The purpose of the hub-and-spoke system is to save airlines money and to give passengers better routes to destinations. Airplanes are an airline's most valuable commodity, and every flight has certain set of costs. Each seat on the plane represents a portion of the total flight

cost. For each seat that is filled by a passenger, an airline lowers its break-even price, which is the seat price at which an airline stops losing money and begins to show a profit on the flight.



Figure1. Example for a hub-and-spoke network [1].

Growth and rapid transformation of the international air transport industry is increasing rapidly. Fuel is a main cost element in air transport industry. A typical airline spends 10% of its operating budget on fuel [2]. The global mobility and freight of passengers increase in international tourism, and the global growth of the economy at large. Various factors, such as the world's largest aviation market, the adoption of mid-sized long-haul aircraft,

* Corresponding author e-mail: altahat@ju.edu.jo.

climate changes and depletion of stratospheric Ozone, and most importantly emissions of greenhouse gases will significantly create substantial fuel related emissions [3]. In 1990 airlines industry contributed to about 3.5% of global gas emissions [4]. This share depends on many factors, and energy efficiency is one of them.

Airlines fuel consumption is a very large cost element in transportation industry; it is highly correlated with emissions and contributes directly to transport externalities [3]. It has been reported how fuel efficiency of commercial aircraft has developed since 1930s [4]. Peeters comparing large piston-engine aircraft with both old and new jet engine, in their macro analysis they revealed an increase in fuel consumption per seat-kilometer as piston-engine aircraft were replaced by jet- one. As economy depends on fuel prices, fuel prices affect airlines operating cost, and affects the demand on travel and cargo. In 2003, fuel represented about 28% of total operating cost for a typical Airbus - A320, by 2006 fuel prices represented about 43% of all operating costs [5]. Many studies on fuel consumption and conservation have been conducted after Arab oil embargo after 1970. David A. Pilati evaluated and discussed various fuel saving strategies, [6]. In [7-9] various models for managing fuel consumption that resulted in fuel saving have been developed in, the operational parameters which effect fuel consumption have been studied in [10-12]. Alan J. Stolzer [2] examined extensively the literature related to fuel consumption efforts, and the related statistical methodologies, he stated that most fuel consumption studies are concerned with engineering rather than operational issues, he recommended that the implementation of a hypothesized Flight Operations Quality Assurance (FOQA) programs at airlines is helpful in this management effort. Recently, Megan et al. [13] developed a model for the estimation of fuel consumption based on two variables, distance and seats. It has been reported that airlines are seeking merger partners strategically to improved fuel efficiency, reduce cost, and boost revenue. That can eliminate network redundancy. The reduction of fuel consumption and its balance against the impact on passengers is also highlighted in [13], across two major US airline mergers, they find that the number of non-stop destinations and flight frequency per connection dropped significantly while the number of passengers increased considerably. It has been found in [13] that the fuel savings achieved by merged both airline networks. Modeling of fuel consumption cost has been considered by several researches. An operating cost model is developed in [14] by summing fuel consumption, labor costs, and other additional costs for specific aircraft types, with the goal of comparing aircraft costs parametrically over fuel price. In 1984 Oster, C. V., Jr., and A. McKey [15] compared the operating costs of different computer aircraft and they performed a parametric analysis of operating cost versus stage length.

A fuel burn in Kilos per seat per Nautical mile [Kg/seat NM] has been standardized in [3] for airplanes using aircraft inventory database. Comparative geographical heterogeneity of fuel burn rates among different distance and routes in the long-haul market is shown in [3], while controlling for seat configuration and stage distance. Zou and others [16] presented deterministic and stochastic

approaches to investigate the efficiency of fuel consumption, in their ratio-based analysis, 15 main airlines operators in the US. Are considered. A multi-objective optimization model has presented in [17] for a robust airline schedules, the considered the incremental changes of flight schedule and of the aircraft maintenance schedule. Their model is solved based simulation; the approach is tested by real world data from KLM Royal Dutch Airlines, significant improvements for the considered objectives was addressed. A network model for airline scheduling is proposed in [18], the scheduling model is solvable in a real-time environment, and it can be used in sophisticated operational and planning systems. The operational crew-scheduling problem is presented in [19] where both the crew pairing, and crew roistering problems are studied simultaneously. The importance of minimizing the total passenger waiting time is highlighted in [20, 21]. A heuristic that minimizes the number of canceled flights and the total passengers waiting time. A network models to determine aircraft swaps and flight cancellations are presented in [22, and 23]. Recent work on scheduling is found in [24-28]. This paper is expected to provide an assessment tool for reducing fuel consumption and consequently costs of transporting passengers and goods by airplanes through the hub and spoke networks. The main idea behind that is to minimize the voyage fuel consumption for a set of aircraft routes, as well as considering an adjustment on airports and the type of airplanes deployed on the destinations, merging airfreight transportation routes through the hub and spoke networks plays a significant value in reducing the redundancy of long flights. The proposed hub and spoke model is expected to enhance transportation efficiency through simplifying a network of routes. Airline companies may take advantage of the concept as it is expected to revolutionize the way airlines are run. A generic operation research model for the hub-and-spoke airlines network shown in figure 2 will be formulated subjected to traveling needs of passengers with the minimum fuel consumption airlines network.

The proposed model should capture some realistic shipping constraints, such as passengers transporting time, demand, destinations, and some other important factors. The main idea of our constructive insertion approach is to minimize fuel consumption for each main aircraft route, as well as considering an adjustment on airports called and the type of airplanes deployed on the main aircraft route. Satisfying the travelling needs of passengers through a hub and spoke networks will enable us to minimize the number of aircrafts travelling through the networks, yielding an expected savings in aircrafts fuel.

2. Materials and Methods

An attempt to formulate a generic model for a worldwide hub-and-spoke airlines network composed of N hubs, each hub composed of (mn) spokes as depicted in Figure 2, will be conducted. The proposed model should result in a route matrix of an adequate number of airplanes, satisfying travelling needs for long distance passengers, with the best fuel consumption, within the whole network paradigm. In this model, passengers are assumed to travel

from any airport source (spoke or hub) through any airport(s) (spoke or hub) to their destination airport.

2.1. Nomenclature

Nomenclature and notations shown in table 1 are used to formulate the proposed model.

2.2. Model Formulation

A suggested mathematical equation for the computation of the fuel consumption per passenger seat occupied for a travelling passenger between airport (i) and airport (j) is as follows:

$$c_{ij} = \frac{(d_{ij})(ac_{ij})(f_{ij})}{(os_{ij})^2(s_{ij})} \quad (1)$$

The objective is to minimize the total fuel consumption as follow:

$$Min z = \sum_{i=1}^L \sum_{j=1}^L c_{ij}(x_{ij}), c_{ij} = \infty \text{ for all } i = j \quad (2)$$

Subject to

$$L = N + \sum_{n=1}^N M_n \quad (3)$$

$$b_i = \sum_{j=1}^L x_{ij}, i = \{1, 2, 3, \dots, L\} \quad (4)$$

$$a_j = \sum_{i=1}^L x_{ij}, j = \{1, 2, 3, \dots, L\} \quad (5)$$

$$\sum_{i=1}^L b_i = \sum_{j=1}^L a_j \quad (6)$$

$$x_{ij} \geq 0, \forall (i), \text{ and } \forall (j) \quad (7)$$

The objective function in equation (2), and the constraints in equations (3), (4), (5), (6), and (7), constitute an operations research model, which can be used to estimate fuel consumption. The model depends on distance between airports (d_{ij}), aircraft performance in terms of rate of fuel consumption per hour of traveling from i to j , and the airplane speed of traveling from i to j in Kilometer per hour.

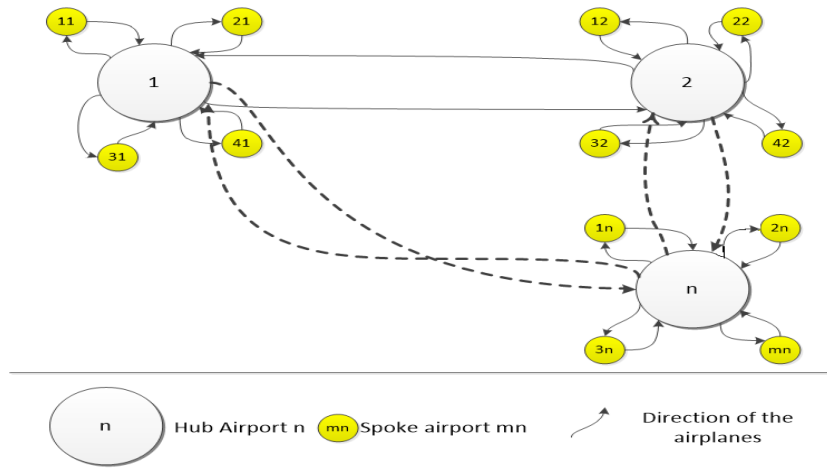


Figure 2. Schematic Illustration of (n) Hub (mn) Spoke Paradigm.

Table 1. Nomenclature and notations

N	Total Number of hubs in the paradigm
n	The n^{th} hub in the paradigm, $n = \{1, 2, \dots, N\}$
M_n	Total Number of spokes of the n^{th} hub paradigm
m_n	The m^{th} spoke of the n^{th} hub in the paradigm, $mn = \{1_n, 2_n, \dots, M_n\}$,
L	Total airports involved in the paradigm
i	Origin city airport index (Source node), $i = \{1, 2, \dots, L\}$,
j	Destination city airport index (Destination node) $j = \{1, 2, \dots, L\}$,
c_{ij}	Unit transportation cost from origin city airport (i) to destination city (j) in term of the fuel consumed per passenger per occupied seat.
x_{ij}	Unit to be shipped from origin city airport (i) to destination city airport (j)
b_i	Unit of supply on origin city airport (i), $b_i = \sum_{j=1}^L x_{ij}, i = \{1, 2, \dots, L\}$
a_j	Unit of demand on destination city airport (j) $a_j = \sum_{i=1}^L x_{ij}, j = \{1, 2, \dots, L\}$
OS_{ij}	Occupied Seats (OS) of an airplane traveling from origin city airport (i) to destination city airport (j). Seat/ airplane
ac_{ij}	Airplane Capacity travelling from origin city airport (i) to destination city airport (j).Seat/ airplane
d_{ij}	Travelling distance in Kilometer from origin city airport (i) to destination city airport (j).
f_{ij}	Rate of fuel consumption per hour of the airplane traveling from origin city airport (i) to destination city airport (j). Litters/(hour. airplane)
s_{ij}	Speed of the airplane traveling from origin city airport (i) to destination city airport (j) in Kilometer per hour.
k_{ij}	Number of airplanes required to be utilized between origin city airports (i) to destination city airport (j).

2.3. Solution Methodology

To obtain a valid solution, the following methodology, which is depicted in Figure 3, is followed:

1. Sketch the situation: A hub and spoke paradigm of (n) hub, (mn) spoke should be formulated as a transshipment network. A regular outline that describes the situation correctly and precisely with relevant data to the situation should be presented.
2. Identify N : Identifying the number of system hubs.
3. Identify the spokes mn for each hub (n), $n = 1, 2, \dots, N$: Identifying spokes and there related hubs.
4. Computing L : Total number of cities is computed using equation (3).
5. I- Vector construction: Identify indices of the airports, usually $i = 1, 2, \dots, L$.
6. J- Vector construction: Identify destination cities airports indices $j = 1, 2, 3 \dots L$.
7. D- Matrix construction: Identify the travel distance (d_{ij}) in Kilometer from origin city i to destination city j .
8. AC- Matrix construction: Identify airplane capacity (ac_{ij}) travelling from i to j .
9. OS- Matrix construction: Identify occupied seats (os_{ij}) of an airplane traveling from i to j .
10. F- Matrix construction: Identify rate of fuel consumed per hour (f_{ij}) by an airplane traveling from i to j .
11. S- Matrix construction: Identify the speed of an airplane (s_{ij}) traveling from i to j .
12. C- Matrix estimation: Estimate a passenger travelling fuel consumption (c_{ij}) from origin city i to destination city j based on equation (1), excel spreadsheets are recommended to be used.
13. A- Vector construction: Identify original demand at every destination city j (a_j), then compute total demand.
14. B- Vector construction: Identify original supply at every origin city i (b_i), then compute total supply.
15. Network balance check: To proceed correctly, total demand should equal total supply. If total demand does not equal total supply, a dummy source/ destination should be added to the network, with a quantity of supply/ demand equal to the difference between total supply and total demand. A zero-cost coefficient should be assigned to all dummy cells; accordingly, all the previous steps should be modified.
16. Buffer (Bu) computation: Buffer is computed using equation (6).
17. AA Vector construction: Compute total demand at every destination city j (aa_j), which is computed according to the following equation:

$$aa_j = \begin{cases} a_j & \text{Pure demand node} \\ a_j + B & \text{Pure transshipment node} \end{cases} \quad (8)$$

$$j = \{1, 2, 3, \dots, L\}$$
18. Computing BB vector, total supply at every origin city i , (bb_i), is computed according to equation (9):

$$bb_i = \begin{cases} b_i & \text{Pure demand node} \\ b_i + B & \text{Pure transshipment node} \end{cases} \quad (9)$$

$$i = \{1, 2, 3, \dots, L\}$$
19. Formulating the transportation model of the problem in tableau format.
20. Solving the problem: Tora software is used.
21. Solution explanation and validation.

3. Variant Real-Life Cases

The core of the problem of this research is to find passengers' routes, which will yield the minimum fuel consumption for the transferring of the passengers within the hub and spoke paradigm. The inputs to the estimation of the fuel consumed per passenger seat problem are just the result of another suboptimal planning problem – the location of hubs and spoke airports problem.

Even the fuel consumed per passenger seat problem described in this thesis is to some extent a simplification of the real problem. By employing a rule modeling tool and generic model, which do not make any assumption on the structure of the problem to be solved, the fuel consumption per passenger seat problem supports a sufficiently accurate modeling of the real-world estimation of fuel consumption in a hypothesized hub and spoke paradigm.

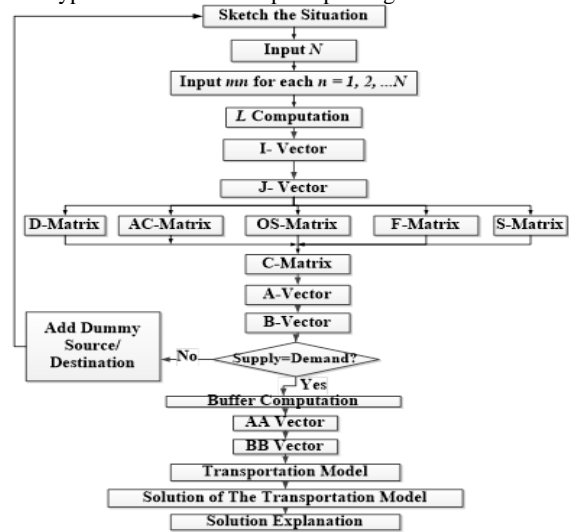


Figure 3. Two hub-spoke groups over other six airports with corresponding supply demand.

3.1. Case Study 1: Royal Jordanian Airplanes outing

The Royal Jordanian (RJ) airlines is the flag carrier airline of Jordan with its head office in Amman, Jordan. RJ offers international services from its main base at Queen Alia International Airport in Jordan. RJ is utilizing two hub-spoke groups connecting long haul passengers through their fleet over other six airports as indicated in figure 4. Cost parameters $\{s_{ij}, f_{ij}, oc_{ij}, ac_{ij}, d_{ij}\}$, demand (b_i) and supply (a_j) between cities airports, are reported in table 2. Using equation (1), the fuel consumed per passenger for a specific route (c_{ij}), (liters per occupied passenger seat) is calculated and recorded in table 3. The transshipment network should be balanced. In this model, the supply is (= 3,746) which equals to the total demand (= 3,746), the Buffer quantity (Bu) is determined; $\{Bu = \text{Total supply} = \text{Total Demand} = 3,746\}$. Airports are classified into: pure demand airport, transit airport, and pure supply airport.

Accordingly, supply and demand are adjusted using equation (8) and equation (9). The resultant transportation model is then solved using TORA Windows ® version 2.00, 2006. TORA is not a solver. It is a demo for students. More standard solvers should be used, but TORA can do the job for this research.

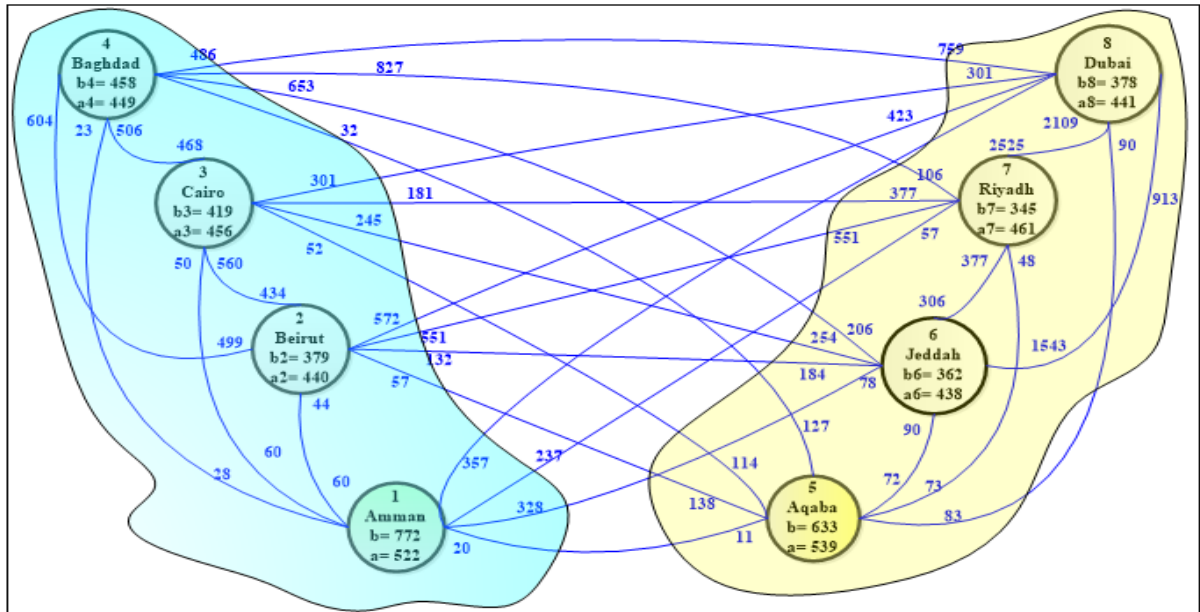


Figure 4. Two hub-spoke groups over other six airports with corresponding supply, demand, and unit transportation costs

Table 2. Cost function parameters between cities airports [14]

		Destination airport (j)								Supply (b _i)	Adjusted Supply (bb _i)	
		1	2	3	4	5	6	7	8			
Origin airport (i)	1	d_{ij}	∞	238	473	631	253	1162	1291	2023	772	4518
		ac_{ij}	-	100	136	110	136	136	136	136		
		oc_{ij}	-	93	90	95	135	119	120	120		
		f_{ij}	-	2000	2000	2000	1600	3900	2800	2850		
	2	s_{ij}	-	124	317	680	276	559	596	676	379	4125
		d_{ij}	238	∞	563	814	447	473	1466	2142		
		ac_{ij}	100	-	136	136	136	136	136	136		
		oc_{ij}	80	-	30	50	64	50	55	50		
	3	f_{ij}	2000	-	4500	4500	2900	4500	3500	3000	419	4165
		s_{ij}	124	-	684	330	312	628	419	826		
		d_{ij}	473	563	∞	1263	381	1218	1614	2417		
		ac_{ij}	136	136	-	136	136	136	283	283		
	4	oc_{ij}	82	35	-	50	67	49	61	75	458	4204
		f_{ij}	2000	4500	-	4000	2950	2000	1750	1500		
		s_{ij}	317	648	-	543	300	563	570	606		
		d_{ij}	631	814	1263	∞	619	1427	614	1400		
	5	ac_{ij}	110	136	136	-	136	136	136	283	633	4379
		oc_{ij}	86	55	52	-	55	80	70	60		
		f_{ij}	2000	4500	4000	-	3000	3500	4000	4000		
		s_{ij}	680	330	543	-	656	514	646	580		
	6	d_{ij}	253	447	381	619	∞	986	1226	2054	362	4108
		ac_{ij}	136	136	136	136	-	136	136	136		
		oc_{ij}	100	100	99	109	-	60	90	75		
		f_{ij}	1600	2900	2950	3000	-	1300	1300	1300		
	7	s_{ij}	276	312	300	656	-	538	559	715	345	4091
		d_{ij}	1162	473	1218	1427	986	∞	853	1701		
		ac_{ij}	136	136	136	136	136	-	136	136		
		oc_{ij}	58	59	49	45	67	-	45	39		
	8	f_{ij}	3900	4500	2000	3500	1300	-	4500	3500	378	4124
		s_{ij}	559	628	563	514	538	-	683	583		
		d_{ij}	1291	1466	1614	614	1226	853	∞	874		
		ac_{ij}	136	136	136	136	136	136	-	136		
Demand (a _j)	oc_{ij}	59	55	61	25	73	50	-	22	3746	-	
	f_{ij}	2800	3500	1750	4000	1300	4500	-	4500			
	s_{ij}	596	419	570	646	559	683	-	524			
	d_{ij}	2023	2142	2417	1400	2054	1701	874	∞			
Adjusted demand (aa _j)	ac_{ij}	136	136	283	283	136	136	136	-	-	-	
	oc_{ij}	57	43	75	75	78	30	20	-			
	f_{ij}	2850	3000	1500	4000	1300	3500	4500	-			
	s_{ij}	676	826	606	580	715	583	524	-			
Demand (a _j)		522	440	456	449	539	438	461	441	-	-	
Adjusted demand (aa _j)		4268	4186	4202	4195	4285	4184	4207	4187	-	-	

Based on North-west corner method solution is obtained, solution is presented in figure 5, it represents the number of passengers who must be transferred between each route, with minimum fuel consumption of \$3,552,307 for the whole paradigm.

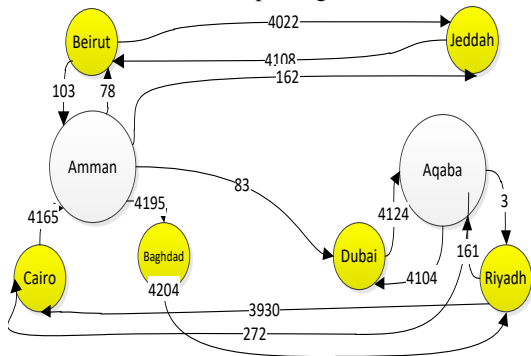


Figure 5. Optimal number of passengers routing through the considered case

Table 3. Fuel consumption per passenger (c_{ij}) computed by equation (1)

i	j	Destination airport							
		1	2	3	4	5	6	7	8
Origin airport	1	∞	44	50	23	11	78	57	81
	2	60	∞	560	604	138	184	551	423
	3	60	434	∞	506	114	245	377	301
	4	28	499	468	∞	127	206	106	759
	5	20	57	52	32	∞	90	48	90
	6	328	132	245	653	72	∞	377	913
	7	237	551	181	827	73	306	∞	2109
	8	357	572	301	486	83	1543	2552	∞

4. Results and discussion

This paper demonstrates a proposed methodology that focuses on creating a route of airplanes between airports of hub and spoke paradigm with the minimum fuel consumption. It develops an operations research model with single linear objective function. The intended model resulted in a routing solution that satisfies some travelling needs of passengers belonging to the hub and spoke network with the minimum fuel consumption of airlines fleets, which is expected to decrease the total costs incurred by airliners. The effectiveness of the proposed model and the efficiency of the proposed methodology have been assessed, using the shown numerical example based that mimic real-life situations.

The model has been created based on the relaxation of the considered hub and spoke paradigm resulting with a capacitated hub and spoke network model, then formulated as transshipment model. The generated transshipment model is then converted to a transportation problem, where hub and spoke airports are considered as a source nodes and a destination nodes. Each source airport has a fixed supply of passengers; the entire supply must be distributed to the destination airports. Similarly, each destination airport has a fixed demand for

passengers, where this entire demand must be received from the sources. A transportation problem will have a feasible solution if and only if, entire supply equals the entire demand, if this not the case the transportation model should be fit by introducing a dummy destination airport or a dummy source airport. The developed model is composed of:

1. A linear single objective function is derived. That depends on:

- Travelling distance $\{d_{ij}$ Kilometer from origin airport (i) to destination airport (j),
- Airplane capacity (ac_{ij}) travelling from i to j,
- (c) standard rate of fuel consumed per hour by an airplane traveling from i to j,
- Occupied seats (os_{ij}) of an airplane traveling from i to j, and
- The standard speed of an airplane (s_{ij}) traveling from i to j.

2. A total number of constraints equals to

$$\left(2L = 2N + 2 \sum_{n=1}^N M_n \right),$$

these constraints assure that the model satisfying all the transshipment demand as well as the original external demand. When there is a need to introduce a dummy source/destination number of constraints equals to $\left(2L + 1 = 2N + 2 \sum_{n=1}^N M_n + 1 \right)$. Accordingly, the considered case has 16 constraints.

3. A total number of decision variables equals to

$$\left(L^2 = \left(N^2 + 2N \sum_{n=1}^N M_n + \left(\sum_{n=1}^N M_n \right)^2 \right) \right)$$

When there is a need to introduce a dummy source/destination number of decision variables equals to

$$\left(L^2 + L = \left(N^2 + 2N \sum_{n=1}^N M_n + \left(\sum_{n=1}^N M_n \right)^2 \right) + L \right)$$

Accordingly, the considered case has 64 decision variables.

4. The considered case has 16 constraints and 15 optimal basic variables.

5. Non-negativity constraints.

A linear formulation of the transshipment network of the considered case is developed as an alternative solution method based on the following; (a) Supply at each pure supply node (i), Table 4. (b) The transshipment quantity at each transshipment node (k) as shown in table 5 and table 6. Transshipment quantity is equal to the buffer quantity if the transshipment node is incapacitated and demand on the transshipment node if any, otherwise is equal to the assigned capacity. And (c) demand at each pure demand node (j) as shown in table 6.

Considering the transshipment network depicted in figure 6, if (x_{ik}) is the transshipped quantity from (i) to (k) with a unit transportation cost of (c_{ik}) , and (y_{kj}) is the transshipped quantity from (k) to (j) with a unit transportation cost of (c_{kj}) . Then the transshipment network can be modeled mathematically by the following set equations.

Table 4. Supply at each pure supply node

Node	Amman	Beirut	Cairo	Baghdad	Aqaba	Jeddah	Riyadh	Daubi	Total
<i>i</i>	1	2	3	4	5	6	7	8	3746
<i>S_i</i>	772	379	419	458	633	362	345	378	

Table 5. Transshipment quantity at each transshipment node (*k*)

Node	Amman	Beirut	Cairo	Baghdad	Aqaba	Jeddah	Riyadh	Daubi	Total
<i>k</i>	1	2	3	4	5	6	7	8	22968
<i>T_k</i>	3746	3746	3746	3746	3746	3746	3746	3746	

Table 6. Demand at each pure demand node (*j*)

Node	Amman	Beirut	Cairo	Baghdad	Aqaba	Jeddah	Riyadh	Daubi	Total
<i>j</i>	1	2	3	4	5	6	7	8	3746
<i>D_i</i>	522	440	456	449	539	438	461	441	

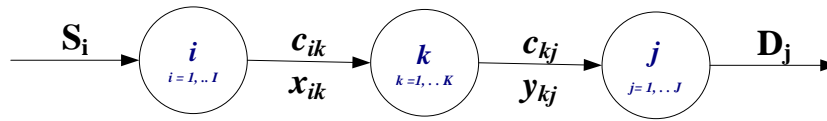


Figure 6. WIP flow and input-output relationship between resources and activity center

$$Min Z = \sum_{i=1}^I \sum_{k=1}^K c_{ik} x_{ik} + \sum_{k=1}^K \sum_{j=1}^J c_{kj} y_{kj}$$

$$\sum_{k=1}^K x_{ik} = s_i \quad \forall i = 1, 2, 3, \dots, I \quad (\text{Supply Constraint at Origin})$$

$$\sum_{i=1}^I x_{ik} = T_k \quad \forall k = 1, 2, 3, \dots, K \quad (\text{Transshipment Constraint})$$

$$\sum_{k=1}^K y_{kj} = D_j \quad \forall j = 1, 2, 3, \dots, J \quad (\text{Demand Constraint at destination})$$

$$\sum_{i=1}^I x_{ik} - \sum_{j=1}^J y_{kj} = 0 \quad \forall k = 1, 2, 3, \dots, K \quad (\text{Transshipment Balancing})$$

$$x_{ik}, y_{kj} \geq 0 \quad \forall i, k, j$$

The problem is solved as a linear operations research model using the roots of Simplex algorithm, Tora for windows version 2 is applied, then solutions are finalized, then the solution is converted into a schedule of airplanes. Validity of solutions has been upraised when the obtained solutions discussed with Royal Jordanian airline scheduling manager, and when model output compared with historical data under similar input conditions. The interpretation of equation (2), (4), (5), and (7) of the proposed model, is also a good indicator for solution validation, it has been found that the optimal fuel consumption cost;

$$z = \left(\sum_{i=1}^I \sum_{j=1}^J c_{ij} (x_{ij}) \right) = 3,552,30700$$

Subject to supply of each origin airport in the travelling paradigm is satisfied, accordingly;

$$\text{For Amman airport}(i = 1) = \sum_{j=1}^J x_{Amman,j} = 4,518$$

$$= (x_{12}) + (x_{14}) + (x_{16}) + (x_{18}) \\ = 78 + 4195 + 162 + 83 \\ = 4,518$$

$$\text{For Beirut airport}(i = 2) = \sum_{j=1}^J x_{Beirut,j} = 4,125 \\ = (x_{21}) + (x_{26}) = 103 + 4,022 \\ = 4,125$$

Similarly, supply of all other origin airport is checked and found to be satisfied. In addition, demand of each destination airport in the travelling paradigm is checked and it has been satisfied for all destination airport, for example;

$$\text{For Riyadh airport}(j = 7) = \sum_{i=1}^I x_{i,Riyadh} \\ = (x_{47}) + (x_{57}) = 4204 + 3 \\ = 4,207$$

$$\text{For Daubi airport}(j = 8) = \sum_{i=1}^I x_{i, Daubi} \\ = (x_{18}) + (x_{58}) = 83 + 4,104 \\ = 4,187$$

5. Conclusions

This research can act as a managerial guide for airlines scheduling as well as a reference for future research in this field. One major finding of this paper is an optimal airline routes that distribute the entire passengers from source locations to their intended destinations in a hub and spoke paradigm, with the minimum fuel consumption, accordingly an airline schedule can be produced. One advantage of the presented model is the ability to convert the solution into schedule of airplanes in term of the number of airplanes to be assigned between any two airports in the paradigm network.

Validation of the results indicates that such routes and schedules can be implemented in hub and spoke airline paradigm where an acceptable fuel consumption cost and a proper behavior of the system is expected. Obtained solutions reveal that the proposed model generates solutions that are adequately reasonable. Model output found to be acceptable it does not include surprises, and it does make sense airline scheduling manager. Therefore, solutions can be implemented.

Furthermore, simulation modeling, queuing theory, dynamic programming may be configured for this type of work as a future extension to obtain a valid model output.

6. Acknowledgement

We thank the anonymous reviewers whose comments and suggestions helped improve and clarify this manuscript.

Work presented in this paper is extracted from a master's thesis prepared by Mowafaq E. Jabri under the supervision of Prof. Dr. Mohammad D. AL-Tahat and Dr. Mohammad Al Janaideh. The University of Jordan approves the thesis in May 2016.

References

- [1]. Howstuffworks. (2015). How Airlines Work. URL: <http://science.howstuffworks.com/transport/flight/modern/airline3.htm>
- [2]. Alan J. Stolzer (2002), fuel consumption modeling of a transport category aircraft using flight operations quality assurance data: A literature review, *Journal of Air Transportation*, Vol. 7, No. 1 – 2002. Pp. 93-103.
- [3]. Park Y. and O'Kelly M., (2014), Fuel burn rates of commercial passenger aircraft: variations by seat configuration and stage distance, *Journal of Transport Geography* 41 (2014), PP. 137–147.
- [4]. Peeters P.M, Middel J., Hoolhorst A. (2005), Fuel efficiency of commercial aircraft: An overview of historical and future trends. National Aerospace Laboratory NLR.
- [5]. Airbus, (2008). Getting to grip with A320 family performance retention and fuel savings. *Flight Operations Support & Services*, Iss. 2.
- [6]. David A. Pilati, (1974), Energy Use and Conservation Alternatives for Airplanes, *Transportation Research*, Vol. 8, 1974, 433-441.
- [7]. Wayne Darnell and Carolyn Loflin, National airline fuel management and allocation model, *Interfaces*, Vol.7, No. 2 (Feb. 1977), pp. 1-16.
- [8]. Barry Nash, A simplified alternative to current airline fuel allocation models, *Interfaces*, Vol. 11, No. 1, February 1981, p.p. 1-9.
- [9]. John S. Stroup and Richard D. Wollmer, A fuel management model for airline industry, *Inform*, Vol. 40, No. 2, (March-April 1992), p.p. 229-237.
- [10]. Pedro Miguel Faria Pereira, Regional Airline's Operational Performance Study and Appropriate Enhancement Techniques, Master of Aerospace Engineering Thesis Work, October, 2009, 1-70.
- [11]. Raffi Babikian, Stephen P. Lukachko, and Ian A. Waitz, The Historical Fuel Efficiency Characteristics of Regional Aircraft from Technological, Operational, and Cost Perspectives, *Journal of Air Transport Management*, Vol. 8, 2002, pp. 389-400.
- [12]. Joosung J. Lee, Can We Accelerate the Improvement of Energy Efficiency in Aircraft Systems? *Energy Conservation and Management*, 51, (2010), 189-196.
- [13]. Megan S. Ryerson and Hyun Kim (2013), Integrating airline operational practices into passenger airline hub definition, *Journal of Transport Geography*, Volume 31, July 2013, pp. 84–93.
- [14]. Ryerson, M.S., Hansen, M. 2010. The Potential of Turboprops for Reducing Aviation Fuel Consumption. *Transport. Res. Part D: Transport and Environment*, Volume 15, Issue 6, pp. 305-314.
- [15]. Oster, C. V., Jr., and A. McKey. 1984. The cost structure of short-haul air service. In *Deregulation and the new airline entrepreneurs*, ed. John R. Meyer and Clinton V. Oster, Jr. Cambridge: MIT Press.
- [16]. Zou B., Elke M., Hansen M., and Kafle N., (2014), Evaluating air carrier fuel efficiency in the US airline industry, *Transportation Research Part A* 59, pp. 306–330.
- [17]. Burke E., et al. (2010), a multi-objective approach for robust airline scheduling, *Computers & Operations Research* 37(2010), pp. 822 – 832.
- [18]. Stojkovic G. et al. (2002), an optimization model for a real-time flight scheduling problem. *Transportation Research Part A* 36 pp. 779–788.
- [19]. Stojkovic, M., Soumis, F., Desrosiers, J., 1998. The operational airline crew-scheduling problem. *Transportation Science* 32 (3), 232–245.
- [20]. Teodorovic, D., Guberinic, S., 1984. Optimal dispatching strategy on an airline network after a schedule perturbation. *European Journal of Operational Research* 15, 178–182.
- [21]. Teodorovic, D., Stojkovic, G., 1990. Model for operational daily airline scheduling. *Transportation Planning and Technology* 14, pp. 273–285.
- [22]. Krishnamurthy, N., 1991. Models for irregular operations at United Airlines. *AGIFORS Proceedings* 31, pp. 81–95.
- [23]. Jarrah, A.I.Z., Yu, G., Krishnamurthy, N., Rakshit, A., 1993. A decision support framework for airline flight cancellations and delays. *Transportation Science* 27, pp. 266–280.
- [24]. Richetta, O., Odoni, A.R., 1993. Solving optimally the static ground-holding policy problem in air traffic control. *Transportation Science* 27 (3), 228–238.
- [25]. Richetta, O., Odoni, A.R., 1994. Dynamic solution to the ground-holding problem in air traffic control. *Transportation Research* 28 (3), 167–185.
- [26]. Bertsimas, D., Stock, S., 1995. The air traffic flow management problem with enroute capacities. Working Paper, Operations Research Center, Massachusetts Institute of Technology.
- [27]. Luo, S., Yu, G., 1997. On the airline schedule perturbation problem caused by the ground delay program. *Transportation Science* 31 (4), 298–311.
- [28]. Hoffman, R., Ball, M.O., 1997. A comparison of formulations for the single-airport ground holding problem with banking constraints. Working Paper, Institute for System Research, University of Maryland.

Prediction Performance of End-Milling Process by Gene Expression Programming

Mohammed T. Hayajneh^{*a}, Majid Abdellahia^b

^aIndustrial Engineering Department, Faculty of Engineering, Jordan University of Science and Technology

^bAdvanced Materials Research Center, Islamic Azad University, Najafabad Branch, Najafabad, Iran

Received 31 March, 2019

Abstract

In this study, two different gene expression programming models were applied to predict surface roughness of end milling. The differences between the two models were the number of genes, chromosomes, head size, and the linking function. To construct the models, 84 pair input-target data were collected by the experimental procedure, randomly parted into 60 and 24 data sets and then were trained and tested respectively by the suggested models. The spindle speed, cutting feed and depth of cut were the independent input parameters. According to these input parameters, the roughness of the surface in the end-milling process at different cutting conditions was predicted. The training and testing results in the gene expression programming models have presented an acceptable potential for predicting roughness values of end-milling in the considered range.

© 2019 Jordan Journal of Mechanical and Industrial Engineering. All rights reserved

Keywords: gene expression programming; end-milling; modeling; surface roughness;

1. Introduction

Surface roughness is one of the most common element measurements in the machining processes. Surface roughness is tangible parameter to quantify the quality of the machined surfaces. In machining processes, surface roughness is needed to be as low as possible. Modeling techniques for the prediction of surface roughness (Ra) can be categorized into three groups which are analytical models, experimental models and Artificial Intelligence (AI)-based models [1]. Analytical and experimental models can be developed by using predictable approaches such as the statistical regression technique. On the other hand, AI-based models are established using non-conventional methodologies such as Fuzzy Logic, Artificial Neural Network, Genetic programming, and gene expression programming (GP) [1].

Different fuzzy logic and artificial neural network schemes have been broadly used for the selection of the working conditions in machining processes [2-10]. Gene expression programming gained broad consideration due to its capability to model nonlinear relationships for input-output mappings. Several studies have employed gene expression programming models for building industry problems. Aldas et al. [11] developed a genetic operation tree to study the effect of machining parameters and reinforcement content on thrust force during drilling of hybrid composites. Sener and Kurtarn [12] employed a genetic algorithm to optimize process parameters for

rectangular cup deep drawing. Yeh and Lien [13] developed a genetic operation tree to predict concrete strength. Vijaykumar et al. [14] applied gene expression programming to control the parameter of bidirectional CFRP composite pipe.

In the present study, surface roughness as a performance indicator of end milling at different variations of spindle speed (N), cutting feed (F) and depth of cut (D) has been modeled by Gene expression programming. A total number of 84 data were collected from the experimental procedures, trained and tested using gene expression programming. The obtained results were compared by experimental ones to test the power of genetic programming for forecasting the surface roughness in the end milling process.

2. Experimental Procedure

The experiment used a Bridgeport end-milling machine. Eight 3/4" four-flute HSS cutting tools were used. Dry machining has been employed. The experiment was performed on aluminum work pieces [2]. Figure 1 shows the experiment setup. The cutting parameters were set as: four levels of spindle speed (750, 1000, 1250, 1500 rpm), seven levels of feed rate (150, 225, 300, 375, 450, 525, 600 mm/min), and three levels of depth of cut (0.25, 0.75, 1.25 mm). In this experimental study, the roughness measurements for surfaces were repeated three times using micro-meters. The measured surface roughness was the response variable. The surface roughness data were

* Corresponding author e-mail: hayajneh@just.edu.jo.

collected randomly for each of the 84 machining conditions defined by the levels of independent variables. Among 84 collected experimental sets, 60 sets were randomly chosen as a training set for the genetic programming models (Table 1) and the remaining 24 sets were used as testing the generalization capability of the proposed models (Table 2).

3. Genetic Programming and Gene Expression Programming Theory

Genetic programming (GP) is proposed by Koza [15]. It is a generalization of genetic algorithms (GAs) [16]. Genetic programming attempts to use computer programs as its data representation. Similarly, to GA, GP needs only the problem to be defined. Then, the program searches for a solution in a problem-independent manner [16]. Genetic programming breeds computer programs to solve problems by implementing the following three steps:

1. Create an initial population of random compositions of the functions and terminals of the problem.
 2. Execute iteratively the following sub steps until the termination criterion has been satisfied:
 - Execute each program in the population and allocate the fitness value using the fitness measure.
 - Create a new population of computer programs by applying the following operations: Reproduction: (i) Copy an existing program to the new population, (ii) Crossover: Generate new offspring program(s) for the new population by remerging arbitrarily chosen parts of two existing programs and (iii) Mutation. Create one new offspring program for the new population by arbitrarily changing a randomly chosen part of one existing program.
 3. The program that is categorized by the method of result designation is selected as the result of the genetic programming system for the run. This result may be a solution (or approximate solution) to the problem [16].
- A flowchart of a typical Genetic programming algorithm is revealed in Figure 2 [17]. The genetic programming approach progresses through the action of three basic genetic operators: reproduction, crossover, and mutation. In the reproduction stage, an approach must be implemented as to which programs should die. In the implementation, a small proportion of the trees with the worst fitness are killed. The population is then filled with the surviving trees according to accepted selection mechanisms, as explained by Sarıdemir [17]. Crossover swamps randomly selected parts of two trees to join good information from the parents and to develop the fitness of the next generation, as shown in Figure 3 [16]. Mutation protects the model against premature convergence and develops the non-local properties of the search, as shown in Figure 4 [16]. Sometimes, one randomly selected node is interchanged by another one from the same set, except itself.

In applying genetic programming with automatic function definition to solving a problem, five major preparatory steps are used. These steps involve determining terminal set, function set, fitness function, control parameter and termination criteria [18].

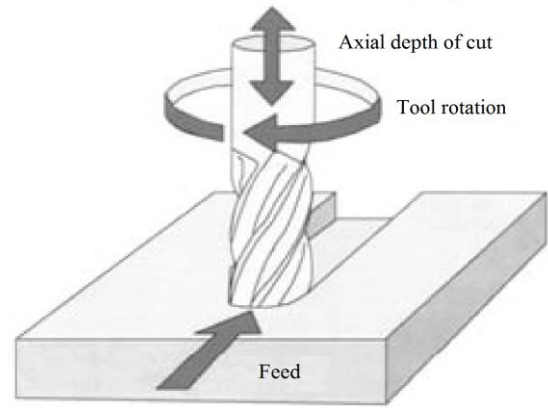


Figure 1. A schematic representation of an end-milling system [2].

Table1. Effect of machining parameters on the surface roughness (training set data set) [2].

No.	N RPM (rpm)	F (mm/min)	D (mm)	Ra (µm)	No.	N (rpm)	F (mm/min)	D (mm)	Ra (µm)
1	750	525	1.25	3.7	31	1000	600	0.25	4.1
2	1250	300	1.25	2.4	32	1500	150	0.25	1.3
3	1000	375	0.25	2.6	33	750	375	1.25	2.6
4	750	600	1.25	4.4	34	1500	525	1.25	3
5	750	300	0.75	2.6	35	1250	300	0.25	2.6
6	1500	375	1.25	2.5	36	1000	300	0.25	3.1
7	1250	450	1.25	2.3	37	1500	225	0.25	1.4
8	1000	300	1.25	2.3	38	750	225	0.75	2.6
9	750	150	1.25	1.9	39	750	150	0.75	1.7
10	1500	600	0.75	2.6	40	750	525	0.75	4
11	1500	450	0.25	3.2	41	1000	600	0.75	4
12	1000	450	0.25	4	42	1250	150	1.25	1.7
13	750	375	0.75	3.1	43	1000	375	0.75	2.6
14	1250	600	0.25	3.8	44	1250	300	0.75	2.5
15	1250	225	0.75	2.1	45	1000	225	0.75	2.4
16	1000	150	1.25	1.6	46	1500	300	0.75	2.1
17	1000	300	0.75	2.1	47	1000	525	0.75	3.9
18	750	450	1.25	3.3	48	1250	225	0.25	2.1
19	1500	600	0.25	3.2	49	1000	150	0.75	1.9
20	1250	525	0.75	2.5	50	1250	375	0.75	2.5
21	1500	450	1.25	2.6	51	1000	150	0.25	1.6
22	750	600	0.75	4.5	52	1000	225	1.25	2.7
23	1000	525	0.25	3.8	53	750	225	1.25	2.5
24	750	300	1.25	2.4	54	1250	450	0.75	2.2
25	1500	225	0.75	1.9	55	1500	300	0.25	2.3
26	1250	150	0.25	1.2	56	750	450	0.25	4.8
27	1250	525	1.25	2.5	57	1250	600	0.75	2.6
28	1250	375	1.25	2.5	58	750	525	0.25	4.5
29	1000	225	0.25	2.3	59	1250	225	1.25	2.4
30	1000	450	0.75	3	60	1250	150	0.75	1.7

Table 2. Effect of machining parameters on the surface roughness (testing set data set) [2].

No.	N (rpm)	F (mm/min)	D (mm)	Ra (µm)	No.	N (rpm)	F (mm/min)	D (mm)	Ra (µm)
1	1000	450	1.25	2.1	13	1250	600	1.25	3.1
2	1500	150	1.25	1.5	14	1250	375	0.25	2.7
3	750	300	0.25	3	15	1000	600	1.25	2.1
4	750	450	0.75	3.7	16	1500	300	1.25	2.4
5	1000	375	1.25	2.6	17	1500	525	0.75	2.6
6	750	225	0.25	2.1	18	1500	525	0.25	3.1
7	1500	375	0.25	2.7	19	1500	600	1.25	3.2
8	1250	525	0.25	3.1	20	750	150	0.25	1.6
9	1500	450	0.75	2.3	21	1250	450	0.25	2.5
10	750	600	0.25	4.7	22	1500	150	0.75	1.4
11	1500	375	0.75	2.1	23	1000	525	1.25	1.5
12	750	375	0.25	3.2	24	1500	225	1.25	1.8

Genetic programming (GP) has two principal elements such as the chromosomes and the expression trees (ETs). The chromosomes may be involved in one or more genes which refer to a mathematical expression. The mathematical code of a gene is identified in two different languages called Karva Language [16]; such as the language of the genes and the language of the expression trees (ETs). The genes have two main parts addressed as the head and the tail. The head comprises some mathematical operators, variables and constants (+, -, *, /, √, sin, cos, 1, a, b, c) which are used to encrypt a mathematical expression. The tail just comprises variables and constants (1, a, b, c) named as terminal symbols. Additional symbols are used if the terminal symbols in the

head are insufficient to define a mathematical expression. A simple chromosome as a linear string with one gene is encrypted in Figure 5. Its ET and the corresponding mathematical equation are also shown in the same figure. The translation of ET to Karva Language is done by starting to read from left to right in the top line of the tree and from top to bottom. The arrangements of genes used in this method are like the arrangements of biological genes and have coding and non-coding parts. On the other hand, more complex mathematical equations are defined by more than one chromosome denoted to multigenic chromosomes. Joining the genes is done by combining functions such as addition, subtraction, multiplication, or division [18].

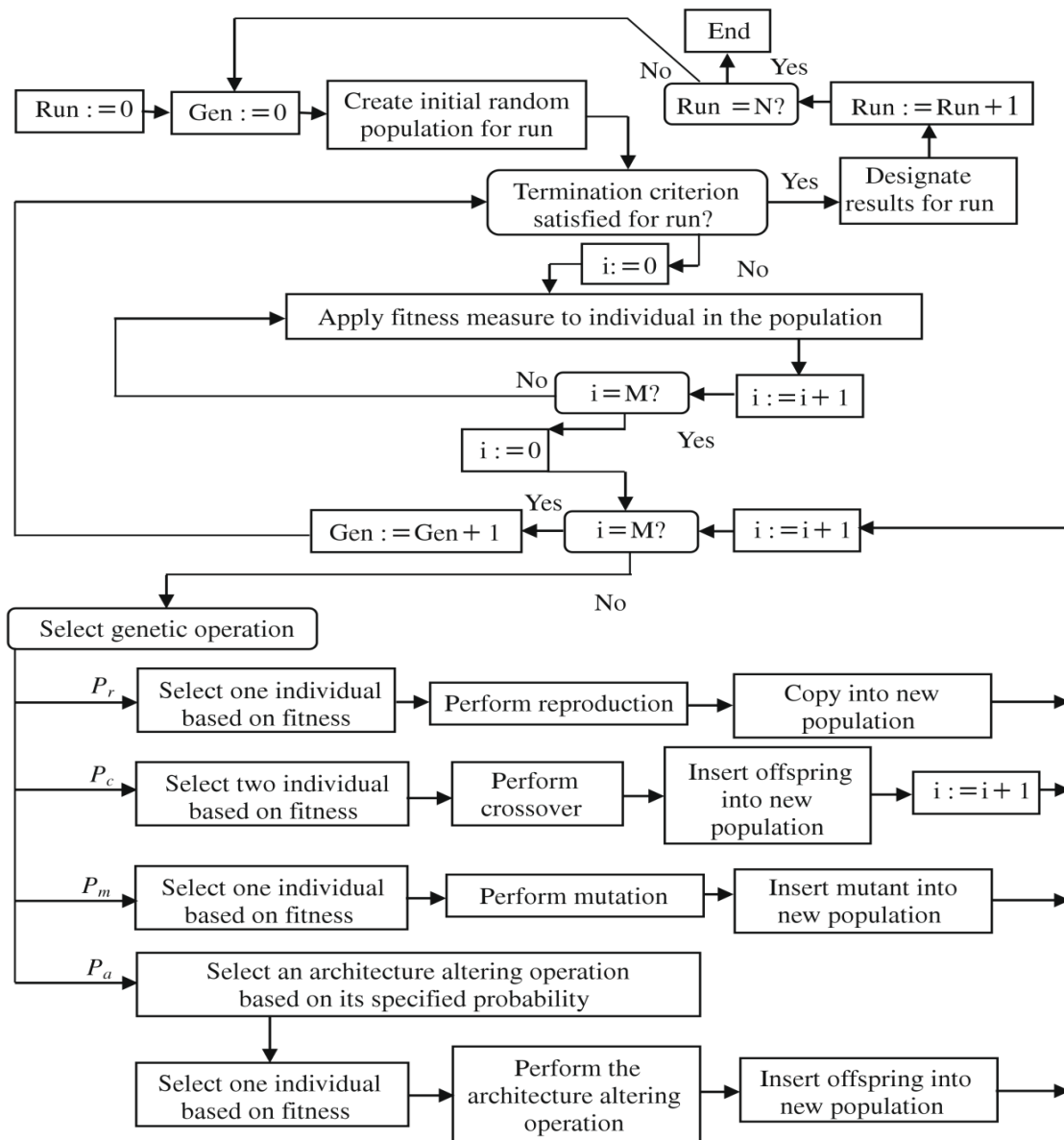


Figure 2. Genetic programming flowchart.

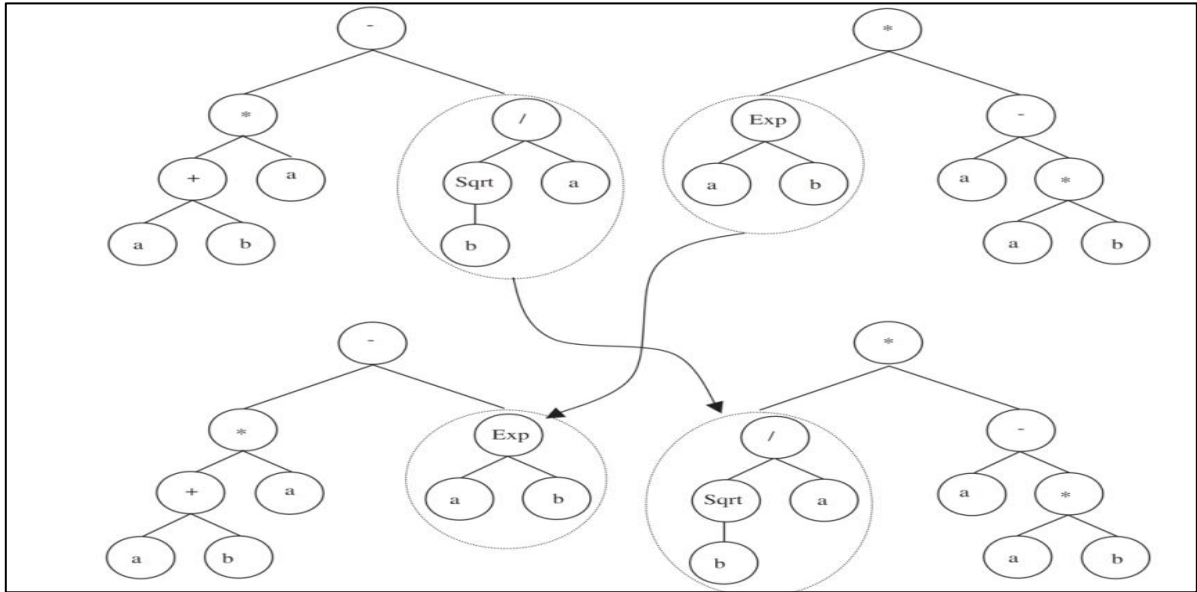


Figure 3. Example of genetic programming crossover

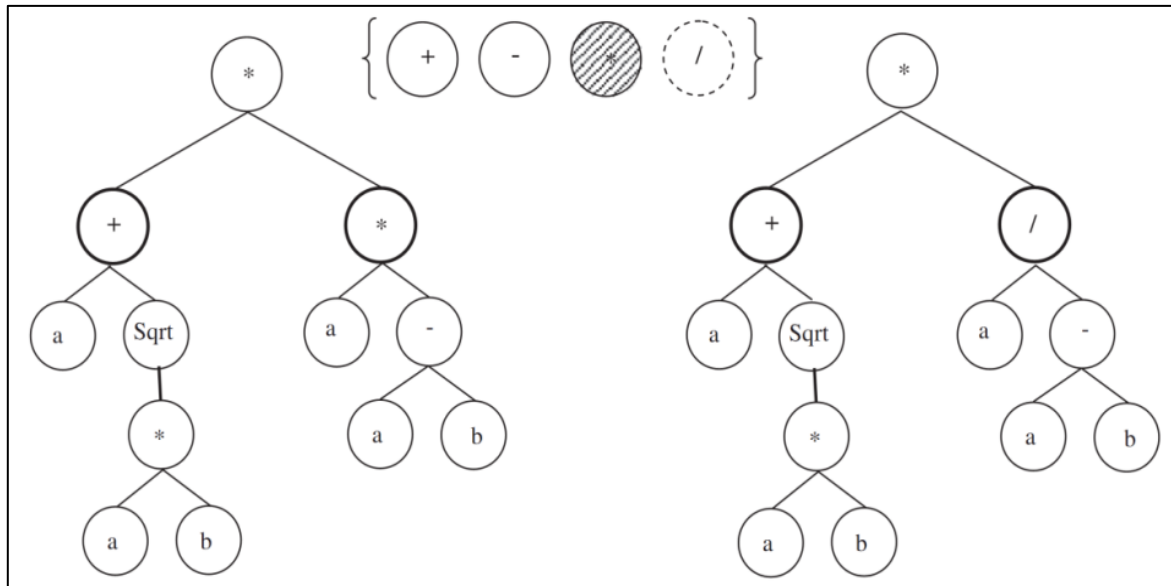


Figure 4. Example of genetic programming mutation

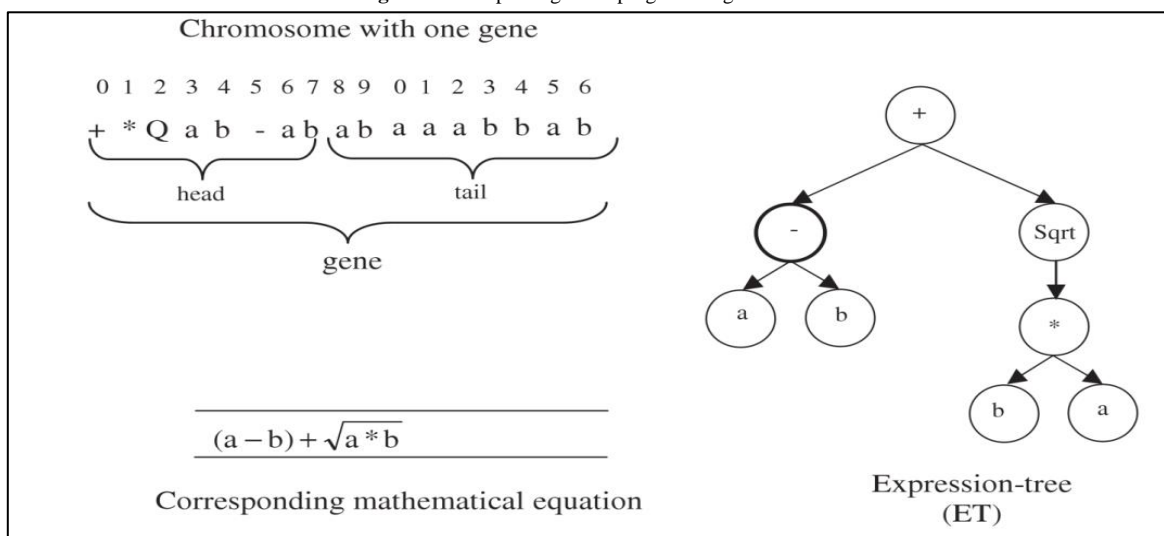


Figure 5. Chromosome with one gene and its expression tree and corresponding mathematical equation

4. Gene Expression Programming Structure and Parameters

In this study the expression trees of two different genetic programming models which were termed GP-I and GP-II were constructed for Ra values of the end-milling process. In the GP-I and GP-II, the number of genes was six and seven (Sub-ETs), and linking function was addition and subtraction, respectively. In the training and testing of GP-I and GP-II models, N, F and D were considered as input data and Ra as independent output data. Among 84 experimental sets, 60 sets were arbitrarily selected as a training set for the GP-I and GP-II modeling and the remaining 24 sets were used as testing the generalization capacity of the proposed models.

For the genetic programming-based formulations, the first is to select the fitness function. For this problem, firstly, the fitness, f_i , of an individual program, i , is measured by Eq. (1):

$$f_i = \sum_{j=1}^{C_t} (M - |C_{(i,j)} - T_j|) \quad (1)$$

where M is the range of selection, $C_{(i,j)}$ is the value returned by the individual chromosome i for fitness case j (out of C_t fitness cases) and T_j is the target value for fitness case j . If the precision $|C_{(i,j)} - T_j|$ is less than or equal to 0.01, then the precision is equal to zero, and $f_i = f_{max} = C_t M$. In this case, $M = 100$ was used, therefore, $f_{max} = 1000$. The benefit of this type of fitness functions is that the systems can find the best solution for itself. The second significant step makes up by selecting the set of terminals T and the set of functions F to generate the chromosomes. In this problem, the terminal set comprises clearly of the independent variable, i.e., $T = \{N, F \text{ and } D\}$. The select of the proper function set is not so obvious, but an appropriate guess can always be done to include all the required functions. In this situation, four basic arithmetic operators (+, -, *, /) and some basic functions (Sqrt, x^2 , x^3 , ln, sin, cos, Arctan, Exp) [19].

The third important step is to determine chromosomal tree, i.e., head length and number of genes. Genetic programming-based formulations firstly use single gene and lengths of 2 heads, and increase the number of genes and heads, one by one while running, and examined the training and testing performance for each formulation [19]. In this study, after several trials, for all the genetic programming-based formulations, number of genes and the length of the head designed as given in table 3. The fourth major step is to choose the linking function. For GP-I and GP-II models, addition and subtraction were created for linking functions, respectively.

Finally, a combination of all genetic operators (mutation, transposition and crossover) was employed as

$$R_{a(GP-I)} = \frac{(\sin(-1.36) + \ln N) + (N^3 \times \ln 2.88)}{\sqrt{F}} + \frac{\cos(D+F-8.93)}{(\tan^{-1} 8.93 - \cos D)(-6.05N)} + \frac{\sqrt{F}}{\ln((N \tan^{-1} 0.34)(D-F) - 9.92)} + \frac{\cos(((N+F) - 584.27)(N \cos -7.17))}{\ln D} + \frac{\cos((F+4.42)(1.26N))}{(\sqrt{4.42-4.42N})(3.50)} - 1.68 + \tan^{-1}(\sqrt{148.03 \tan^{-1} N + \sin F^3}) \quad (6)$$

$$R_{a(GP-II)} = \frac{((9.92-F)N)^2}{2(D-F)} - \sqrt[3]{N} - (\sqrt[3]{2D-9.74})(\ln F - \sqrt[3]{F}) - \exp^{\frac{1}{3}}(\sin N + \cos(93.89N)) - \cos^3 F - \frac{(\cos(7.35+D))(F-9.96)}{(D-9.96)\sqrt[3]{N}} - \tan^{-1}\left(\left(\left((9.71-F) - 841.23\right) + (F/N)\right) - D\right) \quad (7)$$

set of genetic operators. At first, these parameters were well thought-out as the program defined values. Then they were increased step by step and the utmost performance network based on the R^2 values was considered. Parameters of the training of the GP-I and GP-II approach models are given in Table 4. For the GP-I and GP-II approach models, chromosome 32 and 42 were observed to be the best of generation individuals forecasting surface roughness. Explicit formulations based on the GP-I and GP-II approach models for R_a were attained by:

$$R_a = f(N, F, D) \quad (2)$$

The related formulations could be found by the procedure shown in Figure 5.

Table 3. Parameters of GP approach models

Parameter definition	GP-I	GP-II
Chromosomes	32	42
Head size	8	10
Number of genes	6	7
Linking function	addition	subtraction
Mutation rate	0.044	0.044
Inversion rate	0.1	0.1
One-point recombination rate	0.3	0.3
Two-point recombination rate	0.3	0.3
Gene recombination rate	0.1	0.1
Gene transposition rate 0.1	0.1	0.1
Constants per gene	5	5
Weight of functions	7	7
Lower bound	10	10
Upper bound	10	10

5. Results and Discussion

In the present study, in order to assess the capabilities of genetic programming-based formulations, formulas given by some national building codes and the established regression-based formulation, R-square (R^2), root-mean-squared error (RMSE) and mean absolute percentage error (MAPE) were used as the criteria between the experimental and predicted values which are according to the equations (3) – (5), respectively [19]:

$$R^2 = \frac{(n \sum t_i o_i - \sum t_i \sum o_i)^2}{(n \sum t_i^2 - (\sum t_i)^2)(n \sum o_i^2 - (\sum o_i)^2)} \quad (3)$$

$$RMSE = \sqrt{\frac{1}{n} \sum_{i=1}^n (t_i - o_i)^2} \quad (4)$$

$$MAPE = \frac{1}{n} \left[\frac{\sum_{i=1}^n |t_i - o_i|}{\sum_{i=1}^n t_i} \times 100 \right] \quad (5)$$

Where t is the experimental result, o is the obtained result by the formulations and n is the total of data. The related equations to GP-I and GP-II models are in accordance to equations (6) and (7), respectively:

The experimental and the predicted are shown in Figure 6. R-square (R^2), root-mean-squared error (RMSE) and mean absolute percentage error (MAPE) values were shown in Table 4 for the training and testing data. As shown in Figure 6, the results attained from the training and testing in GP-I and GP-II models are in good agreement with the experimental results. As seen in Figure 6a, b and c, d the predicted results from models are compared to the experimental results for training, testing and validation sets, respectively. The training set results demonstrated that the proposed models have remarkably well learned the non-linear relationship between the input and the output variables with high correlation and reasonably low error values. Comparing the GP-I and GP-II approach models' prediction with the experimental results for the testing and training stages proves a high generality capacity of the proposed models and low error values. All these findings show a successful performance of the models for predicting surface roughness in end-milling in training and testing stages. The result of testing phase in Figure 6 shows that the GP-I and GP-II models are capable of generalizing between input and output variables with reasonably good predictions. The performance of the GP-I and GP-II models is shown in Table 4. The best value of R^2 and the minimum value of MAPE and RMSE are 0.923, 0.268 and 0.219, respectively, all for training set in GP-I model. The minimum value of R^2 and the maximum value of MAPE and RMSE are 0.901, 0.339 and 0.471, respectively, all for testing set in GP-II model. The entire R^2 , MAPE and RMSE values show that the proposed GP-I and GP-II models are appropriate and can predict surface roughness

values of end-milling very close to the experimental values.

Table 4. Statistical calculations from GP-I and GP-II training and testing phases

Statistics	GP-I		GP-II	
	Training	Testing	Training	Testing
R^2	0.923	0.920	0.909	0.901
MAPE	0.268	0.314	0.296	0.339
RMSE	0.219	0.411	0.249	0.471

6. Conclusions

This study reports original and efficient models for the formulation of surface roughness in the end-milling process. Two different GP-I and GP-II models were proposed to forecast the roughness values in the end-milling process. The suggested models were based on experimental results. The number of genes in the proposed GP-I and GP-II models was 6 and 7, and the linking functions were addition and subtraction, respectively. All the results attained from the models exhibit excellent agreement with experimental results. The best value of R^2 and the minimum value of MAPE and RMSE are 0.923, 0.268 and 0.219, respectively, all for training set in GP-I model. The minimum value of R^2 and the maximum value of MAPE and RMSE are 0.901, 0.339 and 0.471, respectively, all for the testing set in GP-II model. It was found that GP can be a substitute approach for the assessment of the performance of end-milling process and can calculate their surface-roughness value with suitable input parameters.

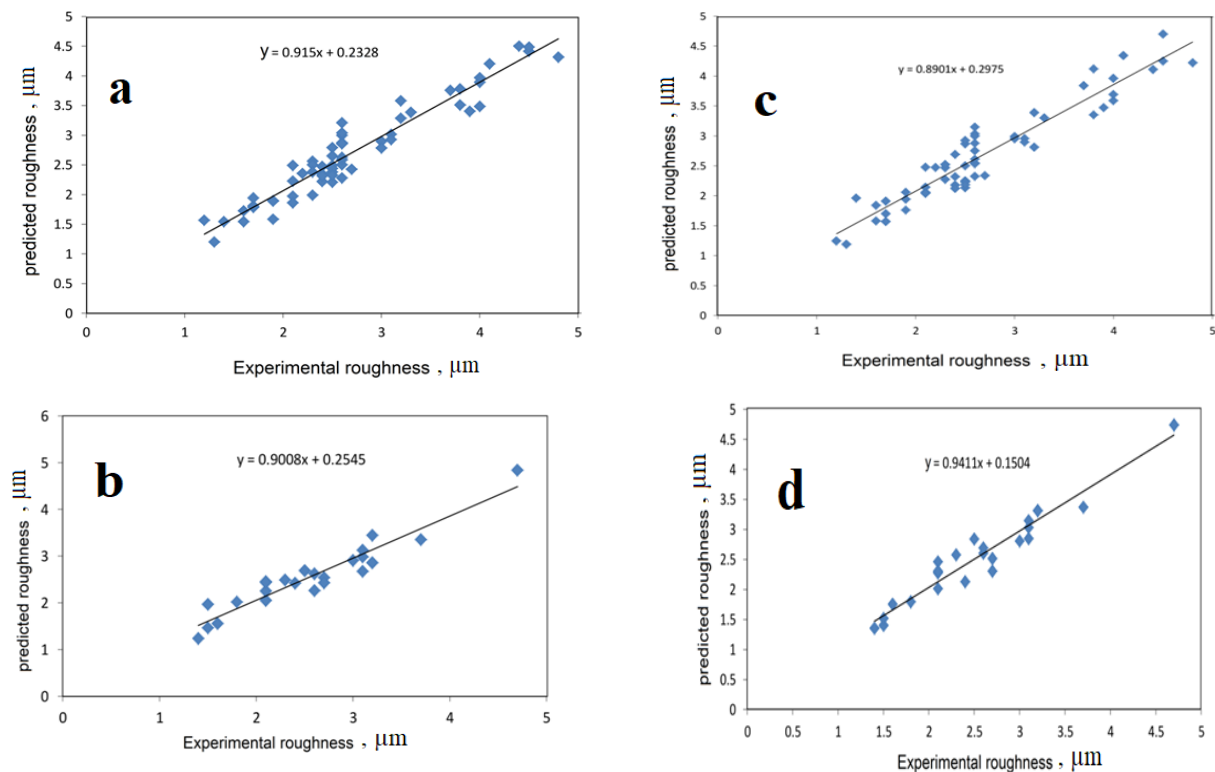


Figure 6. The results obtained from experimental studies and predicted (Model) by using the training and testing results of GP-I and GP-II models. Respectively, (a), (b) training and testing related to GP-I model; (c), (d) training and testing related to GP-II model

References

- [1] P. Benardos and G. osnaikos, Predicting surface roughness in machining: a review. *International Journal of Machine Tools and Manufacture*, vol. 43, No.8, pp. 833–844, 2003.
- [2] M. Hayajneh, M. Tahat, J. Bluhm, A Study of the Effects of Machining Parameters on the Surface Roughness in the End-Milling Process. *Jordan Journal of Mechanical and Industrial Engineering*, vol. 1, no. 1, pp. 1-5, 2007.
- [3] M. Hayajneh, S. Radaideh, Modeling surface finish in end milling process using fuzzy subtractive clustering based system identification method, *Materials and Manufacturing Processes*, vol. 18, no. 4, pp. 653-665, 2003.
- [4] M. Hayajneh, Fuzzy clustering model for surface finish prediction in fine turning process, *International Journal of Machining Science and Technology*, vol. 9, no. 3, pp. 437-451, 2005.
- [5] M. Hayajneh, S. Radaideh, Monitoring hole quality in drilling process using fuzzy subtractive clustering based system identification method, *Journal of Testing and Evaluation*, vol. 35, no. 3, pp. 297-302, 2007.
- [6] M. Hayajneh, A. Hassan, Modelling the machinability of self-lubricated aluminum/alumina/graphite hybrid composites using a fuzzy subtractive clustering-based system identification method, *International Journal of Machining and Machinability of Materials*, vol. 3, no. 3/4, pp. 252-271, 2008.
- [7] H. Al-Wedyan, M. Hayajneh, Prediction and controlling of roundness during the BTA deep hole drilling process: Experimental investigations and fuzzy modeling, *Materials Testing*, vol. 59, no. 3, 2017.
- [8] Hassan, A. Alrashdan, M. Hayajneh, A. Mayyas, Prediction of density, porosity and hardness in aluminum–copper-based composite materials using artificial neural network, *Journal of Materials Processing Technology*, vol. 209, no. 2, pp. 894-899, 2009.
- [9] M. Hayajneh, A. Hassan, A. Alrashdan, A. Mayyas: Prediction of tribological behavior of aluminum–copper based composite using artificial neural network, *Journal of Alloys and Compounds*, vol. 470, no.1, pp. 584-588, 2009.
- [10] M. Hayajneh, A. Hassan, A. Mayyas, Artificial neural network modeling of the drilling process of self-lubricated aluminum/alumina/graphite hybrid composites synthesized by powder metallurgy technique, *Journal of Alloys and Compounds*, vol. 478, no.1, pp. 559-565, 2009.
- [11] K. Aldaş , I. Özkul and M. Hayajneh, Effects of machining parameters and reinforcement content on thrust force during drilling of hybrid composites, *Materials Testing*, vol. 58, no. 3, pp.280-284, 2016.
- [12] Sener and H. Kurtaran, Optimization of process parameters for rectangular cup deep drawing by the Taguchi method and genetic algorithm, *Materials Testing*, vol. 58, no.3, pp. 238-245, 2016.
- [13] Yeh, L. Lien L, Knowledge discovery of concrete material using Genetic Operation Trees. *Expert Systems with Applications*, vol. 36, no.3, pp. 5807-5812, 2009.
- [14] K. Vijaykumar, K. Panneerselvam, and A. Naveen Sait, Machining parameter optimization of bidirectional cfrp composite pipe by genetic algorithm, *Materials Testing*, vol. 56, no.9, pp. 728-736, 2014.
- [15] J. Koza, Genetic programming as a means for programming computers by natural selection. *Statistics and Computing*, vol. 4, no.2, pp. 87-112, 1994.
- [16] Kara, Prediction of shear strength of FRP-reinforced concrete beams without stirrups based on genetic programming. *Advances in Engineering Software*, vol. 42, no.6, pp. 295-304, 2011.
- [17] M. Saridemir, Genetic programming approach for prediction of compressive strength of concretes containing rice husk ash, *Construction and Building Materials*, vol. 24, no.10, pp. 1911-1919, 2010.
- [18] M. Khan, A. Alam, Survey of application, genomics and genetic programming, a new frontier, *Genomics*, vol. 100, no.2, pp. 65-71, 2012.
- [19] M. Saridemir, Empirical modeling of splitting tensile strength from cylinder compressive strength of concrete by genetic programming, *Expert Systems with Applications*, vol. 38, no. 11, pp. 14257-14268, 2011.

Ergonomic Computer Workstation Design for University Teachers in Bangladesh

Md. Golam Kibria*, Md. Rafiquzzaman

Department of Industrial Engineering and Management, Khulna University of Engineering & Technology, Khulna- 9203, Bangladesh

Received 18 May, 2019

Abstract

The ever-growing use of computer in universities due to instructional, administrative, research and study is noticed among the teachers. Prolong sitting-work on the computer workstation causes various pains, discomforts and health related problems. The aim of this study is to design an ergonomic computer workstation to reduce the health-related problems. A Self-reported Nordic questionnaire was developed for conducting ergonomic assessment among 265 participants to evaluate health conditions. Moreover, to determine the potential mismatch, 12 anthropometric measurements and existing furniture dimensions was measured and evaluated. Results showed that most of the teachers were suffered from different types of musculoskeletal disorders (MSDs), particularly, lower back pain and neck pain. Significant numbers of mismatches were found between furniture dimensions and anthropometric measurements. It can be concluded, presence of the musculoskeletal disorders would be the reason of inappropriate furniture dimensions. Finally, an ergonomic computer workstation was proposed by considering anthropometric measurements and guidelines to reduce the musculoskeletal disorders among the teachers. This research can contribute a lot for ergonomic furniture design to the university as well as other organizations and create a sense to overcome the ergonomic problems.

© 2019 Jordan Journal of Mechanical and Industrial Engineering. All rights reserved

Keywords: Anthropometry, Ergonomics, Musculoskeletal Disorders, Computer Workstation;

1. Introduction

Ergonomics is a holistic and human–systems approach for work systems design by considering cognitive, organizational, physical, environmental and other factors [1]. Applications of ergonomic principles improve human-computer interaction and enhance comfort, health and safety of the users [2]. Basically productivity, performance improvement prevention of injuries and fatigue reduction are the main concern of the ergonomics [3]. These objectives are achieved by changing the worker job interface such as work process, work environment, work management and tools [4]. Therefore, it is essential to design an ergonomically adjustable workstation to prevent repetitive body movements, awkward postures and static forces in both sitting and viewing position. Ergonomically designed workstation refers to the proper seat height, desk height, proper placement of monitor, and consider environmental factors, such as proper lighting intensity and noise level [5]. Chair is the vital element that needed to design ergonomically which is adjusted as required to the user intension, comfortable and able to maintain natural postures. Principles of ergonomics suggests working with natural postures, keep work element within easy reach, work at proper heights, minimizing pressure points, provide clearance, work with comfortable weather

[6]. Ergonomic design can be achieved through anthropometric measurements. Anthropometry refers to the scientific measurements of different body parts of the human [7]. It is not feasible to design a work system or equipment that suitable for everyone. Generally, it is targeted that about 90% user can suit with this system. Therefore, to accommodate 90% of the targeted population, it is required to consider 5th percentile of female and 95th percentile of male anthropometry data. Anthropometry is not universal; it is varied among nations, ethnicities and regions. For example, a design of a product for a certain targeted nation may not match with other nations. Anthropometry is vital element to design and modify of product and service [8]. Three basic ergonomics design principles are design for extreme individual, design for average and design for adjustability. Design for extreme individual principle based on 95th percentile of male (maximum population), or 5th percentile of female (minimum population) anthropometric data [9]. Most of the researchers use design for adjustability principle for furniture design [10, 11] and it is based on 5th percentile of female and 95th percentile of male anthropometric data covers 90% of the population [12, 13]. Third principle is design for average whenever adjustability is impractically not possible though it is widely used [14]. Workstation furniture is the vital element that needed to design ergonomically which is adjusted as required to the user

* Corresponding author e-mail: kibria.ipekuet@gmail.com.

intension, comfortable and able maintain natural postures. Design for adjustability principle play vital role for designing ergonomic adjustable furniture that ensures users to work with natural postures, keep work element within easy reach, work at proper heights, minimizing pressure points, provide clearance, and work with comfortably without any discomforts [6]. So, adjustability principle was recommended to design workstation furniture in the current study. Previous studies showed that most of the researchers used adjustability principle to design [10, 11, 14, 15].

In modern world, computer is an integral part of the office. Due to advanced technology and software, computer use in official work is continually increasing. Poor designed workstation and its use are responsible for MSDs and safety problems. Not only visual discomforts and disturbances, but also MSDs problems in neck and shoulders are key problems experienced by the computer users [16]. Moreover, bad postures are the main reason of Musculoskeletal Disorders [17]. Researchers investigated the design parameters of workstation found health related problems among the users. A study was carried out to assess the risks associated with musculoskeletal discomforts by conducting survey among the 292 VDT (Video Display Terminal) users [18]. Results show that MSDs symptoms were observed among different body regions associated with participants. Moreover, researchers concluded improper setting of monitors and keyboards were associated with eye, head, shoulders and back discomforts [18]. Another investigation was carried out to compare postures and muscles patterns among the 40 males and female computer users and found significant differences in both speed typing and repetitive mouse tasking among male and female participants [19]. Furthermore, significant postural variations were observed between genders though chairs and desks of anthropometrically and ergonomically adjusted for both male and female participants. Park et al. (2000) compared discomfort level between adjustable demo chair and conventional chair and concluded that adjustable VDT workstation reduces the discomforts [20]. Straker et al. (2008) investigated neck and upper limb postures of young male and female participants and concluded that no consistent evidence was found between forearm support and posture [21]. Researchers showed that inappropriate design workstation and its use were responsible for shoulder and neck pain [2]. In addition, placement of keyboard above or below the user's elbow height was introduced arm discomfort. Sauter et al. (1991) investigated neck and shoulder pain and suggested the necessity for controlling cervicobrachial pain syndromes in VDT users [22]. The cross-sectional study was conducted by Xue et al. (2013) to evaluate ergonomic hazards of computer workstations among 90 two groups: office and cubicle workers. Neck, shoulders, hands/wrists, upper and lower back discomforts were reported by the workers. It also concluded that the office workers suffered much more neck pain than the cubicle workers, due to an association between longer working computer usages and the frequency of experiencing discomfort [23]. Another research was conducted by lale et. al (2013) to investigate the impact of musculoskeletal discomforts on office workers. They proposed ergonomic computer workstation

based on user's anthropometric measurement to solve the costly health related problems and lost productivity due to perceived musculoskeletal discomfort and relieving the imposed economic burden [24].

When the body dimensions and furniture dimensions are not matched, user feels uncomfortable while sitting, this phenomenon is term as mismatch [25]. Castellucci et al. (2010) conducted a study to evaluate the mismatch between furniture dimension and student anthropometry and found potential mismatch in different dimensions of furniture [26]. Another study conducted in Greece and found high degree of mismatch for seat height and desk height dimensions [27]. The study of Kane et al. (2006) revealed 96% mismatch between furniture dimensions and student's anthropometry [28]. Another study was conducted by Rosyidi et al. (2016) to investigate the mismatch between furniture dimension and student anthropometry and found high percentages of mismatch in three chair and two desk dimensions [29].

On the other hand, researchers recommended ergonomic guidelines and suggestions to solve the ergonomic problems. Workstation furniture is the vital element that needed to design ergonomically which is adjusted as required to the user intension, comfortable and able maintain natural postures. Ergonomically furniture (Chair and Desk) design means design the seat parameters like seat height, seat depth, seat width, backrest, armrest and desk height by considering users anthropometric measurements and ergonomic principles. Haque et. al (2014) considered eleven anthropometric measurements to design ergonomic workstation furniture and these measurements were stature, sitting height, sitting shoulder height, politeal height, sitting elbow height, hip breadth, buttock politeal length, knee height, shoulder breadth and sitting eye height [30]. Design nature of Seat parameters affects the sitting postures of user while sitting [31]. Postural dynamics of users is important element of workstation design that significantly affected by human-computer interface [17][17]. A proper workstation setup is necessary due to use of prolong hours of deskbound computer and routine works [32]. Work postures are affected different parameters like Seat height, Seat depth, Keyboard-to user distance, Monitor height, Monitor-to-user distance, thigh clearance, task lighting etc[33]. Researcher showed that the pressure on legs were greatly reduced by using well height adjusted, rounded edged seat pan [34]. Seat height should be determined in such way that feet freely touch on the floor. However, most of the guidelines suggested that knee bent would be 90 degree with lower leg while seating[35].Haworth (2008) suggested that seat height and seat depth should be adjusted to accommodate large population from 5% female to 95% male user [31]. Seat pan angle is also play a vital role and to reduce MSDs. Researchers found that 10 degree forwarded seat pan angle reduces 30 % intra-disc pressure and concluded that more than 15% inclination of seat pan angle increases muscular tension [36]. Naqv (1994) recommended 15° forward slope of seat pan angle to reduce the intra-disc pressure [37]. Researchers suggested that backrest should be tall and wide sufficiently [38]. Grandjean (1984) recommended 50 cm height and 48 cm width of the backrest to compatible with male anthropometry [39]. Researchers suggested backrest

inclination angle from 90° to 110° are reduce the disc pressure. Another study recommended that backrest inclination angle should be 90° to 120° [40]. Armrest is also an important parameter of chair and it should be appropriately adjusted and well-padded that will support the forearms and elbows to reduce extra pressure exerted on undersides both forearms and elbows [15]. Another study recommended that the length of armrest will be 25.5 cm from the back of the chair [34]. Other researcher Tijerina (1984) suggested that length, width and height should be 44 cm, 6-9 cm, and 18-23 cm (above from the seat pan) respectively [41]. Desk height and seat height should be adjustable in relation to suitable keyboard-forearm relation and adequate leg room [42]. Proper position of display is essential to prevent neck and visual problems. One study recommended that preferable viewing distance should be 63 to 85 cm[40]. Sommerich et al. (2001) investigated the trade-off between visual and musculoskeletal strain and proposed a u-shaped model to maintain viewing angle from 0° to 45° while using computer [43]. Another study suggested the viewing angle range from 15° to 25° below gaze inclination [44].

Ever growing use of computer in everyday life increases the risks of musculoskeletal disorders and visual problems. Various national and international standards and guidelines for computer workstation design have developed around the world to counter these problems[45]. International Organization for Standardization ISO-9241[46] and Occupational Safety and Health Administration, OSHA (2008) [47] are the two international standards. The prominent national standards are Canadian Standard Can/CSA Z412-M89 (Canada) [48], American Standard ANSI/HFES-100 (United States), and Australian Standard AS-3590.2 (Australia) [49], whereas national guidelines are Australian National Code of Practice for the Prevention of Occupational Overuse Syndrome and A Guide to Work with Computers published by the Labor Department (Hong Kong). Europe, Australia, America and other developed countries continuously active in endorsing and participating in ergonomics standards development. Unfortunately, there are no established ergonomic standards in Bangladesh. In the current study, worldwide prominent computer workstation guidelines were followed to design the proposed computer workstation.

The common and widely recognized guideline for furniture design is BIFMA (The Business and Institutional Furniture Manufacturer's Association) (BIFMA). BIFMA is a group that addresses common concerns in the furniture industry and provides office furniture design guidelines for fit and function [50]. Some furniture design standards have been recognized in various countries, for instance Colombia (ICONTEC 1999), Chile (INN 2002), the European Union (CEN 2012), Japan (JIS 2011) and the United Kingdom (BSI 2006) [25]. Yet not much has been done on office furniture and moreover, there are no established standards for Bangladeshi office furniture.

In Bangladesh, computer is an integral part of office used for different purposes such as, for internet browsing, emailing, chatting and other communicating purposes, especially for the university teachers. So, prolonged period (average more than 6 hours per day) is spend in front of computer with inappropriate sitting postures to do research

and other academic activities. They are associated with the risks of MSDs due to continuous computer usages. The furniture used by the teachers are manufactured by local producers and suppliers [30]. Suppliers mainly follow "one-size-fits-all" approach for making Most of the teachers are unaware about their sitting postures and surrounding environmental factors, and they do not take any institutional training on ergonomics and safety related issues furniture without considering user anthropometry. Thus, all users are not compatible with the furniture dimensions. This fixed and unadjusted furniture can lead to awkward postures. As a result, awkward postures lead to fatigue and discomfort in the different body parts of the furniture users [51]. A pilot study of Bangladesh health profession institution reported that 53% computer users are affected by lower back problems, and more than 30% of the users are affected by rest of form of MSDs problems due to absence of ergonomic intervention [52]. Users are affected not only by health risks, but also by financial losses [53]. A report of US labor department in 2013 showed that 20 billion of US dollars were spent as direct cost, and 100 billion US dollar on indirect cost for MSDs incidents (OSHA, 2014). There is no existence of cost related data and enough researches on MSDs in Bangladesh. So, all these incidents and information about their workstation is an alarming for the teachers and signifies the necessity of redesigning the existing workstation setup.

Although a lot of research work was done on computer workstation by considering postural, psychological and environmental factors which affect the musculoskeletal system of the user working in office, there were few of the studies solely address teacher's ergonomic problems around the world. As far the author's knowledge, very few studies were conducted on University teacher's ergonomic problems especially in developing country like Bangladesh. Therefore, aim of the research is to find out ergonomic problems among the university teachers, and design an ergonomic computer workstation by considering anthropometric measurements and following various ergonomic guidelines and suggestions to reduce the health-related problems.

2. Methodology

2.1. Participants

A Total of 265 university teachers from different engineering universities of Bangladesh with their demographical information shown in Table 1 participated in this research. Sample size was calculated by using one source [54].

$$n = N / (1 + Ne^2) \quad (1)$$

Where n is the sample size and N is the total population of the group and e is the degree of accuracy at 95% confidence level.

2.2. Ergonomic Assessment (Health Survey)

Ergonomic assessment was conducted among the teachers to evaluate the risk of WMSD (Work Related Musculoskeletal Disorder) Symptoms working as because of prolong sitting on their desk. A set of self-reported

Nordic questionnaire was developed by extensive literature review shown in the Appendices A. Musculoskeletal pain frequency was classified in the three categories, such as: “constantly” (most of time of the day) “occasionally” (two to four times a month) and “frequently” (more than four times a month). Prevalence of pain was measured with percentages of “Yes” and “No” reported by the participants.

Table 1. Demographical information of the participants

Biographical characteristics	Frequency, n	Percentage (%)
Age(years)		
23-30	158	59.62
31-40	63	23.77
41-60	44	16.60
Gender		
Male	200	65.33
Female	65	34.67
Employment Status		
Lecturer	122	32
Assistant Professor	65	30
Associate Professor	36	21.33
Professor	42	16.67

2.3. Anthropometric Measurements, Equipment and Procedures

Harpenden Anthropometer was used to measure the anthropometric dimensions of the participants. Consent of the participants was taken before the data collection process and participants were chosen had no physical disabilities. Standard sitting posture was maintained during measurements. Moreover, subjects were wearing less clothes without shoes. The measurements were taken with help of two research assistants, and they were trained for using measurements, tools and techniques. To ensure the accuracy and consistency of the recorded data, each dimension was taken three times and average value was recorded. Flowing anthropometric measurements were considered to design ergonomic furniture (chair, desk) shown in table 2. Fig.1 shows the anthropometric measurements and definitions of those dimensions were adopted from one source [55].

2.4. Furniture dimensions

Furniture dimensions such seat height, seat width, seat depth, backrest height, and seat to desk clearance, desk height were considered to evaluation in the current study and the definitions of the dimensions were adopted from one source [56].

Seat Height (SH): The vertically distance measured from front edge of seat to surface of the floor.

Seat Depth (SD): The horizontal distance measured from back of the seating surface to seat front.

Seat Width (SW): Distance measured horizontally from outer left side to the outer right side.

Backrest Height (BH): The vertical distance from the top side of the seat surface to the highest point of the backrest.

Desk Height (DH): The distance measured vertically from the front top edge of the desk to floor.

Seat to Desk Clearance (SDC): The distance measured vertically from top edge of the seat surface to underneath surface of the desk.

2.5. Furniture and body dimensions mismatch

Equations (2) to (7) were used to evaluate the potential mismatch between furniture dimension and user's anthropometric measurements. Six furniture dimensions were check against the anthropometric measurements shown in the Table 2.

Table 2. Anthropometric dimensions

S/N.	Anthropometric dimensions	Definition
1	Sitting height	It is the vertical distance measured from vertex to the sitting surface.
2	Sitting Shoulder Height	The distance measured vertically distance from the sitting surface to top of the shoulder.
3	Popliteal Height	Distance measured vertically with 90° knee flexion from footrest to popliteal surface of the knee.
4	Hip Breadth	It is the maximum horizontal distance across the hips when subjects in sitting position.
5	Sitting Elbow Height	It is the vertical distance from the sitting surface to bottom of the elbow.
6	Buttock-Popliteal Length	Distance measured horizontally With 90° knee flexion from posterior surface to buttock.
7	Buttock-Knee Depth	Distance measured horizontally With 90° knee flexion from knee cap to uncompressed buttock.
8	Thigh Clearance	Distance measured vertically from highest point on the top of the right thigh to sitting surface.
9	Sitting eye height	It is distance measured vertically from the sitting surface to the inner canthus (corner) of the eye.
10	Shoulder (bideltoid) breadth	It is the maximum distance between two deltoid muscles.
11	Sitting Knee Height	Distance measured vertically With 90° knee flexion from knee quadriceps muscles to footrest.

2.6. level of compatibility

To compare furniture dimensions with participants' anthropometric measurements, there are two types of equations i.e. one-way limit and two-way limits equations. Match and mismatch classifications were defined to measure compatibility by using one-way limit equation. For two-way relationships, three classifications were defined: (a) high mismatch (lowest limit of the relationship is greater than anthropometric measurement); (b) low mismatch (highest limit of the relationship is lower than anthropometric measurement); and (c) match (anthropometric measurement is between the limits).

2.7. Data analysis

The software SPSS 16.0 was used analysis the data. Therefore, different percentile values (5th, 50th, 95th), mean, standard deviation (SD), maximum (Max), minimum (Min) were calculated shown Table 6.

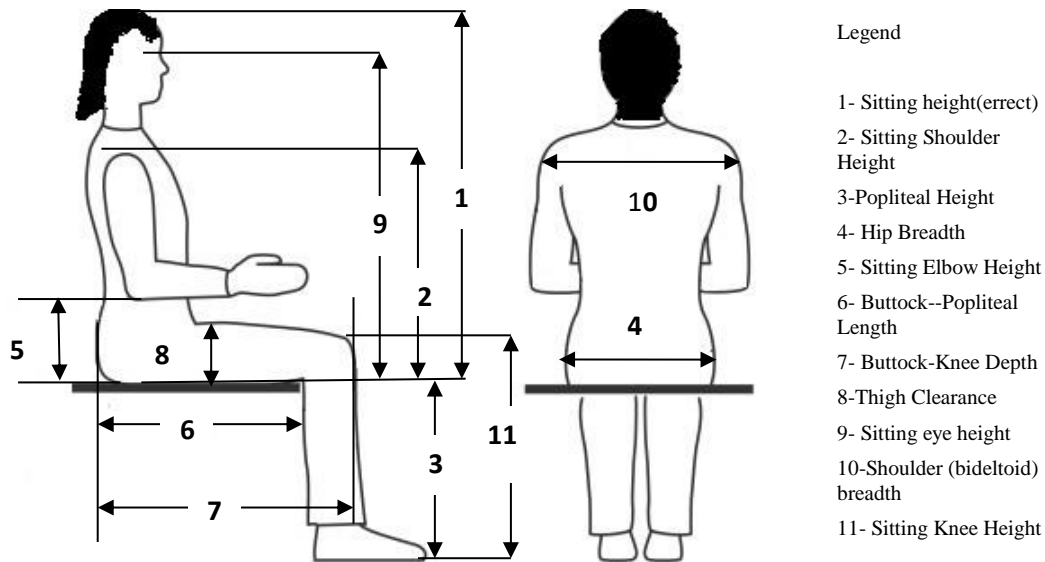


Figure 1. Anthropometric measurements

3. Results and Discussion

3.1. Ergonomic assessment (Health Survey) report

Table 4 shows MSDs frequency percentages among different body parts such as shoulder, wrist, neck, and ankle elbow regions reported by participants. No common presence of MSDs is found when it is observed in three separate categories. But the combination of occasional and frequent category shows the high frequencies percentage of pain. Majority of the participants (65.28%) experienced lower back pain. 58.49% participants suffered from neck pain whereas 48.3% participants reported that they were suffered by Hips/Buttocks/Thighs pain. 47.16%, 41.88%, 27.55%, 37.35% and 30.19% participants suffered from different kinds of pain on the body, such as shoulder/upper arm body, such as Shoulders/Upper arm, Upper back, Elbow/forearm, Knees and legs, and Feet/Ankles respectively. A few percentages of participants suffered from lower and upper back pains constantly. Frequently occurring pain in lower back, hips and neck were reported 33.20%, 33.321% and 30.56% respectively by the participants. This MSDs Prevalence is slightly higher compared to other study[57], and nearly similar to another study conducted in Bangladesh[52].

Prevalence of MSDs indicates that there were large percentages of incompatibility between user anthropometry and furniture dimensions. As a result, most of the users did not maintain the appropriate sitting postures while sitting and workstations setup were inappropriate and unadjusted for the users. However, incompatible furniture and unadjusted workstation setup leads to user discomfort for working activities it introduces to Musculoskeletal Disorders (MSDs) among different body parts. In the current study, 58.49% participants worked on their computer workstation more than 5 hours and 13.58% were spent their time more than 8 hours per day in computer related work (shown in Table 1). Many participants (155) did their regular computer related activities by spending 5-8 hours or more time per day. This prolonged sitting work, incorrect postures, and inappropriate workstation setup would be the reason of high frequency

of MSDs. Other studies showed that discomforts are the main reason of poor ergonomic workstation design, excessive hours of computer usage, continuous awkward sitting Postures, psychosocial environmental factors and longer work load [58, 57]. These findings were congruent with the current study. After the critical literature review, authors reached a conclusion that incorrect postures and inappropriate workstation setup were significantly associated with MSDs (shown in Table 5).

3.2. Anthropometric data analysis

Anthropometric data were analyzed in the form of different percentiles values (5th, 50th and 95th), average (Mean), standard deviation (SD), maximum (Max), minimum (Min), and shown in Table 6. From Table 6, average sitting height of the male participants was 85.21cm and 90% of the male participants cover the stature range from 79cm to 92.05cm (standard deviation 4.24cm). Similarly rest of the dimensions, Shoulder height(44.00-65.005 cm), popliteal height(42-52 cm), Hip breadth(29-47.47 cm), Elbow height(20-29.55 cm), Buttock-popliteal length(39.00-49.05 cm), Buttock-knee length(47-61 cm), Thigh clearance(11-25 cm), Eye height(58-81.16 cm), Shoulder (bilateral) breadth(36-51.05 cm) , Knee height(47-63.69 cm), covers the mentioned range . The highest standard deviations were found in case of sitting shoulder height and eye height that are respectively 7.37 cm and 6.69 cm respectively. In case of female data, sitting height (76.26-85.40 cm), Shoulder height(49.20-59.08 cm), popliteal height(32.68-46.18 cm), Hip breadth(, 30.72-48.21 cm), Elbow height(17.20-30.92 cm), Buttock-popliteal length(38.02-49.48 cm), Buttock-knee length(, 48.20-58.40 cm), Thigh clearance(9.76-15 cm), Eye height(64.06-73.32 cm), Shoulder (bilateral) breadth(34.60-50.80 cm) , Knee height(44.92-54.24) covers the mentioned range. The highest standard deviations were found in case of hip breadth and shoulder breadth that are 4.83 cm and 4.45 cm respectively. Finally, it can be concluded that all dimensions of male were higher than female except hip breadth. All data (male and female) statistically checked and found normally

distributed with strong nature of normal curve (shown in figure 3). As anthropometric regional variability is absence in Bangladesh, therefore collected data represents the whole country's anthropometric image of ages from 23-60.

3.3. Participant's Match and Mismatch History with Furniture

Table 7 shows the match and mismatch percentages between existing furniture dimensions, and participant anthropometry. High percentages of mismatches were found particularly on seat height, backrest height, desk height, seat to desk clearance. 74% female participants were mismatched on seat whereas male participants were less. About 50% both male and female participants were mismatched on seat depth. Almost all participants were matched on seat width and very few of them were mismatched. Backrest was totally inappropriate for all participants. 87.7 % female participants were mismatched on seat to desk height that was slightly higher than male. 100% of the female participants had not enough desk clearance. Seat height and desk height were so taller for the female participants. The potential mismatch found

between furniture dimensions and participant anthropometry measurements indicated the high frequency of MSDs problems existence among the participants (shown in Table 4). This mismatch history will be alarming for the participants and this situation will be overcome by redesigning the workstation for better welfare of participants and organization.

3.4. Computer Workstation Design

From Table 4 and Table 6, research found the mismatch between furniture dimensions and participant anthropometry, and large frequency of MSDs among different body parts of participants. So, the only solution will be the redesign of workstation's furniture and setup. Workstation furniture (Chair and Desk) was designed on user's anthropometric measurements and following various ergonomic guidelines and suggestions (shown in figure 4). Placement of monitor and other accessories were adjusted maintaining postural guidelines following worldwide prominent ergonomic standard and guidelines for computer workstation setup (shown in figure 5).

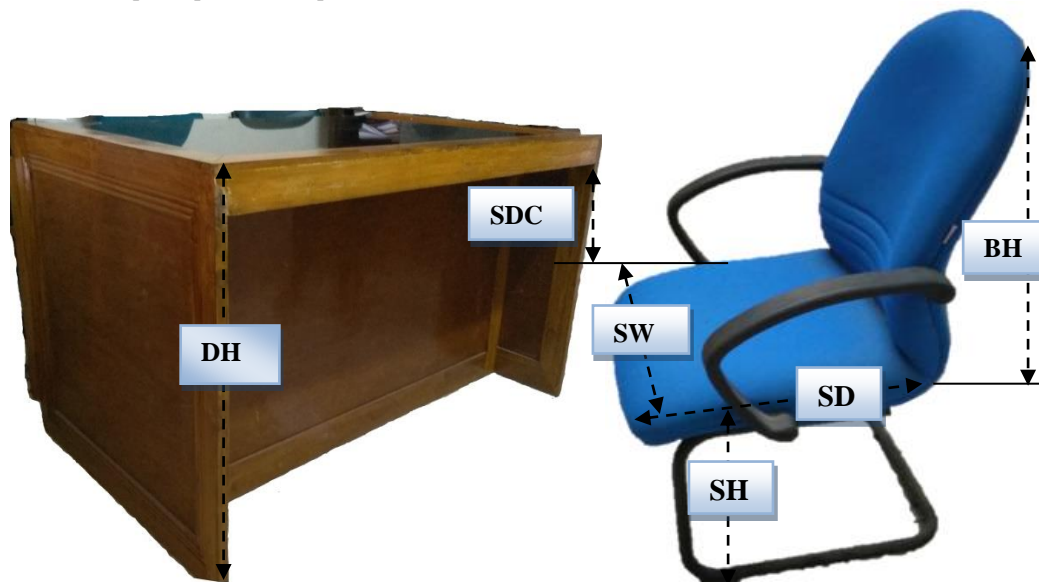


Figure 2. Furniture dimensions

Table 3. Match Criteria equations

Seat dimensions against anthropometric dimensions	Equations		References
Sitting Height (SH) against popliteal height :	$(PH + 3) \cos 30 \leq SH \leq (PH + 3) \cos 5$	2	[70]
Seat depth (SD) against buttock popliteal length (BPL):	$0.80BPL \leq SD \leq 0.95BPL$	3	[71]
Seat Width (SW) against Hip breadth(HB):	$1.10HB \leq SW \leq 1.30HB$	4	[72]
Desk Height (DH) against Sitting Elbow Height(SEH):	$SEH \leq DH \leq SEH + 5$	5	[27]
Backrest Height (BH) against Sitting Shoulder Height(SSH):	$0.60SSH \leq BH \leq 0.80SSH$	6	[73]
Seat to Desk Clearance (SDC) against Thigh clearance(TC):	$(TC + 2) < SDC$	7	[71]

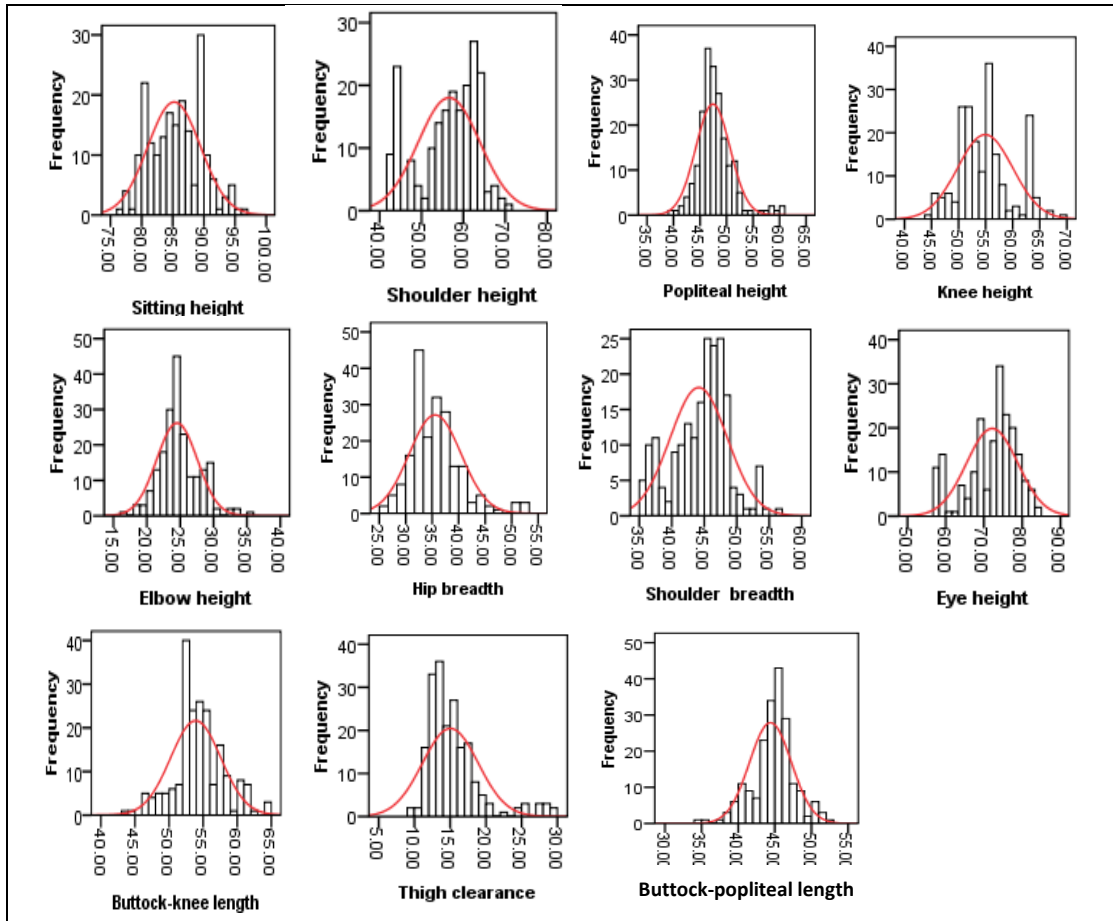


Figure 3. Normality distribution curves of anthropometric data (male)

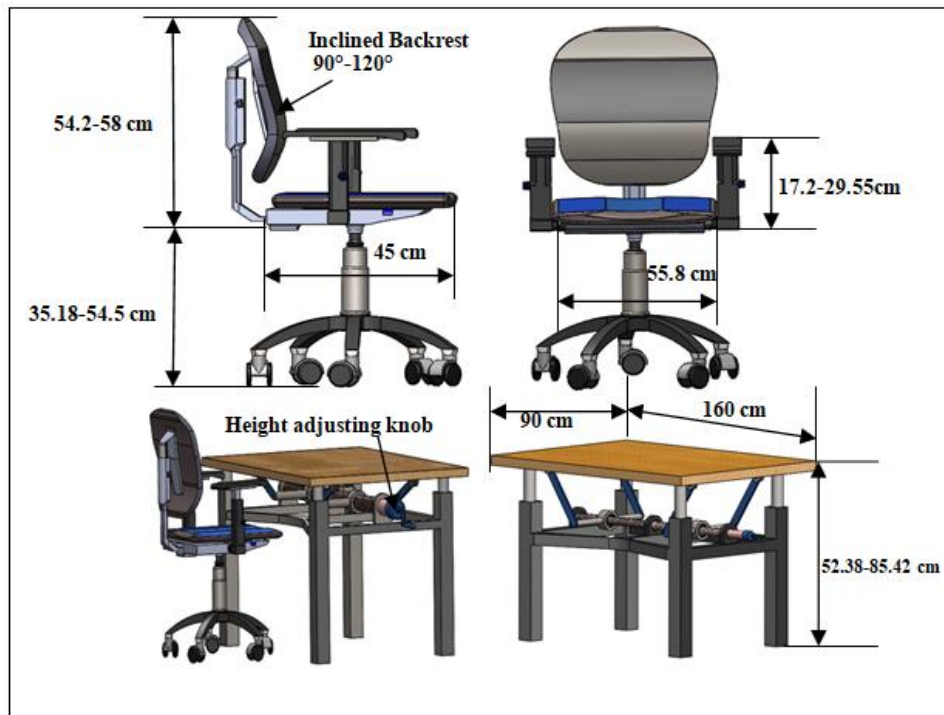


Figure 4. Proposed workstation design (chair and desk)

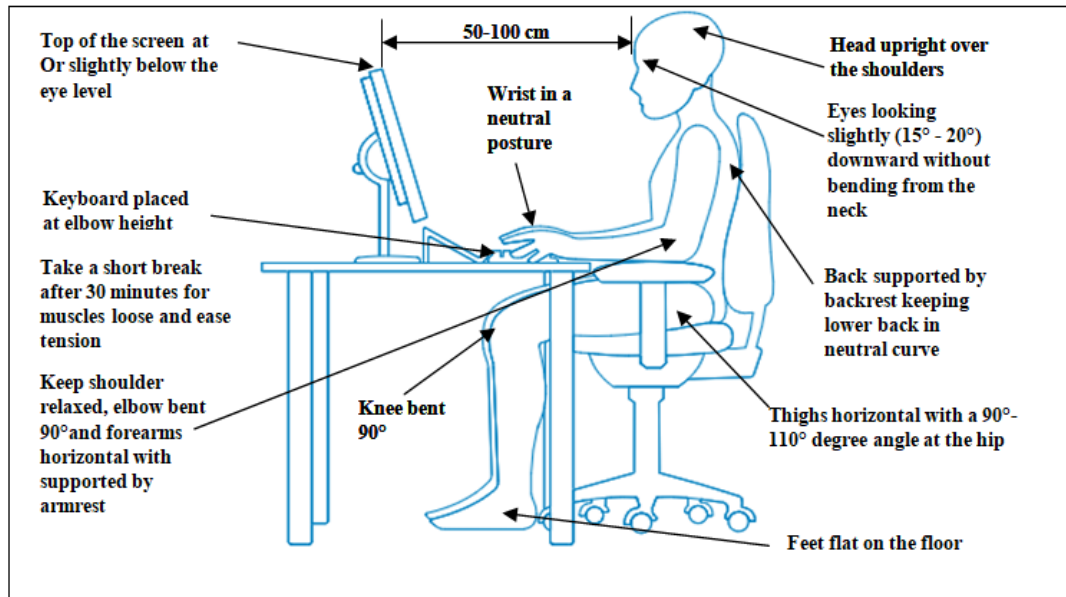


Figure 5. Recommended ergonomic guidelines for monitor, keyboard, mouse placement and sitting postures

Table 4. Frequency distribution of musculoskeletal pain

Pain in the following body regions	Constantly, (%)	Frequently, (%)	Occasionally, (%)	Total, (%)
Neck	3.39	30.56	24.52	58.49
Shoulders/Upper arm	2.26	28.67	16.22	47.16
Upper back	6.79	24.52	10.57	41.88
Lower back	7.92	33.20	24.15	65.28
Elbow/forearm	1.51	9.81	16.22	27.55
Wrist/Hand	0	9.81	30.19	40
Hips/Buttocks/Thighs	5.28	33.21	9.81	48.3
Knees and legs	0	17.35	20	37.35
Feet/Ankles	0	10.19	20	30.19

Table 5. Association of MSDs with sitting posture and workstation setup

Body parts with incorrect posture	Part of workstation with inappropriate setup	Body part affected
Torso	Seating	Lower back
Wrist and hands	Input devices	Wrist(left right)
Forearm and elbow	Seating	forearm
Head neck	Monitor	Neck and upper back
Head and neck	Monitor	Right and left shoulder
Shoulder and arm	Monitor	Right and left shoulder

Table 6. Anthropometric data for the teachers

Dimensions	Gender	Min	Max	Mean	SD	5 th percentile	50 th percentile	95 th percentile
Sitting height (erect) (cm)	Male	76.00	96.00	85.21	4.24	79.00	85.05	92.05
	female	73.00	88.90	80.35	3.03	76.26	79.756	85.4
Shoulder height, sitting (cm)	Male	47.00	71.00	56.57	7.37	44.00	58.00	65.05
	female	42.00	64.00	54.22	3.24	47.10	54.20	59.08
Popliteal height (cm)	Male	39.00	60.00	47.43	3.24	43.00	47.00	52.00
	female	28.00	47.00	39.71	4.19	32.68	39.90	46.18
Hip breadth, sitting (cm)	Male	25.00	53.00	35.54	4.89	29.00	35.00	44.47
	female	29.00	52.00	36.17	4.83	30.72	35.00	48.21
Elbow height, sitting (cm)	Male	17.00	35.00	24.52	3.05	20.00	24.00	30.92
	female	16.20	34.00	23.56	4.06	17.2	23.10	29.01
Buttock-popliteal length (cm)	Male	34.00	52.00	44.40	2.86	39.00	45.00	49.48
	female	35.00	52.07	43.43	3.42	38.02	43.60	49.05
Buttock-knee length (cm)	Male	43.00	64.00	53.90	3.69	47.00	54.00	61.00
	female	45.50	60.71	52.90	3.26	48.20	52.70	58.40
Thigh clearance (cm)	Male	9.00	29.21	15.02	3.90	11.00	14.00	25.00
	female	8.70	17.02	12.30	1.76	9.76	12.00	15.00
Eye height, sitting (cm)	Male	57.00	85.00	72.15	6.69	58.00	74.00	81.16
	female	60.20	76.90	68.70	3.22	64.06	68.20	73.32
Shoulder (bideltoid) breadth (cm)	Male	35.00	56.00	44.14	4.41	36.00	45.00	51.05
	female	33.00	55.00	40.43	4.45	34.60	40.00	50.80
Knee height (cm)	Male	44.00	69.00	54.90	5.10	47.00	54.00	63.69
	female	40.60	58.00	49.47	3.18	44.92	49.20	54.24

Table 7. Match and mismatch history

Furniture dimensions	Participants	Match	High mismatch	Low mismatch	Total mismatch
Seat Height	Male	68.5%	32.5%	0%	32.5%
	Female	26%	50%	14%	74%
Seat depth	Male	52%	14%	34%	48%
	Female	46%	28%	26%	54%
Seat width	Male	90%	10%	0%	10%
	Female	98%	2%	0%	2%
Backrest height	Male	00%	100%	0%	100%
	Female	4.6%	95.4%	0%	95.4%
Seat to desk height	Male	32.5%	0%	67.5%	67.5%
	Female	12.3%	0%	87.7%	87.7%
Seat to desk clearance	Male	37%			63%
	Female	0%			100%

3.4.1. General Requirements for Chair Design

Seat height: Seat height is the vital parameter of proper design of office chair and according to OSHA (2008) [60] and BIFMA furniture guidelines [50], it should be adjusted to accommodate a large population for preventing MSDs on back, legs, buttocks and arms. For example, *ANSI/HFES-100* specifies the seat height should be adjustable up to 56 cm [61], which has a much higher value than 51 and 52 cm recommended in *AS-3590.2* and *CAN/CSA-Z412-M89*, respectively. Seat should be adjustable with suitable keyboard-forearm relation and adequate leg room [42]. According to Parvez et al. (2018), seat height is related to popliteal height [25], while another researcher showed that seat height should be lower than popliteal height or else most users will be unable to rest their feet on the floor [62]. Popliteal height is the determinant of seat height [25], and Haworth (2008) suggested adjustable seat height that was ranged from 5th percentile of female and 95th percentile of male popliteal height [31]. So, researchers proposed adjustable seat height considering 5th percentile of female and 95th percentile of male popliteal height with added a shoes allowance of 2.5 cm and it was ranged from 35.18 cm to 54.5 cm (shown in figure 4).

Seat depth: Seat depth dimension should be considered in such way that shortest users cannot exceed their buttock popliteal length [63]. According to OSHA (2008), seat depth should be not too short and not too long to avoid creating pressure on buttock of taller users and knee of shorter users [60]. Taifa et. al proposed 50th percentile of male buttock popliteal length for seat depth [14]. That's why, 50th percentile of male buttock-popliteal length was taken to determine the seat depth dimension and it was 45 cm (shown in figure 4).

Seat width: Seat width should be designed in such way those users who has wider hip can accommodate with the seat [64] and consider the cloth allowance for easy movement. ISO-9241 proposes to consider large hip breadth for determining dimension of seat width [46]. Taifa et.al (2017) and BIFMA guidelines proposes seat width should be determined considering 95th percentile of female hip breadth added with clothing allowance for easy movement [14, 50]. In this research, 95th of the female hip breadth with cloth and movement allowance was considered to determine the seat width and it was 55.8 cm (shown in figure 4).

Backrest: Backrest should be designed that will support the individual body load and stabilize reclining posture with supporting head/neck when extreme reclining

posture [65]. *CAN/CSA-Z412-M89* specifies the backrest height should be adjustable [48]. OSHA (2008) recommended that backrest should be contoured and adjustable for maintaining neutral posture by the users [47]. It should be enough taller and wider for better supporting of reclining sitting without restricting elbow movement comfortably and impede upper body mobility [24]. Other researchers proposed that backrest should be adjustable from 50th percentile of male and female sitting shoulder height [15] and The inclination angle of 90-120 degree was recommended by Grandjean et.al [40]. Authors recommended the adjustable backrest considering 50th percentile of male and female sitting shoulder height and it was ranged from 54.2 cm to 58 cm and backrest inclination angle was 90 to 105 degree adopted from OSHA(2008)[47] (shown in figure 4).

Armrest: Armrests should be adjusted and made of a soft material and have rounded edges [60]. The armrest must support the forearms. Armrest should be designed in such way that is capable of holding forearms without creating pressure on median curve which leads to carpal tunnel syndrome [34]. Sitting elbow height is the detriment of armrest height. So, it was recommended that the adjustable armrest height ranged from 17.2 cm to 29.55 cm considering the elbow height of female 5th percentile to male 95th percentile [15] from the sitting surface (shown in figure 4).

3.4.2. General Requirements for Desk Design

Desk size: *AS-3590.2* suggests 120cm length x 90cm wide desk size for solely performed computer working [49]. In this research, target users perform computer working and other activities like reading. So, the desk size was recommended by 160 cm length x 90 cm wide as official desk in considering work envelope concept, nature of task and anthropometric dimensions of the target users (shown in figure 4).

Desk height: Most of the computer workstation guidelines such as *OSHA (2008)*, *CAN/CSA-Z412*, *ISO-9241*, *ANSI/HFES-100*, *AS-3590.2*, and other researchers recommend the height adjustable desk for easily accommodate the knee without any problems [15, 47-49, 61]. Desk height should be adjustable with suitable keyboard-forearm relation and adequate leg room [42]. Desk height was recommended by considering the summation of popliteal height and sitting elbow height values from female 5th percentile to male 95th percentile with added the shoes allowance 2.5 cm that was ranged from 52.38 cm to 85.42 cm (shown in figure 4).

3.4.3. Placement of Computer Accessories with Postural Guidelines

Keyboard: Placement of keyboard should in such way that it will not create any problem on arms, wrists, neck and shoulders. So, it was recommended to place the keyboard at least at elbow height [66].

Monitor: Computer monitor should be placed in such way that will prevent eyestrain and neck pain. Placement depends on individual's visual capacities, task requirements, screen characteristics, comfortable viewing distance. Recent studies suggested that computer monitor placement should be placed according to the individual's need of user within a moderate height range below the eye level with physiologically favorable head inclination [45, 67]. *OSHA (2008)* proposes to place the monitor 50-100cm away from the users with maintaining viewing angle 15° - 20°[47]. *AS-3590.2* proposes a low monitor position that is between 32° and 45° below horizontal eye level [49] while *ANSI/HFES-100* proposes a mid-position that is between 15° and 25°[61]. *AS-3590.2* specifies viewing distances between 35 and 75 cm which are closer than those recommended in *CAN/CSA-Z412-M89* and *ANSI/HFES-100*[48, 49, 61]. However, user often reports that 50cm viewing distance causes more fatigue than 100 cm [68]. Most of the authors recommended that monitor should be placed 63-85 cm away from users at or below the eye level with comfortable viewing angle [40, 69]. In the current study suggested monitor should be placed 50-100 cm way from the user with maintaining viewing 15° - 20° (shown in figure 5).

Posture: In this research, authors recommended to maintain neutral postures while sitting (shown in figure 5).

4. Conclusion and Recommendations

4.1. Conclusion

The primary focus of the current study was to investigate the prevalence of ergonomic issues/problems among the teachers and their workstations through a design of an ergonomic workstation to overcome these problems. High prevalence of musculoskeletal pain was observed among the users reported by ergonomic assessment (Health survey). It was also noticed that most of users were mismatched with their workstation furniture compared to their anthropometric measurements. Prevalence of MSDs, in the current study indicates that these problems are directly associated with physical workstation characteristics (office equipment), workload characteristics, human behaviors and perceptions towards ergonomics. An ergonomic computer workstation was designed for the teachers based on their anthropometric dimensions and related ergonomic guidelines. It is expected that implementation of suggestions and ergonomic guidelines in physical workstation designing, will reduce user's discomfort and enhancing their performance and productivity.

It is a common practice nowadays to buying furniture following the concept of "one-size-fits-all" in educational institution rather than adjustable furniture due to excessive cost of furniture that accommodate 90% of the target population. Very few researches have been conducted on cost reduction of ergonomic adjustable furniture. In this

regard, the focus will be placed on reducing manufacturing cost. This research can contribute a lot for ergonomic furniture design to the university authorities as well as other organizations and create a sense to overcome the ergonomic problems. All these factors contribute to organizational effectiveness, productivity, health and safety of computer users. Moreover, arrangement of basic ergonomic training like workstation setup, posture practicing and related other issues by the organization is necessary to overcome this threat. Similar study can be conducted to other organization to assess the health condition and ergonomic practices of the computer users which can inspire to manufacturers to design ergonomic furniture.

4.2. Recommendations

Ergonomic problems can be solved to redesign the existing workstation's furniture and its adjustment. As it is difficult to eliminate all critical problems of health survey just collecting anthropometric measurements, all responsible administrations and managements of universities are recommended to consider the following.

1. Anthropometric considerations must be incorporated with furniture procurement process to avoid musculoskeletal symptoms caused by prolonging computer usage.
2. QFD (Quality Function Deployment) and Kano Model with ergonomic integrations should be incorporated with the furniture designing process.
3. It is highly recommended that frequent seminar and workshop should be arranged by the universities creating awareness on negative effect of poor posture and practice neutral posture practicing when working.

Acknowledgement

The authors are very much grateful to Khulna University of Engineering and Technology (KUET), Bangladesh, for providing its lab facility to pursue this research.

References

- [1] Salvendy, G., Handbook of human factors and ergonomics. 2012: John Wiley & Sons.
- [2] Shikdar, A.A. and M.A. Al-Kindi, Office ergonomics: deficiencies in computer workstation design. *International Journal of Occupational Safety and Ergonomics*, 2007. 13(2): p. 215-223.
- [3] Darling, D., S. Kraus, and M. Glasheen-Wray, Relationship of head posture and the rest position of the mandible. *Journal of Prosthetic Dentistry*, 1984. 52(1): p. 111-115.
- [4] Darnell, M.W., A proposed chronology of events for forward head posture. *Journal of craniomandibular practice*, 1983. 1(4): p. 49-54.
- [5] S, E., *Office Ergonomics*. 2007.
- [6] Serina, E.R., R. Tal, and D. Rempel, Wrist and forearm postures and motions during typing. *Ergonomics*, 1999. 42(7): p. 938-951.
- [7] Akhter, Z., et al., Stature estimation using head measurements in Bangladeshi Garo adult females. *Bangladesh journal of anatomy*, 2009. 7(2): p. 101-104.

- [8] Lin, Y.-C., M.-J.J. Wang, and E.M. Wang, The comparisons of anthropometric characteristics among four peoples in East Asia. *Applied ergonomics*, 2004. 35(2): p. 173-178.
- [9] Khaspuri, G., S. Sau, and P. Dhara, Anthropometric consideration for designing class room furniture in rural schools. *Journal of Human Ecology*, 2007. 22(3): p. 235-244.
- [10] Al-Saleh, K.S., M.Z. Ramadan, and R.A. Al-Ashaikh, Ergonomically adjustable school furniture for male students. *Educational Research and Reviews*, 2013. 8(13): p. 943-955.
- [11] Ziefle, M., Sitting posture, postural discomfort, and visual performance: a critical view on the interdependence of cognitive and anthropometric factors in the VDU workplace. *International Journal of Occupational Safety and Ergonomics*, 2003. 9(4): p. 503-514.
- [12] Kothiyal, K. and S. Tettey, Anthropometry for design for the elderly. *International Journal of Occupational Safety and Ergonomics*, 2001. 7(1): p. 15-34.
- [13] Alrashdan, A., L. Alsudairi, and A. Alqaddoumi. Anthropometry of Saudi Arabian female college students. in *IIE Annual Conference. Proceedings*. 2014. Institute of Industrial and Systems Engineers (IISE).
- [14] Taifa, I.W. and D.A. Desai, Anthropometric measurements for ergonomic design of students' furniture in India. *Engineering Science and Technology, an International Journal*, 2017. 20(1): p. 232-239.
- [15] Deros, B.M., et al., Recommended chair and work surfaces dimensions of VDT tasks for Malaysian citizens. *Eur. J. Sci. Res*, 2009. 34(2): p. 156-167.
- [16] Bergqvist, U.O. and B.G. Knave, Eye discomfort and work with visual display terminals. *Scandinavian journal of work, environment & health*, 1994: p. 27-33.
- [17] Karwowski, W., et al., The effects of computer interface design on human postural dynamics. *Ergonomics*, 1994. 37(4): p. 703-724.
- [18] Fogleman, M. and R.J. Lewis, Factors associated with self-reported musculoskeletal discomfort in video display terminal (VDT) users. *International Journal of Industrial Ergonomics*, 2002. 29(6): p. 311-318.
- [19] Yang, J.-F. and C.-Y. Cho, Comparison of posture and muscle control pattern between male and female computer users with musculoskeletal symptoms. *Applied ergonomics*, 2012. 43(4): p. 785-791.
- [20] Park, M.-Y., J.-Y. Kim, and J.-H. Shin, Ergonomic design and evaluation of a new VDT workstation chair with keyboard-mouse support. *International Journal of Industrial Ergonomics*, 2000. 26(5): p. 537-548.
- [21] Straker, L., et al., The impact of computer display height and desk design on 3D posture during information technology work by young adults. *Journal of electromyography and kinesiology*, 2008. 18(2): p. 336-349.
- [22] Sauter, S.L., L.M. Schleifer, and S.J. Knutson, Work posture, workstation design, and musculoskeletal discomfort in a VDT data entry task. *Human factors*, 1991. 33(2): p. 151-167.
- [23] Xue, Liu, R.K., Kee-Hean. Ong. [cited 2013; Available from: <https://www.astm.org/studentmember/images/2010SaintLouisUniversity.pdf>.
- [24] Lale, K., & Korhan, O, Anthropometric computer workstation design to reduce perceived musculoskeletal discomfort. In *International Conference on Industrial Engineering and Operations Management Istanbul*, 2013.
- [25] Parvez MS, R.A., Tasnim N, Ergonomic mismatch between students anthropometry and university classroom furniture. *Theoretical Issues in Ergonomics Science*, 2019. 6: p. 1-30.
- [26] Castellucci, H., P. Arezes, and C. Viviani, Mismatch between classroom furniture and anthropometric measures in Chilean schools. *Applied ergonomics*, 2010. 41(4): p. 563-568.
- [27] Gouvali, M. and K. Boudolos, Match between school furniture dimensions and children's anthropometry. *Applied ergonomics*, 2006. 37(6): p. 765-773.
- [28] Kane, P., M. Pilcher, and S. Legg, Development of a furniture system to match student needs in New Zealand schools. in *16th World Congress on Ergonomics*. 2006.
- [29] Rosyidi, C.N., et al., Mismatch analysis of elementary school furniture in several regions of Central Java, Indonesia, and redesign recommendations. *SAGE Open*, 2016. 6(3): p. 2158244016664386.
- [30] Hoque, A., et al., Ergonomic design of classroom furniture for university students of Bangladesh. *Journal of Industrial and Production Engineering*, 2014. 31(5): p. 239-252.
- [31] Haworth. *The Ergonomic Seating Guide*. 2008 [cited 2018 20 December]; Available from: <http://www.haworth.com/en-us/Knowledge/Workplace-Library/Documents/Ergonomic-Seating-Guide.pdf>.
- [32] Kumah, D., et al., Ergonomic Challenges of Employees Using Computers at Work in a Tertiary Institution in Ghana. *Optom open access*, 2016. 1(107): p. 2476-2075.1000107.
- [33] Chowdhury, N., A Comparative Assessment of Ergonomic Risk Factors in University Personnel Using RULA and REBA Aiming to Study the Cause and Effect Relationship. 2015.
- [34] Lueder, R., *The ergonomics payoff: Designing the electronic office*. 1986: Nichols Pub Co.
- [35] Ontario Ministry of Labour, C., *Computer Ergonomics: Workstation Layout and Lighting. Health and Safety Guidelines*. 2004.
- [36] Lelong, C., et al., Spinal biomechanics and the sitting position. *Revue du Rhumatisme et des Maladies Osteo-articulaires*, 1988. 55(5): p. 375-380.
- [37] NAQVI, A., Study of forward sloping seats for VDT workstations. *Journal of human ergology*, 1994. 23(1): p. 41-49.
- [38] Chaffin, D.B., and G. Andersson., *Occupational Biomechanics*. 1984: New York: John and Wiley Sons.
- [39] Grandjean, E., *Postures and the design of VDT workstations. Behaviour & Information Technology*, 1984. 3(4): p. 301-311.
- [40] Grandjean, E., W. Hünting, and M. Pidermann, VDT workstation design: preferred settings and their effects. *Human factors*, 1983. 25(2): p. 161-175.
- [41] Tijerina, L., *Video display terminal workstation ergonomics*. 1984: Dublin, Ohio: OCLC.
- [42] Sauter, S. and R. Arndt, Ergonomics in the automated office: gaps in knowledge and practice. *Human computer interaction*, 1984: p. 411-414.
- [43] Sommerich, C.M., S.M. Joines, and J.P. Psihogios, Effects of computer monitor viewing angle and related factors on strain, performance, and preference outcomes. *Human factors*, 2001. 43(1): p. 39-55.
- [44] Chen, C. and T. Zhong, *An Ergonomic Development for VDT Workstation*. Published by the Institute of Occupational Safety and Health Council of Labor Affairs, Executive Yuan, Republic of China, IOSH88-H326, 1999.
- [45] Woo, E., P. White, and C. Lai, Ergonomics standards and guidelines for computer workstation design and the impact on users' health—a review. *Ergonomics*, 2016. 59(3): p. 464-475.
- [46] ISO, *Ergonomic Requirements for Office Work with Visual Display Terminals (VDTs) Part 5, in Workstation Layout and Postural Requirements (ISO 9241-5:1998)*1998, International Organization for Standardization.: Switzerland.
- [47] Occupational Safety and Health Administration. 2008. "OSHA Ergonomic Solutions: Computer Workstations ETool." Accessed January 14. <https://www.osha.gov/SLTC/etools/computerworkstations/>

- [48] CSA (Canadian Standards Association). 1989. A Guideline on Office Ergonomics: A National Standard of Canada (CAN/CSA-Z412-M89). Rexdale: Canadian Standards Association.
- [49] Standards Australia. 1990. Australian Standard: Screen-based Workstations. Part 2: Workstation Furniture (AS 3590.2-1990). Sydney: Standards Australia.
- [50] BIFMA International, Ergonomics Guidelines for VDT (Video Display Terminal) Furniture Used in Office Workspaces. Document G1-2002. February 28, 2002.
- [51] Tayyari, F. and J.L. Smith, Occupational ergonomics: Principles and applications (Manufacturing systems engineering series). 1997: United Kingdom: Chapman & Hall London.
- [52] Habib, M. and S. Yesmin, A pilot study of prevalence and distributions of musculoskeletal symptoms (MSS) among paper based office workers in Bangladesh. *Work*, 2015. 50(3): p. 371-378.
- [53] Lee, T.-H., Ergonomic comparison of operating a built-in touch-pad pointing device and a trackball mouse on posture and muscle activity. *Perceptual and motor skills*, 2005. 101(3): p. 730-736.
- [54] Odunaiya, N.A., D.D. Owonuwa, and O.O. Oguntibeju, Ergonomic suitability of educational furniture and possible health implications in a university setting. *Advances in medical education and practice*, 2014. 5: p. 1.
- [55] Gordon, C.C., et al., Anthropometric survey of US Army personnel: Summary statistics, interim report for 1988, 1989, ANTHROPOLOGY RESEARCH PROJECT INC YELLOW SPRINGS OH.
- [56] Bhadrabati Biswas, F.B.Z., Rahat Ara, M.S. Parvez,*, A.S.M. Hoque, Mismatch between classroom furniture and anthropometric measurements of Bangladeshi primary school students. *International Conference on Mechanical, Industrial and Energy Engineering*, 2014.
- [57] Labeodan, T.A. and I. Olaseha, Knowledge of Computer Ergonomics among Secretarial Staff in a Nigerian University Community. *International Journal of Health, Wellness & Society*, 2012. 2(3).
- [58] Akodu, A., et al., Work-related musculoskeletal disorders of the upper extremity with reference to working posture of secretaries. *South African Journal of Occupational Therapy*, 2015. 45(3): p. 16-22.
- [59] Mirmohammadi, S.J., et al., Effects of training intervention on non-ergonomic positions among video display terminals (VDT) users. *Work*, 2012. 42(3): p. 429-433.
- [60] Occupational Safety and Health Administration. 2008. "OSHA Ergonomic Solutions: Computer Workstations ETool." Accessed January 14. <https://www.osha.gov/SLTC/etools/computerworkstations/>
- [61] ANSI (American National Standards Institute). 2007. American National Standard for Human Factors Engineering of Computer Workstations (ANSI/HFES 100-2007). Santa Monica, CA: The Human Factors Society.
- [62] Castellucci, H.I., Arezes, P. M., & Molenbroek, J. F. M. (2015). Equations for defining the mismatch between students and school furniture: A systematic review. *International Journal of Industrial Ergonomics*, 48, 117-126., Equations for defining the mismatch between students and school furniture: A systematic review. *International Journal of Industrial Ergonomics*, 2015. 48: p. 117-126.
- [63] Thariq, M.M., H. Munasinghe, and J. Abeysekara, Designing chairs with mounted desktop for university students: Ergonomics and comfort. *International Journal of Industrial Ergonomics*, 2010. 40(1): p. 8-18.
- [64] O Ismaila, S., et al., Anthropometric design of furniture for use in tertiary institutions in Abeokuta, South-western Nigeria. *Engineering Review: Međunarodni časopis namijenjen publiciranju originalnih istraživanja s aspekta analize konstrukcija, materijala i novih tehnologija u području strojarstva, brodogradnje, temeljnih tehničkih znanosti, elektrotehnike, računarstva i građevinarstva*, 2013. 33(3): p. 179-192.
- [65] Bergqvist, U., et al., The influence of VDT work on musculoskeletal disorders. *Ergonomics*, 1995. 38(4): p. 754-762.
- [66] Bergqvist, U., et al., Musculoskeletal disorders among visual display terminal workers: individual, ergonomic, and work organizational factors. *Ergonomics*, 1995. 38(4): p. 763-776.
- [67] Weidling, P. and W. Jaschinski, The vertical monitor position for presbyopic computer users with progressive lenses: how to reach clear vision and comfortable head posture. *Ergonomics*, 2015. 58(11): p. 1813-1829.
- [68] Jaschinski-Kruza, W., Visual strain during VDU work: the effect of viewing distance and dark focus. *Ergonomics*, 1988. 31(10): p. 1449-1465.
- [69] Hon, C.K., A.P. Chan, and F.K. Wong, An analysis for the causes of accidents of repair, maintenance, alteration and addition works in Hong Kong. *Safety Science*, 2010. 48(7): p. 894-901.
- [70] Sanders, M. and E. McCormick, Applied anthropometry, work-space design and seating. *Human factors in engineering and design*, 1993. 7.
- [71] Parcels, C., M. Stommel, and R.P. Hubbard, Mismatch of classroom furniture and student body dimensions: empirical findings and health implications. *Journal of adolescent health*, 1999. 24(4): p. 265-273.
- [72] Evans, W., A. Courtney, and K. Fok, The design of school furniture for Hong Kong schoolchildren: An anthropometric case study. *Applied ergonomics*, 1988. 19(2): p. 122-134.
- [73] Dianat, I., et al., Classroom furniture and anthropometric characteristics of Iranian high school students: proposed dimensions based on anthropometric data. *Applied ergonomics*, 2013. 44(1): p. 101-108.

Appendices A

Ergonomic Assessment (Health Survey)

Name:
Designation:
Age:
Date of Assessment:

Question: Do you experience pain or discomfort in any following parts of the body when using your computer? If “yes”, mention please which part of your body?

- a) Neck b) Shoulders/upper arm c) Upper back d) Lower back e) Elbow/ forearm
f) Wrist/Hand g) Hips/Buttocks/Thighs h) Knees and legs i) Feet/ Ankles

Please mention in which form is affected?

- i) Constantly (most time of the day)
ii) Frequently (more than four times a month)
iii) Occasionally (two to four times a month)
iv) Never

User Signature

Production and Distribution Decisions for a Multi-product System with Component Commonality, Postponement Strategy and Quality Assurance Using a Two-machine Scheme

Singa Wang Chiu ^a, Jyun-Sian Kuo ^b, Yuan-Shyi Peter Chiu ^{b*}, Huei-Hsin Chang ^c

^aDepartment of Business Administration, Chaoyang University of Technology, Taichung 413, Taiwan

^bDepartment of Industrial Engineering & Management, Chaoyang University of Technology, Taichung 413, Taiwan

^cDepartment of Finance, Chaoyang University of Technology, Taichung 413, Taiwan

Received 9 Jan. 2019

Abstract

Coping with present-day's more demanding customer requests on variety, fast delivery, and quality, a growing number of corporations constantly redesign their production scheme and reorganize their supply chains. Motivated by the benefits gained from postponement policy in multi-item manufacturing systems and response to customer's actual needs, this study adopts a two-machine fabrication scheme to explore the optimal fabrication-delivery policy for a two-stage multi-item system with common part, postponement policy and product quality reassurance (including product screening, scrap and rework). In the first stage, machine one is utilized to fabricate common parts that shared by all finished products. Then, in stage two, a separate machine produces the finished items under a rotation cycle time order. With the help of mathematical modeling, optimization methods, and a numerical illustration, our proposed fabrication system is capable of not only deciding the best fabrication-delivery policy, but also demonstrating its beneficial choice in cost saving and cycle length reduction in comparison with the results from a system using single-machine scheme.

© 2019 Jordan Journal of Mechanical and Industrial Engineering. All rights reserved

Keywords: Production-distribution Decision, Multi-product System, Two-stage Two-machine Scheme, Postponement, Component Commonality, Quality Assurance;

1. Introduction

Postponing product differentiation is an effective strategy which is often assessed by production managers when planning production of multiproduct that have a part in common, for it can reduce production cycle time and lower overall fabrication relevant costs. Zinn [1] presented four different heuristics to help identify the potentials of postponement in order to assess savings of safety stock from postponement. He provided a real example to applying heuristics to support his findings. Lee and Tang [2] developed a model to capture expenses and benefits relating to redesign of manufacturing strategy. Their model was applied to analyze some special cases of real examples. As a result, they identified and formalized three different ways of product/process redesigns. They are; the standardization, modular design, and process reforming, for delaying differentiation from these real examples. Some special theoretical cases were also studied to characterize the optimal point of product differentiation and derive managerial insights. Swaminathan and Tayur [3] observed a few leading producers in computer industry who adopted the delayed differentiation strategy in managing their product lines to lower cost while keeping

customer service. Although this strategy is a challenging assignment, it is used to cope with stochastic demands by storing the half-way finished products to serve the fabrication needs for multiple end products. Accordingly, they modeled the problem as a two-stage integer program and employed the structural decomposition along with sub-gradient derivative methods in their solution process. A computational section is provided to express applicability of their solution procedure and offer insights on system characteristics, performances, and merits. Van Hoek et al. [4] provided a detailed investigation of the experiences from firms that handle process changes relating to adoption of postponement policy. They evaluated the benefits from implementing postponement strategy in each business environment, recognized the relevant managerial characteristics and potential bottlenecks, and suggested on how to successfully carry out the postponement strategy. Yang and Burns [5] explored the issues of decoupling spot, controlling, integrating, and planning capacity of the supply chain system from the viewpoint of postponement. Their objective was to expand the significance of postponement to the real-life supply-chain systems. Kumar and Wilson [6] investigated and explored the connection among inventory, delayed differentiation, and off-shoring. They

* Corresponding author e-mail: ypchiu@cyut.edu.tw.

pointed out the risks and reasons of off-shoring, the costs/benefits of delayed differentiation, and the relations and impacts of delayed differentiation and off-shoring on stock status. Then, the inventory impact of scenarios including diverse levels of delayed differentiation for an off-shore fabricated product is investigated using a set of real-world data. As a result, the best scenario is determined. Sensitivity analysis on the key variables was conducted and joint uncertainty owing to demand and cycle were identified as the significant input to every scenario. For any given strategy, they presented a fast approach to identify the dominated point within the uncertainty formula that affects stock status. Saghiri and Hill [7] explored the effect of supplier relationship on adopting delayed differentiation for a buying firm. Three separate postponement policies were proposed with 219 empirical data from manufacturing firms to test for the hypothetical connections between supplier relationships. The results indicated that buying firm's ability on implementing postponement in product design phase is positively related to supplier's level of commitment, anticipation of a long-lasting relationship, and joint actions with buyer. But another finding showed that buying firm's ability on implementing postponement in procurement phase is positively related to only the coordinated actions of supplier and buyer. Their findings provided greater insight into how different aspects of supplier relationship practically impact different types of postponement. Chiu et al. [8] derived optimal fabrication-distribution policy for a multiproduct system with quality reassurance and product differentiation. A single-machine two-stage manufacturing scheme is implemented. Consequently, they not only decided a closed-form optimal fabrication-distribution policy, but also showed a significant system cost savings and notable reduction in cycle time in comparison with the result from a single-stage scheme. Additional works [9-17] that also investigated diverse features of postponement issues in manufacturing systems.

In real-life production processes, owing due to diverse unpredictable factors fabrication of nonconforming items is inevitable. Product's quality assurance has always been a challenging and critical task for production managers. Studies related to product's quality assurance matters including inspection, scrap, and rework issues have been broadly performed in past years [18-42]. To cope with present-day's more demanding customer needs in terms of variety, fast delivery, and quality, an increasing number of corporations constantly redesign their production scheme and restructure their supply chains. Motivated by the possible advantages of postponement policy in multiproduct manufacturing systems and response to actual customer's needs, this study uses a dual-machine scheme to reconsider Chiu et al.'s problem [8]. The main difference between the present study and prior work [8] is that two separate machines are used in our proposed scheme, wherein in the first production stage machine one fabricates all common parts, and in the second stage machine two makes finished products under a

rotation cycle time discipline, with the intention of further reducing cycle time. Past literature showed that combined impacts of postponement, quality reassurance, and a two-machine scheme to the multiproduct fabrication-distribution problem have not been explicitly explored. We aim to fill the gap.

2. Description, Modeling, and Formulation

Suppose that demands λ_i per year for L products must be met (where $i = 1, 2, \dots, L$) and these products share a common part which are produced in advance by a machine (i.e., in stage 1, see Figure 1). Then, right after that, in stage 2 a second machine manufactures L customized end products in sequence (see Figure 2) under a rotation cycle time discipline. Such a two-machine scheme aims to reduce manufacturing cycle length and cut down total fabrication relevant cost. In stage 1, the manufacturing rate for common parts is $P_{1,0}$ per year, and the fabricating rate for finished items in stage 2 by a separate machine is $P_{1,i}$ per year.

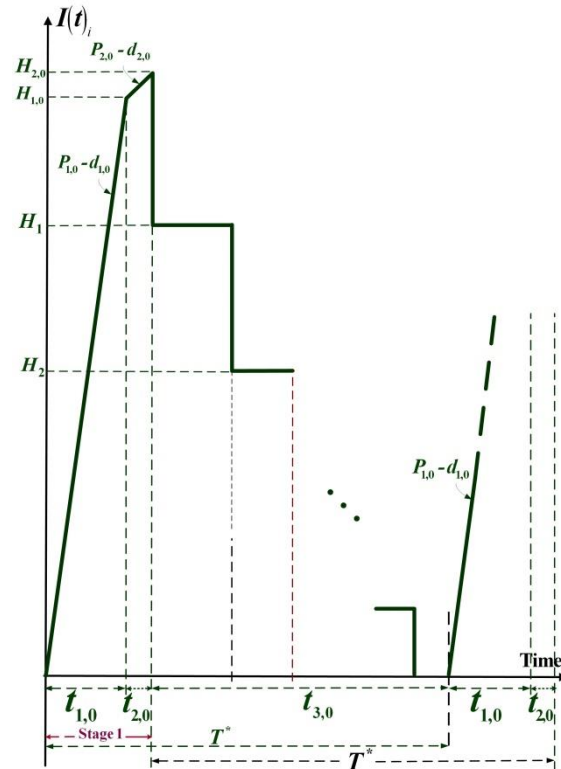


Figure 1. Level of on-hand common parts in stage 1 in the proposed model with a two-machine manufacturing scheme

All manufactured items are screened in both stages, cost of screening is a part of unit manufacturing cost C_i . Assuming x_i proportion of defective products may be manufactured randomly in both stages of the fabrication processes, at a rate of $d_{1,i}$ per year; so $d_{1,i} = P_{1,i} x_i$ (where $i = 0, 1, 2, \dots, L$; and $i = 0$ represents fabrication of common part in stage 1).

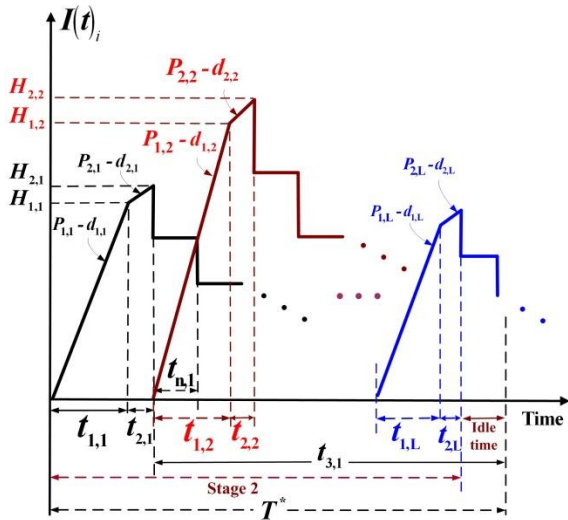


Figure 2. Level of on-hand finished items in stage 2 (machine 2) in proposed model using a two-machine production scheme

A portion $\theta_{1,i}$ of the nonconforming items are scraps (where $0 \leq \theta_{1,i} \leq 1$) and the rest are rework-able. The rework process immediately follows the regular fabrication, at $P_{2,i}$ items per year. During the rework, a $\theta_{2,i}$ portion fails (where $0 \leq \theta_{2,i} \leq 1$) that need to be scrapped (see Figures 3 and 4). Without permission of stock out, we further assume that $P_{1,i} - d_{1,i} - \lambda_i > 0$. In stage 2, when each rework process ends, fixed-quantity n installments of each finished batch are shipped to buyers at fixed time interval in $t_{3,i}$.

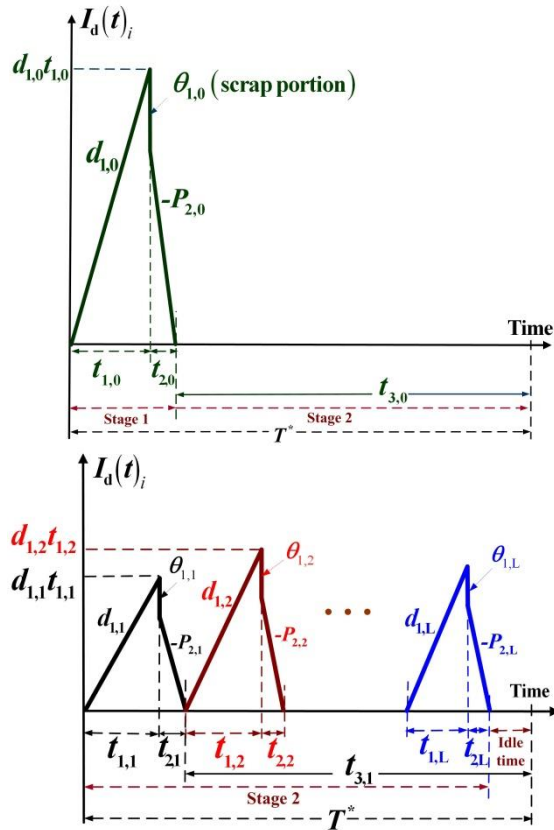


Figure 3. Inventory levels of on-hand defective common parts in stage 1 (left-hand side) and defective finished items in stage 2 (right-hand side) in a cycle

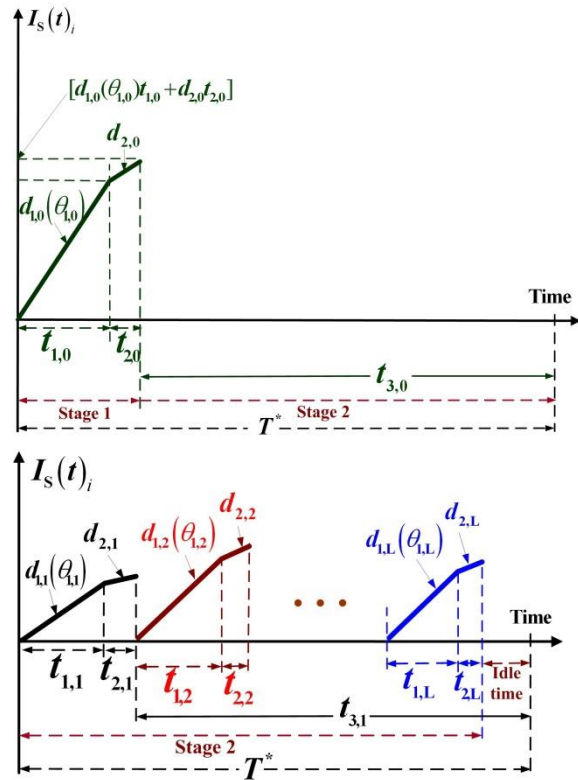


Figure 4. Inventory levels of scrapped common parts in stage 1 (left-hand side) and scrapped finished items in stage 2 (right-hand side) in a cycle

Inventory level of on-hand common parts awaiting the second stage's fabrication is exhibited in Figure 5. Nomenclature is exhibited in Appendix A.

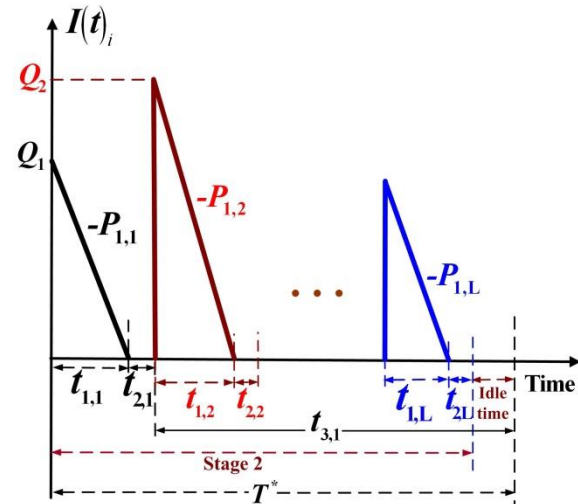


Figure 5. Inventory level of on-hand common parts awaiting the second stage's fabrication

2.1. Formulations and Mathematical Modeling

Since the proposed two-stage multi-product EPQ system using a two-machine production scheme, it releases the workload of fabricating the common intermediate parts from machine two. Therefore, an efficient end-item fabrication is expected stage two. The proposed solution procedure begins with deciding optimal rotation cycle

length for stage 2. Then, uses the rotation cycle time for fabrication of common parts in stage one.

In order to satisfy demands, enough capacity must be ensured in stage 2 for fabricating L distinct products under the rotation cycle discipline. So, the prerequisite formulas (1) and (2) must hold:

$$\sum_{i=1}^L (t_{1,i} + t_{2,i}) < T \quad \text{or} \quad \sum_{i=1}^L Q_i \left[\frac{1}{P_{1,i}} + \frac{E[x_i](1-\theta_{1,i})}{P_{2,i}} \right] < T \quad (1)$$

or

$$\sum_{i=1}^L \left(\frac{\lambda_i}{[1-\phi_i E[x_i]]} \right) \left[\frac{1}{P_{1,i}} + \frac{E[x_i](1-\theta_{1,i})}{P_{2,i}} \right] < 1 \quad (2)$$

To meet product demands λ_i and by observing Figures 2 to 5, we obtain formulas for stage two as follows (for $i = 1, 2, \dots, L$):

$$Q_i = \frac{\lambda_i T}{1 - \phi_i E[x_i]} \quad (3)$$

$$T = t_{1,i} + t_{2,i} + t_{3,i} = \frac{Q_i (1 - \phi_i E[x_i])}{\lambda_i} \quad (4)$$

$$\phi_i = \theta_{1,i} + \theta_{2,i} (1 - \theta_{1,i}) \quad (5)$$

$$Q_i = P_{1,i} (t_{1,i}) \quad (6)$$

$$H_{1,i} = (P_{1,i} - d_{1,i}) t_{1,i} \quad (7)$$

$$H_{2,i} = H_{1,i} + (P_{2,i} - d_{2,i}) t_{2,i} \quad (8)$$

$$t_{1,i} = \frac{Q_i}{P_{1,i}} = \frac{H_{1,i}}{P_{1,i} - d_{1,i}} \quad (9)$$

$$t_{2,i} = \frac{x_i Q_i (1 - \theta_{1,i})}{P_{2,i}} = \frac{d_{1,i} t_{1,i} (1 - \theta_{1,i})}{P_{2,i}} = \frac{H_{2,i} - H_{1,i}}{P_{2,i} - d_{2,i}} \quad (10)$$

$$t_{3,i} = n t_{n,i} \quad (11)$$

$$d_{1,i} \cdot t_{1,i} = P_{1,i} x_i \cdot t_{1,i} \quad (12)$$

At buyer's side, the inventory level in any given cycle is illustrated in Figure 6. From where, the following equations can be observed:

$$D_i = \frac{H_{2,i}}{n} \quad (13)$$

$$I_i = D_i - \lambda_i t_{n,i} \quad (14)$$

$$n I_i = \lambda_i (t_{1,i} + t_{2,i}) \quad (15)$$

$$TC_2(T, n) = \sum_{i=1}^L \left\{ \begin{aligned} & C_i Q_i + K_i + C_{R,i} [x_i (1 - \theta_{1,i}) Q_i] + C_{S,i} [x_i \phi_i Q_i] + n K_{1,i} + C_{T,i} [Q_i (1 - \phi_i x_i)] \\ & + h_{1,i} \left[\frac{Q_i}{2} (t_{1,i}) + \frac{H_{1,i} t_{1,i}}{2} + \frac{H_{2,i} + H_{1,i}}{2} (t_{2,i}) + \left(\frac{n-1}{2n} \right) H_{2,i} t_{3,i} + \frac{d_{1,i} t_{1,i}}{2} (t_{1,i}) \right] \\ & + h_{2,i} \left(\frac{P_{2,i} t_{2,i}}{2} \right) (t_{2,i}) + h_{3,i} \left[\frac{n(D_i - I_i) t_{n,i}}{2} + \frac{n(n+1)}{2} I_i t_{n,i} + \frac{n I_i (t_{1,i} + t_{2,i})}{2} \right] \\ & + h_{4,i} (x_i Q_i) T \end{aligned} \right\} \quad (21)$$

From Figure 3, total holding costs during rework time $t_{2,i}$ are as follows:

$$\sum_{i=1}^L \left[h_{2,i} \left(\frac{P_{2,i} t_{2,i}}{2} \right) (t_{2,i}) \right] \quad (16)$$

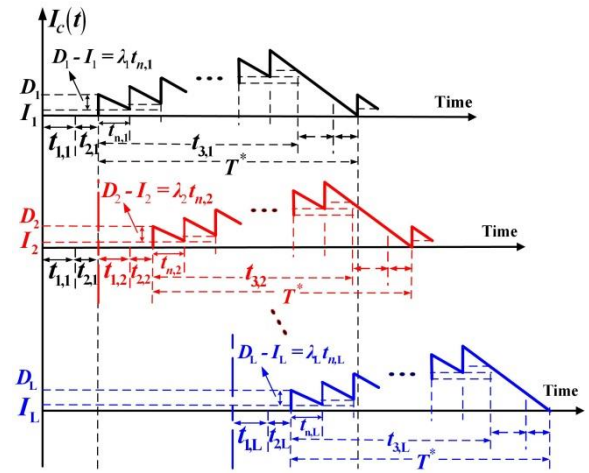


Figure 6. Inventory level of stocks at the buyer's in any given cycle

From Figure 5, total holding costs for common parts awaiting next stage of fabrication are as follows:

$$\sum_{i=1}^L \left\{ h_{1,i} \left[\frac{Q_i}{2} (t_{1,i}) \right] \right\} \quad (17)$$

In delivering time $t_{3,i}$ (stage 2), total holding costs are as follows:

$$\sum_{i=1}^L \left\{ h_{3,i} \left(\frac{n-1}{2n} \right) H_{2,i} t_{3,i} \right\} \quad (18)$$

In any given cycle, the fixed and variable shipping costs are

$$\sum_{i=1}^L \left\{ n K_{1,i} + C_{T,i} [Q_i (1 - \phi_i x_i)] \right\} \quad (19)$$

At buyer's side (Figure 6), total holding costs in a given cycle are as follows [8]

$$\sum_{i=1}^L \left\{ h_{3,i} \left[\frac{n(D_i - I_i) t_{n,i}}{2} + \frac{n(n+1)}{2} I_i t_{n,i} + \frac{n I_i (t_{1,i} + t_{2,i})}{2} \right] \right\} \quad (20)$$

Therefore, overall system costs in a cycle for stage two, $TC_2(T, n)$ includes summation of setup, variable manufacturing, disposal, and rework costs, producer's inventory and safety stock holding costs, fixed and variable shipping costs, and buyer's holding costs. Hence, $TC_2(T, n)$ is

By substituting Eqs. (1) to (15) in Eq. (21), and using the expected values of x_i to cope with randomness of x_i , and after additional derivations, $E[TCU_2(T, n)]$ becomes

$$E[TCU_2(T, n)] = E[TC_2(T, n)] / E[T] = \sum_{i=1}^L \left\{ \left[C_i \lambda_i \pi_{0,i} + \frac{K_i}{T} + C_{R,i} \lambda_i (1 - \theta_{1,i}) \pi_{1,i} + C_{S,i} \lambda_i \varphi_i \pi_{1,i} + \frac{nK_{1,i}}{T} + C_{T,i} \lambda_i \right] + \frac{h_{1,i} T \lambda_i^2}{2} \left[\pi_{3,i} + \pi_{4,i} - \frac{\pi_{5,i}}{n} \right] \right. \\ \left. + \frac{h_{2,i} T \lambda_i^2 \pi_{1,i}^2}{2} \left[\frac{(1 - \theta_{1,i})^2}{P_{2,i}} \right] + \frac{h_{3,i} T \lambda_i^2}{2} \left[\frac{2\pi_{0,i}}{P_{1,i}} + \frac{2(1 - \theta_{1,i})\pi_{1,i}}{P_{2,i}} - \frac{1}{\lambda_i} + \left(1 + \frac{1}{n} \right) \pi_{5,i} \right] + Th_{4,i} \lambda_i \pi_{1,i} \right\} \quad (22)$$

where

$$\pi_{0,i} = \frac{1}{(1 - \varphi_i E[x_i])}; \pi_{1,i} = \frac{E[x_i]}{(1 - \varphi_i E[x_i])}; \text{ and } \pi_{2,i} = (1 - \theta_{1,i})(1 - \theta_{2,i}) \text{ for } i = 1, 2, \dots, L; \\ \pi_{3,i} = \left[\frac{\pi_{0,i}^2}{P_{1,i}} + \frac{(1 - E[x_i])(1 - \theta_{1,i})\pi_{0,i}\pi_{1,i}}{P_{2,i}} \right] \text{ for } i = 1, 2, \dots, L; \\ \pi_{4,i} = \left[\frac{1 - E[x_i]}{\lambda_i} \pi_{0,i} + \frac{\pi_{2,i}\pi_{1,i}}{\lambda_i} + \frac{\pi_{0,i}\pi_{1,i}}{P_{1,i}} [1 - \pi_{2,i}] \right] \text{ for } i = 1, 2, \dots, L; \\ \pi_{5,i} = \left[\pi_{4,i} - \pi_{3,i} - \frac{(1 - \theta_{1,i})\pi_{2,i}\pi_{1,i}^2}{P_{2,i}} \right] \text{ for } i = 1, 2, \dots, L \quad (23)$$

On the other hand, in stage one, in order to supply in time enough common parts (see Figure 1) to satisfy the needs of stage two's fabrications, machine 1 must fabricate common parts ($t_{1,0} + t_{2,0}$) early. By observing Figures 1, 3, 4, and 5, we obtain the following formulations directly:

$$\sum_{i=1}^L Q_i = \lambda_0 T \quad (24) \quad H_{2,0} = H_{1,0} + (P_{2,0} - d_{2,0})t_{2,0} \quad (30)$$

$$Q_0 = \frac{\sum_{i=1}^L Q_i}{1 - \varphi_0 E[x_0]} \quad (25) \quad t_{2,0} = \frac{x_0 Q_0 (1 - \theta_{1,0})}{P_{2,0}} = \frac{d_{1,0} t_{1,0} (1 - \theta_{1,0})}{P_{2,0}} = \frac{H_{2,0} - H_{1,0}}{P_{2,0} - d_{2,0}} \quad (31)$$

$$T = t_{1,0} + t_{2,0} + t_{3,0} = \frac{Q_0 (1 - \varphi_0 E[x_0])}{\lambda_0} \quad (26) \quad H_1 = H_{2,0} - Q_1 \quad (32)$$

$$\varphi_0 = \theta_{1,0} + \theta_{2,0} (1 - \theta_{1,0}) \quad (27) \quad H_{2,0} = \sum_{i=1}^L Q_i \quad (33)$$

$$H_{1,0} = t_{1,0} (P_{1,0} - d_{1,0}) \quad (28) \quad H_i = H_{(i-1)} - Q_i \text{ for } i = 2, 3, \dots, L \quad (34)$$

$$t_{1,0} = \frac{Q_0}{P_{1,0}} = \frac{H_{1,0}}{P_{1,0} - d_{1,0}} \quad (29) \quad H_L = H_{(L-1)} - Q_L = 0 \quad (35)$$

For stage 1, total cost in a cycle, $TC_1(T, n)$ comprises setup cost, variable manufacturing, disposal, and rework costs, inventory and safety stock holding costs. Hence, $TC_1(T, n)$ becomes:

$$TC_1(T, n) = \left\{ C_0 Q_0 + K_0 + C_{R,0} [x_0 (1 - \theta_{1,0}) Q_0] + C_{S,0} [x_0 \varphi_0 Q_0] + h_{2,0} \left[\frac{d_{1,0} t_{1,0} (1 - \theta_{1,0})}{2} \right] (t_{2,0}) \right. \\ \left. + h_{1,0} \left[\frac{H_{1,0} t_{1,0}}{2} + \frac{H_{2,0} + H_{1,0}}{2} (t_{2,0}) + \frac{d_{1,0} t_{1,0}}{2} (t_{1,0}) + \sum_{i=1}^L H_i (t_{1,i} + t_{2,i}) \right] + h_{4,0} (x_0 Q_0) T \right\} \quad (36)$$

The prerequisite assumption for stage 1 is

$$(t_{1,0} + t_{2,0}) < T \text{ or } \left[Q_0 \left(\frac{1}{P_{1,0}} + \frac{E[x_0](1 - \theta_{1,0})}{P_{2,0}} \right) \right] < T \quad (37)$$

or

$$\left\{ \left(\frac{\lambda_0}{[1 - \varphi_0 E[x_0]]} \right) \left[\frac{1}{P_{1,0}} + \frac{E[x_0](1 - \theta_{1,0})}{P_{2,0}} \right] \right\} < 1 \quad (38)$$

Substituting Eqs. (24) to (35) in Eq. (36) and using the expected values of x_i to cope with its randomness, and after additional derivations, $E[TCU_1(T, n)]$ becomes

$$E[TCU_1(T, n)] = E[TC_1(T, n)] / E[T] \tag{39}$$

$$= \left[C_0 \lambda_0 \pi_{0,0} + \frac{K_0}{T} + C_{R,0} \lambda_0 (1 - \theta_{1,0}) \pi_{1,0} + C_{S,0} \lambda_0 \phi_0 \pi_{1,0} + \gamma_0 T \right]$$

where

$$\pi_{0,0} = \frac{1}{(1 - \phi_0 E[x_0])}; \pi_{1,0} = \frac{E[x_0]}{(1 - \phi_0 E[x_0])}; \pi_{0,j} = \frac{1}{(1 - \phi_j E[x_j])} \quad \text{for } j = 1, \dots, i$$

$$\gamma_0 = \left\{ \begin{aligned} & \left[\frac{h_{1,0} \lambda_0^2 (\pi_{0,0})^2}{2} \left[\frac{1}{P_{1,0}} + \frac{2E[x_0](1 - \theta_{1,0})(1 - E[x_0])}{P_{2,0}} + \frac{E[x_0]^2 (1 - \theta_{1,0})^2 (1 - \theta_{2,0})}{P_{2,0}} \right] \right. \\ & \left. + h_{1,0} \sum_{i=1}^L \left\{ \left(\frac{\lambda_i \pi_{0,i}}{P_{1,i}} + \frac{\lambda_i (1 - \theta_{1,i}) \pi_{1,i}}{P_{2,i}} \right) \left[\sum_{i=1}^L (\lambda_i \pi_{0,i}) - \sum_{j=1}^i (\lambda_j \pi_{0,j}) \right] \right\} \right. \\ & \left. + h_{4,0} \lambda_0 \pi_{1,0} + \frac{h_{2,0} \lambda_0^2 (\pi_{1,0})^2}{2} \left[\frac{(1 - \theta_{1,0})^2}{P_{2,0}} \right] \right\} \end{aligned} \right. \tag{40}$$

Therefore, $E[TCU(T, n)]$ consists of the expected costs of both stages as follows:

$$E[TCU(T, n)] = E[TCU_1(T, n)] + E[TCU_2(T, n)]. \tag{41}$$

2.2. Deriving the Optimal Production and Shipment Policy

To decide the optimal fabrication-distribution policy, the convexity of $E[TCU_2(T, n)]$ has to be proved first. That is Eq. (42) the Hessian matrix equations [43] must hold.

$$[T \ n] \cdot \begin{pmatrix} \frac{\partial^2 E[TCU(T, n)]}{\partial T^2} & \frac{\partial^2 E[TCU(T, n)]}{\partial T \partial n} \\ \frac{\partial^2 E[TCU(T, n)]}{\partial T \partial n} & \frac{\partial^2 E[TCU(T, n)]}{\partial n^2} \end{pmatrix} \cdot \begin{bmatrix} T \\ n \end{bmatrix} > 0 \tag{42}$$

From Eq. (22) we have

$$\frac{\partial E[TCU_2(T, n)]}{\partial T} = \sum_{i=1}^L \left\{ \left[\frac{-K_i}{T^2} - \frac{nK_{1,i}}{T^2} \right] + \frac{h_{1,i} \lambda_i^2}{2} \left\{ \pi_{3,i} + \pi_{4,i} - \frac{\pi_{5,i}}{n} \right\} + \frac{h_{2,i} \lambda_i^2 \pi_{1,i}^2}{2} \left[\frac{(1 - \theta_{1,i})^2}{P_{2,i}} \right] \right. \tag{43}$$

$$\left. + \frac{h_{3,i} \lambda_i^2}{2} \left[\frac{2\pi_{0,i}}{P_{1,i}} + \frac{2(1 - \theta_{1,i}) \pi_{1,i}}{P_{2,i}} - \frac{1}{\lambda_i} + \left(1 + \frac{1}{n} \right) \pi_{5,i} \right] + h_{4,i} \lambda_i \pi_{1,i} \right\}$$

$$\frac{\partial E[TCU_2(T, n)]}{\partial T^2} = \sum_{i=1}^L \left(\frac{2K_i}{T^3} + \frac{2nK_{1,i}}{T^3} \right) \tag{44} \quad \frac{\partial E[TCU_2(T, n)]}{\partial n^2} = \sum_{i=1}^L \left\{ \frac{T \lambda_i^2}{n^3} [(h_{3,i} - h_{1,i}) \pi_{5,i}] \right\} \tag{46}$$

$$\frac{\partial E[TCU_2(T, n)]}{\partial n} = \sum_{i=1}^L \left\{ \frac{K_{1,i}}{T} + \frac{T \lambda_i^2}{2n^2} [(h_{1,i} - h_{3,i}) \pi_{5,i}] \right\} \tag{45} \quad \frac{\partial^2 E[TCU_2(T, n)]}{\partial T \partial n} = \sum_{i=1}^L \left\{ -\frac{K_{1,i}}{T^2} + \frac{\lambda_i^2}{2n^2} [(h_{1,i} - h_{3,i}) \pi_{5,i}] \right\} \tag{47}$$

By substituting equations (44), (46), and (47) in Eq. (42) and after more derivations, Eq. (48) can be obtained.

$$[T \ n] \cdot \begin{pmatrix} \frac{\partial^2 E[TCU_2(T, n)]}{\partial T^2} & \frac{\partial^2 E[TCU_2(T, n)]}{\partial T \partial n} \\ \frac{\partial^2 E[TCU_2(T, n)]}{\partial T \partial n} & \frac{\partial^2 E[TCU_2(T, n)]}{\partial n^2} \end{pmatrix} \cdot \begin{bmatrix} T \\ n \end{bmatrix} = \sum_{i=1}^L \frac{2K_i}{T} > 0 \tag{48}$$

Since T and K_i are both positive, so Eq. (48) is positive. Therefore, for all n and T different from zero $E[TCU_2(T, n)]$ is strictly convex. Then, to simultaneously decide the fabrication and distribution policies, the linear system of the first derivatives (Eqs. (43) and (45)) of

$E[TCU_2(T, n)]$ with respect to T and n , needs to be solved, respectively. Let these partial derivatives equal to zero and with extra derivations, the following can be gained:

$$T^* = \sqrt{\frac{\sum_{i=1}^L (K_i + nK_{1,i})}{\sum_{i=1}^L \left\{ \frac{h_{1,i}\lambda_i^2}{2} \left[\pi_{3,i} + \pi_{4,i} - \frac{\pi_{5,i}}{n} \right] + \frac{h_{2,i}\lambda_i^2\pi_{1,i}^2}{2} \left[\frac{(1-\theta_{1,i})^2}{P_{2,i}} \right] + h_{4,i}\lambda_i\pi_{1,i} \right.}}}$$

$$\left. + \frac{h_{3,i}\lambda_i^2}{2} \left[\frac{2\pi_{0,i}}{P_{1,i}} + \frac{2(1-\theta_{1,i})\pi_{1,i}}{P_{2,i}} - \frac{1}{\lambda_i} + \left(1 + \frac{1}{n}\right)\pi_{5,i} \right] \right\}} \quad (49)$$

and

$$n^* = \sqrt{\frac{\left(\sum_{i=1}^L K_i \right) \sum_{i=1}^L \left\{ \frac{\lambda_i^2}{2} [(h_{3,i} - h_{1,i})\pi_{5,i}] \right\}}{\left(\sum_{i=1}^L K_{1,i} \right) \sum_{i=1}^L \left\{ \frac{h_{1,i}\lambda_i^2}{2} (\pi_{3,i} + \pi_{4,i}) + \frac{h_{2,i}\lambda_i^2\pi_{1,i}^2}{2} \left[\frac{(1-\theta_{1,i})^2}{P_{2,i}} \right] + h_{4,i}\lambda_i\pi_{1,i} \right.}}}$$

$$\left. + \frac{h_{3,i}\lambda_i^2}{2} \left[\frac{2\pi_{0,i}}{P_{1,i}} + \frac{2(1-\theta_{1,i})\pi_{1,i}}{P_{2,i}} - \frac{1}{\lambda_i} + \pi_{5,i} \right] \right\}} \quad (50)$$

3. Numerical Example with Sensitivity Analysis

In this section, we use a numerical example to explain the practical usage of our obtained results. Suppose five end items have annual demand rates λ_i : 3,800, 3,600, 3,400, 3,200, and 3,000 units; and $\alpha = 0.5$. We first assume the linear relationship between α and relevant system variables. Hence, in stage 1 we have $P_{1,0} = 120,000$ (calculating by $P_{1,0} = (1/\alpha) * (\text{the mean of } P_{1,i}'\text{s})$) and $P_{2,0} = 96,000$ (computing by $P_{2,0} = (1/\alpha) * (\text{the mean of } P_{2,i}'\text{s})$). The same linear relationship is also applied to other system variables and to relieve readers' comparison efforts, we adopt the same values of parameters as in [8] as follows:

- $K_0 = \$8,500,$
- $C_0 = \$40,$
- $C_{R,0} = \$25,$
- $C_{S,0} = \$10,$
- $h_{1,0} = \$5,$
- $h_{2,0} = \$15,$
- $h_{4,0} = \$5,$
- $x_0 =$ uniformly distributed over the interval of $[0, 0.04],$
- $\theta_{1,0} = 0.2,$
- $\theta_{2,0} = 0.2,$
- $P_{1,i} = 128,276, 124,068, 120,000, 116,066,$ and $112,258$ units, respectively; and $P_{1,i} = 1/(1/P_{1,i} - 1/P_{1,0}),$
- $P_{2,i} = 102,621, 99,254, 96,000, 92,852,$ and $89,806$ units, respectively; and $P_{2,i} = 1/(1/P_{2,i} - 1/P_{2,0}),$
- $K_i = \$10,500, \$10,000, \$95,000, \$90,000,$ and $\$8,500,$ respectively,
- $C_i = \$80, \$70, \$60, \$50,$ and $\$40,$
- $C_{R,i} = \$45, \$40, \$35, \$30,$ and $\$25,$
- $C_{S,i} = \$30, \$25, \$20, \$15,$ and $\$10,$
- $\theta_{1,i} = 0.30, 0.25, 0.20, 0.15,$ and $0.10,$
- $\theta_{2,i} = 0.30, 0.25, 0.20, 0.15,$ and $0.10,$
- $x_i =$ uniformly distributed over the ranges of $[0, 0.01], [0, 0.06], [0, 0.11], [0, 0.16],$ and $[0, 0.21],$ respectively,
- $h_{1,i} = \$30, \$25, \$20, \$15,$ and $\$10,$
- $h_{2,i} = \$50, \$45, \$40, \$35,$ and $\$30,$
- $h_{4,0} = \$30, \$25, \$20, \$15,$ and $\$10,$
- $K_{1,i} = \$2,200, \$2,100, \$2,000, \$1,900,$ and $\$1,800,$
- $C_{T,i} = \$0.5, \$0.4, \$0.3, \$0.2,$ and $\$0.1,$
- $h_{3,i} = \$90, \$85, \$80, \$75,$ and $\$70,$ respectively.

Applying equations (49), (50), and (41), we found $n^* = 3, T^* = 0.4444,$ and $E[TCU(T^*, n^*)] = \$2,209,197.$ The

impacts of different cycle times T to $E[TCU(T, n)]$ is depicted in Figure 7.

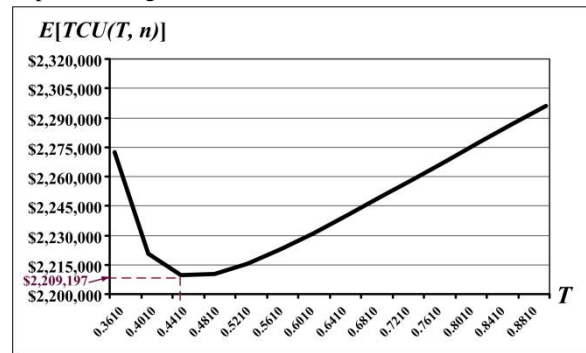


Figure 7. The impacts of different cycle times T to $E[TCU(T, n)]$

Figure 8 shows joint impacts of diverse expected values of x_i and ϕ_i on $E[TCU(T, n)]$. As both expected values of x_i and ϕ_i increase, $E[TCU(T, n)]$ goes up significantly. These analytical results revealed the important/realistic information on production quality costs.

The behavior of $E[TCU(T, n)]$ with respect to the completion rate α of common part is displayed in Figure 9. It indicates that as α increases, $E[TCU(T, n)]$ decreases significantly, and a savings in cost 4.63% revealed at $\alpha = 0.5$. That is the system costs decline to \$2,209,197 (from \$2,316,483) in comparison with the result from a prior work which utilized a fabrication scheme with a single stage.

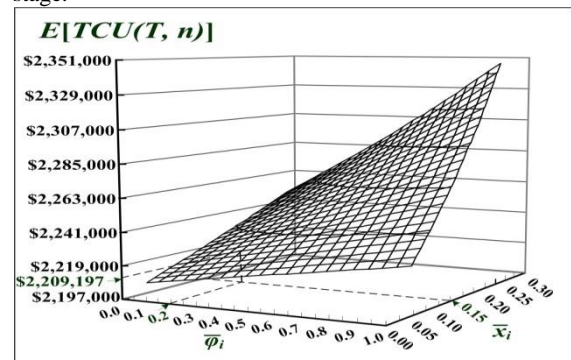


Figure 8. Joint impacts of diverse expected values of x_i and ϕ_i on $E[TCU(T, n)]$

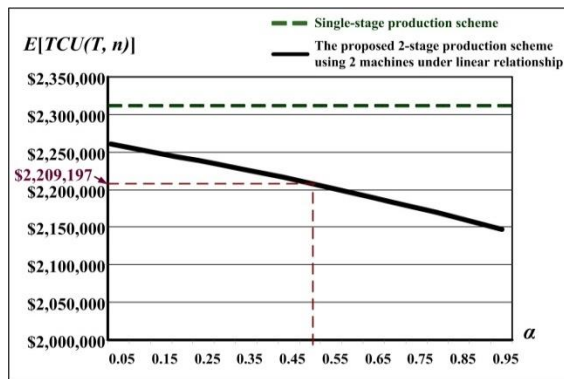


Figure 9. Behavior of $E[TCU(T, n)]$ with respect to the completion rate α

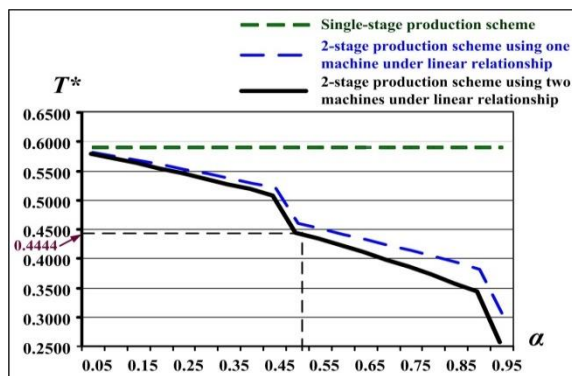


Figure 10. The impacts of different values of completion rate α to T^* for both the fabrication schemes with single-machine and two-machine

3.1. Exploration of Nonlinear Cost Relationship

This section examines the nonlinear relationship between α and its corresponding fabrication cost. It is assumed that ' $\alpha^{1/3}$ ' is the relating factor. Therefore, we have $C_0 = [\alpha^{1/3}]C_1 = [(0.5)^{1/3}](\$80) = \$63$, so its fabrication cost (or value) is higher than \$40 as assumed linearly. Similarly, the following values of other parameters can also be obtained: $h_{1,0} = \$8$, $K_0 = \$13493$, $h_{2,0} = \$24$, $C_{S,0} = \$16$, $h_{4,0} = \$8$, and $C_{R,0} = \$40$. For stage 2, we also have $C_{R,i} = \$30, \$25, \$20, \15 , and $\$10$, respectively; $C_i = \$57, \$47, \$37, \27 , and $\$17$; $K_i = \$5,507, \$5,007, \$4,507, \$4,007$, and $\$3,507$; and $C_{S,i}$ are $\$24, \$19, \$14, \9 , and $\$4$; and x_i are uniform distributed over the ranges $[0, 0.01], [0, 0.06], [0, 0.11], [0, 0.16]$, and $[0, 0.21]$, respectively. Other values of parameters remain the same as in earlier sub-section: $x_0 = [0, 0.04]$; $\theta_{1,0} = 0.20$; $\theta_{2,0} = 0.20$; $\varphi_0 = 0.36$; scrap rates $\theta_{1,i} = 0.10, 0.15, 0.20, 0.25$, and 0.30 ; $\theta_{2,i} = 0.10, 0.15, 0.20, 0.25$, and 0.30 , respectively; $P_{2,0} = 96,000$; and $P_{1,0} = 120,000$.

Applying equations (49), (50), and (22), we found $T^* = 0.3659$, $n^* = 3$, and $E[TCU(T^*, n^*)] = \$2,164,111$. The behavior of $E[TCU(T, n)]$ with respect to different α values under both nonlinear and linear relationships is displayed in Figure 11. It shows that as α increases, $E[TCU(T, n)]$ declines. Specifically, $E[TCU(T, n)]$ is reduced by 2.04% at $\alpha = 0.5$. That is a savings of \$45,086 (for it decreases from \$2,209,197) in comparison with the result from the earlier linear case. This analytical outcome reveals as common part's value is higher, $E[TCU(T, n)]$ decreases further in comparison with the earlier linear case.

For comparison purpose, Figure 10 exhibits impacts of different values of completion rate α to T^* for both the fabrication schemes with single-machine and two-machine. It reveals that as α increases, T^* decreases significantly, and T^* has reduced by 24.75% at $\alpha = 0.5$ (i.e., it declines from 0.5906 to 0.4444) as compared to the result from a prior work which employed a fabrication scheme with single stage [30]. Additional analysis also indicates that T^* has reduced 3.39% further (at $\alpha = 0.5$) comparing to the result from a two-stage fabrication scheme using one machine [8]. Clearly, the fabrication cycle length (or response time) is notably reduced in the proposed fabrication scheme in comparison with either the single-stage [30] or the two-stage single-machine production models [8].

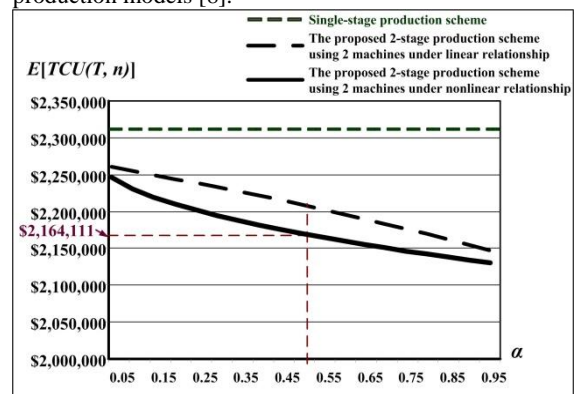


Figure 11. The behavior of $E[TCU(T, n)]$ with respect to different α values under both nonlinear and linear relationships

Figure 12 illustrates the impacts of different values of α to T^* for both two-machine and single-machine manufacturing schemes under both nonlinear and linear relationships. It specifies that as α increases, T^* declines notably. Moreover, at $\alpha = 0.5$, T^* is shortened by 17.66% (i.e., it decreases from 0.4444 to 0.3659) in comparison with earlier linear case. Additional analysis points out that at $\alpha = 0.5$, T^* is cut down by 8.32% (i.e., T^* declines from 0.3991 to 0.3659) in comparison with the result in a prior work on a multiproduct two-stage single-machine manufacturing system with postponement and under the same nonlinear relationship [8]. Finally, if we judge the obtained results of nonlinear relationship case against that of a single-stage multi-item production system [30], we realize a significant 38.05% reduction in production cycle time at $\alpha = 0.5$ (i.e., T^* declines from 0.5906 to 0.3659).

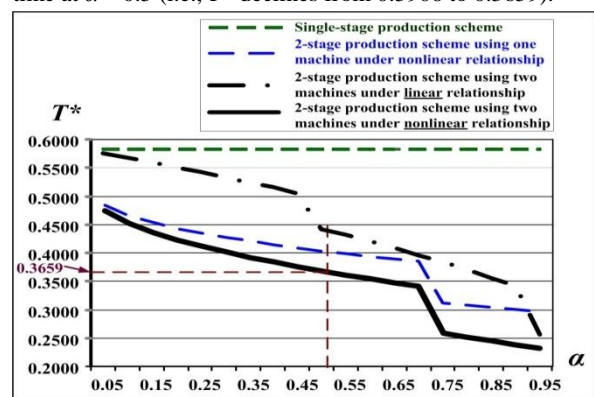


Figure 12. The impacts of different values of α on T^* for both two-machine and single-machine manufacturing schemes under both nonlinear and linear relationships

4. Conclusions

A two-machine fabrication scheme is proposed to re-explore a multiproduct manufacturing system featuring commonality of part, postponement strategy, and quality assurance (which was investigated previously [8] using a single-machine scheme). The objective is to further shorten the cycle time. Distinctively, in the first fabrication stage, machine one exclusively fabricates all common parts that needed by production of end products, and in stage two, a separate machine fabricates the end-product under a rotation cycle time discipline. With the help of mathematical modeling, optimization methods, and a numerical illustration, the proposed system is capable of not only deriving the best fabrication-delivery policy (see Figure 7), but also demonstrating that the proposed fabrication scheme is a beneficial choice in saving cost and shortening fabrication cycle length (Figures 9–12) in comparison with that obtained from a single-machine scheme.

The obtained analytical results exclusively expose the following valuable managerial information: (a) the behavior of $E[TCU(T, n)]$ with respect to α ; (b) the impacts of different α values to T^* for both the fabrication schemes with single-machine and two-machine, and under both nonlinear and linear relationship of component's value; (c) the behavior of $E[TCU(T, n)]$ with respect to α for both nonlinear and linear relationships.

In summary, without an in-depth exploration on such a particular multi-item system utilizing a two-machine manufacturing scheme, the aforementioned valuable information remains inaccessible to managerial decision makings. For future research, examining effect of machine failure on the operating decisions is a practical direction.

Acknowledgements

This study was supported by the Ministry of Science and Technology of Taiwan (grant #: MOST 102-2410-H-324-015-MY2).

References

- [1] W. Zinn, "Developing heuristics to estimate the impact of postponement on safety stock". *International Journal of Logistics Management*, Vol. 1 (1990) 11-16.
- [2] H.L. Lee, C.S. Tang, "Modelling the costs and benefits of delayed product differentiation". *Management Science*, Vol. 43 (1997) 40-53.
- [3] J.M. Swaminathan, S.R. Tayur, "Managing broader product lines through delayed differentiation using vanilla boxes". *Management Science*, Vol. 44 (1998) S161-S172.
- [4] R.I. Van Hoek, B. Vos, H.R. "Commandeur, Restructuring European Supply Chains by Implementing Postponement Strategies". *Long Range Planning*, Vol. 32 (1999) 505-518.
- [5] B. Yang, N. Burns, "Implications of postponement for the supply chain". *International Journal of Production Research*, Vol. 41 (2003) 2075-2090.
- [6] S. Kumar, J. Wilson, "A manufacturing decision framework for minimizing inventory costs of a configurable off-shored product using postponement". *International Journal of Production Research*, Vol. 47 (2009) 143-162.
- [7] S.S. Saghir, A. Hill, "Supplier relationship impacts on postponement strategies". *International Journal of Production Research*, Vol. 52 (2014) 2134-2153.
- [8] S.W. Chiu, J-S. Kuo, V. Chiu, Y-S.P. Chiu, "Cost minimization for a multi-product fabrication-distribution problem with commonality, postponement, and quality assurance". *Mathematical and Computational Applications*, Vol. 21(3) (2016) Art. No. 38, 1-14.
- [9] D.A. Collier, "Aggregate safety stock levels and component part commonality". *Management Science*, Vol. 28 (1982) 1296-1303.
- [10] Y. Gerchak, M. Henig, "An inventory model with component commonality". *Operations Research Letters*, Vol. 5(3) (1986) 157-160.
- [11] A. Garg, C.S. Tang, "On postponement strategies for product multiple points of differentiation". *IIE Transactions*, Vol. 29 (1997) 641-650.
- [12] R. Ernst, B. Kamrad, "Evaluation of supply chain structures through modularization and postponement". *European Journal of Operational Research*, Vol. 124 (2000) 495-510.
- [13] R.S. Tibben-Lembke, Y. Bassok, "An inventory model for delayed customization: A hybrid approach". *European Journal of Operational Research*, Vol. 165 (2005) 748-764.
- [14] G.A. Graman, "A partial-postponement decision cost model". *European Journal of Operational Research*, Vol. 201 (2010) 34-44.
- [15] F. Bernstein, G.A. DeCroix, Y. Wang, "The impact of demand aggregation through delayed component allocation in an assemble-to-order system". *Management Science*, Vol. 57(6) (2011) 1154-1171.
- [16] S. Qrunfleh, M. Tarafdar, "Lean and agile supply chain strategies and supply chain responsiveness: The role of strategic supplier partnership and postponement". *Supply Chain Management*, Vol. 18 (2013) 571-582.
- [17] Y-S.P. Chiu, J-S. Kuo, S.W. Chiu, Y-T. Hsieh, "Effect of delayed differentiation on a multi-product vendor-buyer integrated inventory system with rework". *Advances in Production Engineering & Management*, Vol.11(4) (2016) 333-344.
- [18] M.J. Rosenblatt, H.L. Lee, "Economic production cycles with imperfect production processes". *IIE Transaction*, Vol.18 (1986) 48-55.
- [19] M. Henig, Y. Gerchak, "Structure of periodic review policies in the presence of random yield". *Operations Research*, Vol. 38 (1990) 634-643.
- [20] A.M. Zargar, "Effect of rework strategies on cycle time". *Computers & Industrial Engineering*, Vol. 29 (1995) 239-243.
- [21] H-M. Wee, Y-S. Shum, "Model development for deteriorating inventory in material requirement planning systems". *Computers & Industrial Engineering*, Vol. 36 (1999) 219-225.
- [22] R.H. Teunter, S.D.P. Flapper, "Lot-sizing for a single-stage single-product production system with rework of perishable production defectives". *OR Spectrum*, Vol.25 (2003) 85-96.
- [23] D. Ojha, B.R. Sarker, P. Biswas, "An optimal batch size for an imperfect production system with quality assurance and rework". *International Journal of Production Research*, Vol. 45 (2007) 3191-3214.
- [24] W-N. Ma, D-C. Gong, G.C. Lin, "An optimal common production cycle time for imperfect production processes with scrap". *Mathematical and Computational Modelling*, Vol. 52 (2010) 724-737.
- [25] T. Chakraborty, S.S. Chauhan, B.C. Giri, "Joint effect of stock threshold level and production policy on an unreliable production environment". *Applied Mathematical Modelling*, Vol. 37 (2013) 6593-6608.
- [26] P. Jawla, S. R. Singh, "Multi-item economic production quantity model for imperfect items with multiple production setups and rework under the effect of preservation technology and learning environment". *International Journal*

- of Industrial Engineering Computations, Vol. 7(4) (2016) 703-716.
- [27] Y. Hu, Z. Li, J. Zhao, L. Ren, D. Wang, "Optimization of hydraulic fracture-network parameters based on production simulation in shale gas reservoirs." *Journal of Engineering Research*, Vol. 4(4) (2016) 214-235.
- [28] J. Gómez, I. Salazar, P. Vargas, "Sources of information as determinants of product and process innovation". *PLoS ONE*, Vol. 11(4) (2016) Article No. e0152743.
- [29] S.W. Chiu, S-W. Chen, C-K. Chang, Y-S.P. Chiu, "Optimization of a multi-product intra-supply chain system with failure in rework." *PLoS ONE*, Vol. 11(12) (2016) Article No. e0167511.
- [30] A. Romero-Jabalquinto, A. Velasco-Téllez, P. Zambrano-Robledo, B. Bermúdez-Reyes, "Feasibility of manufacturing combustion chambers for aeronautical use in Mexico". *Journal of Applied Research and Technology*, Vol. 14(3) (2016) 167-172.
- [31] B. Mičičeta, J. Herčko, M. Botka, N. Zrnčić, "Concept of intelligent logistic for automotive industry". *Journal of Applied Engineering Science*, Vol.14(2) (2016) 233-238.
- [32] K.S. Dinesh, A.R. Ashwanth, S. Karthikeyan, G.K. Nithyanandam, "Investigation to improve the new product development process of mono block pump using additive manufacturing". *International Journal of Mechanical and Production Engineering Research and Development*, Vol. 6(2) (2016) 77-88.
- [33] N. Abilash, M. Sivapragash, "Optimizing the delamination failure in bamboo fiber reinforced polyester composite". *Journal of King Saud University - Engineering Sciences*, Vol. 28(1) (2016) 92-102.
- [34] M. Rakyta, M. Fusko, J. Herčko, L. Závodská, N. Zrnčić, "Proactive approach to smart maintenance and logistics as a auxiliary and service processes in a company". *Journal of Applied Engineering Science*, Vol. 14(4) (2016) 433-442.
- [35] P. Jindal, A. Solanki, "Integrated supply chain inventory model with quality improvement involving controllable lead time and backorder price discount". *International Journal of Industrial Engineering Computations*, Vol. 7(3) (2016) 463-480.
- [36] A. Ajbar, E. Ali, "Study of advanced control of ethanol production through continuous fermentation". *Journal of King Saud University – Engineering Science*, Vol. 29(1) (2017) 1-11.
- [37] S. Kovalevskyy, O. Kovalevska, P. Dašić, D. Ješić, P. Kovač, "Engineering consulting technology in production engineering intelligent mobile machines". *International Journal of Industrial Engineering and Management*, Vol. 8(4) (2017) 203-208.
- [38] L. Oblak, M.K. Kuzman, P. Grošelj, "A fuzzy logic-based model for analysis and evaluation of services in a manufacturing company". *Journal of Applied Engineering Science*, Vol. 15(3) (2007) 258-271.
- [39] I.D. Wangsa, "Greenhouse gas penalty and incentive policies for a joint economic lot size model with industrial and transport emissions". *International Journal of Industrial Engineering Computations*, Vol. 8(4) (2017) 453-480.
- [40] M. Abubakar, U. Basheer, N. Ahmad, "Mesoporosity, thermochemical and probabilistic failure analysis of fired locally sourced kaolinitic clay". *Journal of the Association of Arab Universities for Basic and Applied Sciences*, Vol. 24 (2017) 81-88.
- [41] H. Kaylani, A. Almuhtady, A. M. Atieh, "Novel approach to enhance the performance of production systems using lean tools". *Jordan Journal of Mechanical and Industrial Engineering*, Vol. 10(3) (2016) 215-229.
- [42] Y-S.P. Chiu, C-J. Liu, M-H. Hwang, "Optimal Batch Size Considering Partial Outsourcing Plan and Rework". *Jordan Journal of Mechanical and Industrial Engineering*, Vol. 11(3) (2017) 195-200.
- [43] R.L. Rardin, *Optimization in Operations Research*, Int. Ed., Prentice-Hall, New Jersey, 1998.

Appendix A

Nomenclature

For $i = 0, 1, 2, \dots, L$

- Q_i = fabrication batch size,
 φ_i = scrap rate of product i , where $0 \leq \varphi_i \leq 1$,
 $t_{1,i}$ = uptime of product i ,
 $t_{2,i}$ = rework time of product i ,
 $t_{3,i}$ = shipping time of product i ,
 $H_{1,i}$ = level of perfect quality product i when regular production ends,
 $H_{2,i}$ = level of perfect quality product i when rework process finishes,
 K_i = setup cost,
 C_i = unit manufacturing cost,
 $C_{R,i}$ = unit rework cost,
 $C_{S,i}$ = unit disposal cost,
 $h_{1,i}$ = holding cost per product,
 $h_{2,i}$ = holding cost per reworked item,
 $h_{4,i}$ = holding cost per safety stock,

For $i = 1, 2, \dots, L$

- $K_{1,i}$ = fixed cost per delivery of product i ,
 $C_{T,i}$ = unit shipping cost of product i ,
 $t_{n,i}$ = fixed time interval between two succeeding deliveries,
 H_i = level of common part in the beginning of fabrication of end item i ,
 $I_c(t)_i$ = customer's stock level of product i at time t ,
 $h_{3,i}$ = holding cost per product for customer's stock,
 I_i = the left-over quantities of product i in each $t_{n,i}$ at customer's side,
 D_i = quantities of finished items for product i per delivery.

Other notation:

- T = rotation cycle length – a decision variable,
 n = number of deliveries per cycle – a decision variable,
 α = common part's completion rate in comparison with finished product,
 $E[T]$ = the expected fabrication cycle length,
 $TC_1(T, n)$ = stage one's total cost per cycle,
 $E[TC_1(T, n)]$ = stage one's expected cost per cycle,
 $E[TCU_1(T, n)]$ = stage one's expected cost per unit time,
 $TC_2(T, n)$ = stage two's total cost per cycle,
 $E[TC_2(T, n)]$ = stage two's expected total cost per cycle,
 $E[TCU_2(T, n)]$ = stage two's expected total cost per unit time,
 $E[TCU(T, n)]$ = the expected system cost per unit time.

Optimal Off-Grid Hybrid Renewable Energy System for Residential Applications Using Particle Swarm Optimization

Osama Abuzeid^{a,*}, Amjad Daoud^b, Mahmoud Barghash^c

^a Mechanical Engineering Department, The University of Jordan, Amman 11942, Jordan

^b Engineering Department, Higher Colleges of Technology, United Arab Emirates, Al Ain

^c Industrial Engineering Department, The University of Jordan, Amman 11942, Jordan

Received 1 May, 2019

Abstract

We propose a hybrid off-grid energy system that comprises photovoltaic panels, wind turbines, diesel generators, and a battery bank. The proposed system could be adjusted to reflect real world conditions in order to optimize the cost of energy. Using Particle Swarm optimization searching methods, an optimal combination that follows load demand data of a typical house is found. From this configuration, the optimal mix that minimizes the leveled cost of energy (LCE) is formed and is found to be comparable to the cost of grid electricity.

© 2019 Jordan Journal of Mechanical and Industrial Engineering. All rights reserved

Keywords: off-grid, hybrid, Particle Swarm optimization (PSO), Levelized Cost of Energy (LCE);

Nomenclature

This part includes explanation of the symbols used in Equations 1 and 2, represent the core of the PSO algorithm [2,4,12,17,24,30].

V_i^K : denotes the velocity of particle i at the K_{th} iteration (scalar value).

V_i^{K+1} : the updating the velocity of particle i at the $(K+1)_{th}$ iteration (scalar value).

X_i^K : denotes the position of particle i at the K_{th} iteration (scalar value).

X_i^{K+1} : the updating the position of particle i at the $(K+1)_{th}$ iteration (scalar value).

w : weighting inertial coefficient; its value is typically between 0.8 and 1.2, which can either dampen the particle's inertia or accelerate the particle in its original direction. Thus a large value of w makes the algorithm constantly explore new areas without much local search and hence fails to find the true optimum. To achieve a balance between global and local exploration to speed up convergence to the true optimum, an inertia weight w whose value decreases linearly with the iteration number has been used.

c_1 : A cognitive (individual) learning coefficient; usually close to 2 and affects the size of the step the particle takes toward its individual best candidate solution.

c_2 : A social (group) learning coefficient; is typically close to 2 and represents the size of the step the particle takes toward the global best candidate solution the swarm has found up until that point.

The parameters c_1 and c_2 denote the relative importance of the memory (position) of the particle itself to the memory (position) of the swarm.

r_1 and r_2 are uniformly distributed random numbers in the range 0 and 1.

The random values r_1 in the cognitive (individual) component and r_2 in the social (group) component cause these components to have a stochastic influence on the velocity update. This stochastic

nature causes each particle to move in a semi-random manner heavily influenced in the directions of the individual best solution of the particle and global best solution of the swarm.

P_{best}^k : Every particle has a memory of its own best position; denoted by personal best. It is the best experience of the particle i .

g_{best}^k : In addition to this personal best there is a common best experience – among the members of the swarm denoted by global; global common experience among the members of the swarm.

Each particle tries to modify its position using the following information:

1. The current positions, X_i^k
2. The current velocities, V_i^k
3. The distance between the current position and personal best; $P_{best}^k - X_i^k$
4. The distance between the current position and the global best; $g_{best}^k - X_i^k$

The three terms of Equation 1:

$w^k \cdot V_i^k$: This first term is the inertia component, responsible for keeping the particle moving in the same direction it was originally heading.

$c_1 \cdot r_1 \cdot (P_{best}^k - X_i^k)$: This second term, called the cognitive (individual) component, acts as the particle's memory, causing it to tend to return to the regions of the search space in which it has experienced high individual fitness.

$c_2 \cdot r_2 \cdot (g_{best}^k - X_i^k)$: This third term, called the social (group) component, causes the particle to move to the best region the swarm has found so far.

1. Introduction

Rural communities face a major obstacle in sourcing their modest energy needs; mainly lighting and electric appliances. So, it is difficult for rural households living off-grid to keep their lights on affordably and reliably levels; a major impediment to the development of their

* Corresponding author e-mail: oabuzeid@ju.edu.jo.

communities. This is even more evident in developing countries [1-5].

Also, sometimes it is cost prohibitive to connect them to the nearest electricity grid; a problem known as “*the last mile problem*” and “*power loss problem*” [6] may make connecting them unattractive to major electric distributors. So the only practical solution is to generate electricity locally or what is called “*distributed generation*”.

Distributed generation from renewable energy sources (*RES*) has attracted the attention of many policy makers, universities and scientists looking for practical and realistic off-grid methods of electric generation and storage that can effectively replace conventional fossil fuels of oil, gas and coal. Renewable energy sources allow the use of natural resources, but their intermittency would prove inadequate mainly when the wind is not blowing, the sun is not shining, or the rivers are shallow. However, combining these natural renewable energy sources with conventional diesel generation and energy storage systems in “*hybrid renewable energy systems*” (*HRES*) may offer a reliable electric distributed generation and minimal diesel requirements to cope with the “*worst month*” problem [7]. *HRES* advantages include best use of the renewable power generation technologies operating characteristics and efficiencies higher than that could be obtained if a single power source is used [8]. The utilization of two or more *RES* may provide an economic solution as well for off-grid locations with significant weather changes and seasonal variations. It can be either grid connected or stand-alone mode. Stand-alone or off-grid is preferable due to recent advances in renewable energy technologies and highly efficient power electronics converters which are used to convert the unregulated power generated from renewable sources into useful power where it is required at the load end [9]; eliminating “*the power loss problem*” altogether.

Furthermore, *HRES* addresses *RES* limitations in terms of flexibility, efficiency, reliability, emissions and economics:

- Fossil fuel flexibility: Usually off-grid systems would rely solely on diesel generators, but due to the high cost of sourcing fossil fuel, diesel-based electric generation became uneconomic and costly.
- Reliability and cost are two of *HRES* advantages: it is possible to confirm that hybrid generation systems are usually more reliable and less costly than systems that rely on a single source of energy [5, 10-12].
- The rise of importance of renewable energy sources that fill the gap between nonrealistic free energy sources such as nuclear fusion and the need to provide electric services during the day from wind and solar panels when the sun shines and at night from the wind and battery storage.
- In various research papers [13-18, 2], it has been proven that hybrid renewable electrical systems in off-grid applications are economically viable; especially in remote locations. In addition, climate can make one type of hybrid system more profitable than another type. For example, photovoltaic hybrid systems (Photovoltaic–Diesel–Battery) are ideal in areas with warm climates [5,19].
- Lastly, it has been studied that due to the high initial cost of the system, government subsidies are required to adopt the system on a large-scale basis in remote

areas [20,21]. Even though the cost of distributed generation of electricity from most of the hybrid energy systems are higher than that of the national grid electricity tariff, “*the last mile problem*” makes the cost of national grid extension to these remote areas difficult and uneconomical [5,16,17].

A common solution for off-grid power supply in small and medium-sized energy systems is a fuel generator set [22]; however, the following current developments have sought to improve the competitiveness and desirability of alternative off-grid hybrid renewable energy systems:

- Steeply decreasing production costs of renewable energy technologies like solar, wind and biomass caused a boom in the respective technologies in developed countries,
- Expanding research in electric storage devices sparked by the plans of several countries to use electric vehicles in the near future,
- Increasing environmental concerns and awareness of climate changes provoked by *CO₂* emissions produced by the combustion of fossil fuels and
- Increasing operation costs for fuel generator sets due to rising oil prices.
- Several literatures have studied the sizing of hybrid energy systems:
- A simple general method for the optimization of the power generated from Hybrid Renewable Energy Systems (*HRES*) to achieve a typical house electric load as an example was presented in [6]. Particle Swarm Optimization Technique (*PSO*) is utilized as the optimization searching algorithm due to its advantages over other techniques for minimizing the “*Levelized Cost of Energy*” (*LCE*) with an acceptable production rate and minimal power loss [6].

Others [2,4,17,23,24] concluded that focusing on the installation cost alone is not enough for a hybrid renewable energy system (*HRES*) sizing methodology and the sizing model will be based on a simplified cost analysis. Besides the installation cost, Operation and maintenance (*O&M*) costs take up a large proportion of the overall cost of the system over its lifetime and must be taken into consideration. Thus, a method was developed to calculate long-term energy production costs for a hybrid wind–diesel system by taking into consideration fixed and variable costs of maintenance, operation and financing, and initial costs [2,4,17,23,24].

Alternatively, in [25] an algorithm was developed to optimize the size of a standalone hybrid wind–diesel system considering reactive power balancing conditions.

The optimal combination of components of a hybrid renewable energy system (*HRES*) were evaluated to meet the power demand and its reliability considering the loss of load probability (*LOLP*) [26].

The loss of load probability (*LOLP*) sensitivity analysis on total installation cost of the considered hybrid renewable energy system (*HRES*) was studied in [27].

From a different perspective, authors in [28] described an optimal energy storage sizing method by considering the compensation cost of wind power and load curtailment. Furthermore, authors in [1] researched the optimal size of batteries and diesel generator usage in a hybrid system which consists of wind turbines, photovoltaic panels (*PV*), diesel generator and battery storage. They introduced a

sizing model that predicts the optimum configuration of a hybrid system and implemented it as a graphical user interface. In particular, their paper's sizing model simulates real time operation of the hybrid system, using the annual measured hourly wind speed and solar irradiation. The benefit of using time series approach is that it reflects a more realistic situation; here, the peaks and troughs of the renewable energy resource are a central part of the sizing model [1].

A general model of a hybrid off-grid energy system using linear programming methods was developed in [29]. This algorithm can be adjusted to reflect real conditions in order to achieve economical and ecological optimization of off-grid energy systems. The operation of this model was tested in two real off-grid energy systems, where both optimization processes resulted in hybrid energy systems, utilizing photovoltaic (PV), lead-acid batteries and a diesel generator as a load-balancing facility [29].

2. Particle swarm optimization, PSO

Particle Swarm Optimization simulates the social behavior of birds flocking or other natural creatures. Each bird represents a feasible solution in PSO. The solution in this case if two vectors representing position in solution space and a velocity. PSO in this case attempts to discover optimal solution through iteratively calculating the position solutions and modifying the velocities to follow the best known solutions. This is similar to birds following their leader in a spectacular view of intelligence. PSO was invented by Kennedy and Eberhart [30] and represents an important population-based metaheuristic algorithm. Using iterative methodology, the particles fly through the

N -dimensional space to discover the global optimal. Two main equations are traditionally used to govern the PSO namely velocity equation and position equation.

$$V_i^{k+1} = w^k \cdot V_i^k + c_1 \cdot r_1 \cdot (P_{best}^k - X_i^k) + c_2 \cdot r_2 \cdot (g_{best}^k - X_i^k) \quad (1)$$

Equation 1 shows the velocity equation for the PSO algorithm in an iterative manner. The $k+1$ iteration velocity for particle i is a combination of a memory value of the same velocity multiplies by an inertia parameter w , and a tendency value towards the current best value P_{best} and the global best g_{best} for the k^{th} iteration multiplied by a limiting acceleration constant values c_1 and c_2 . Random variables r_1 and r_2 are used to enhance the search through varying the tendency components from iteration to iteration and from particle to another particle.

$$X_i^{k+1} = X_i^k + V_i^k \quad (2)$$

Equation 2 shows the position equation for the PSO algorithm. This is a simple linear distance calculation assuming the time difference equal to iteration difference between the $k+1$ and k which is 1. To assist the PSO in focusing in finding the optimal value, the velocity memory value inertia factor is reduced iteratively through the use of Equation 3.

$$w = w_{Max} - \left(\frac{w_{Max} - w_{Min}}{iter} \right) \times iter \quad (3)$$

where w_{Max} and w_{Min} are the initial and final values of the inertia weight, respectively, and $iter$ is the maximum number of iterations used in PSO. The values of $w_{Max} = 0.9$ and $w_{Min} = 0.4$ are commonly used.

A full schematic for the operation of the PSO is shown in Figure 1 below.

3. Hybrid system optimization Algorithm

The algorithm is shown in Figure 2. Initially, hourly solar irradiance (kW/m^2) and wind speed (m/s) for the University of Jordan with Latitude: $32^\circ 00' 30.00''$ N and Longitude: $35^\circ 52' 13.19''$ E were obtained using HOMER, [31]. Such data were used in order to determine the feasibility of our system and to perform the optimization. An energy load profile, or consumption profile; explains how energy used throughout the day, is obtained. The load profile is assumed constant all over the year, and it is also integrated to the data tables extracted from HOMER.

We then obtain the produced power using rate 1 kW using the following simplified equations:

$$P_w(kW) = \begin{cases} k_w \times v_w; & 3 < v_w < 25 \\ 0; & otherwise \end{cases} \quad (4)$$

where P_w is the wind generated power, v_w : is the wind speed, m/s, and $k_w = 0.03$ is a constant considered for simplified LCE.

$$P_s(kW) = k_s * SI \quad (kW/m^2) \quad (5)$$

where P_s : the solar generated power, SI is the solar irradiance; the power per unit area received from the sun, and $k_s = 1.9$ is a constant considered for simplified LCE.

The PSO particle represents a solution (not optimal yet) for the system that is composed of three parameters and a complementary fourth:

1. Solar system solution kW,
2. Wind solution kW,
3. Battery storage solution kWh and
4. Generator maximum rated capacity in kW.

For each particle, the system is run for a full year and for each hour of the year. We calculate the extra needed power which is the power produced by both solar and wind that is more than the household load power needed as in Figure 3.

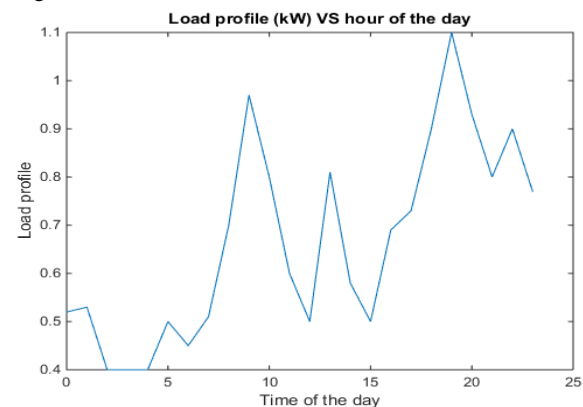


Figure 3. Load Profile

The algorithm then goes into deciding if this amount can be stored into the battery system and if so, the power is stored into the battery. Otherwise, the power is dumped. If the extra power turned to be negative that is less power is generated than load profile power needed.

If the power stored in the battery is greater than the needed power; it is pulled from the battery; otherwise we use the generator to generate the extra amount. Now we modify the capacity of the generator according to the new requirement.

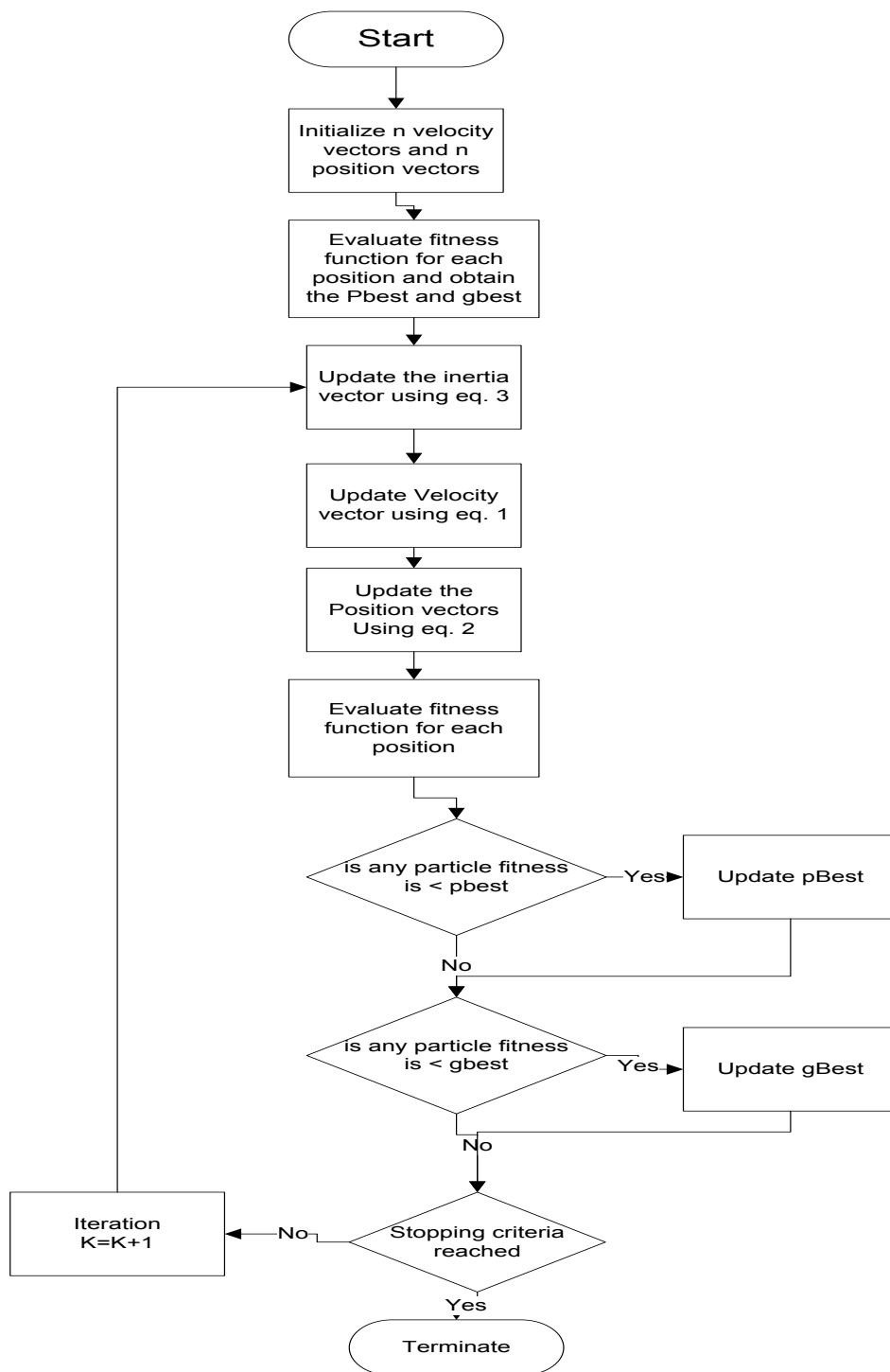


Figure 1. PSO flow chart

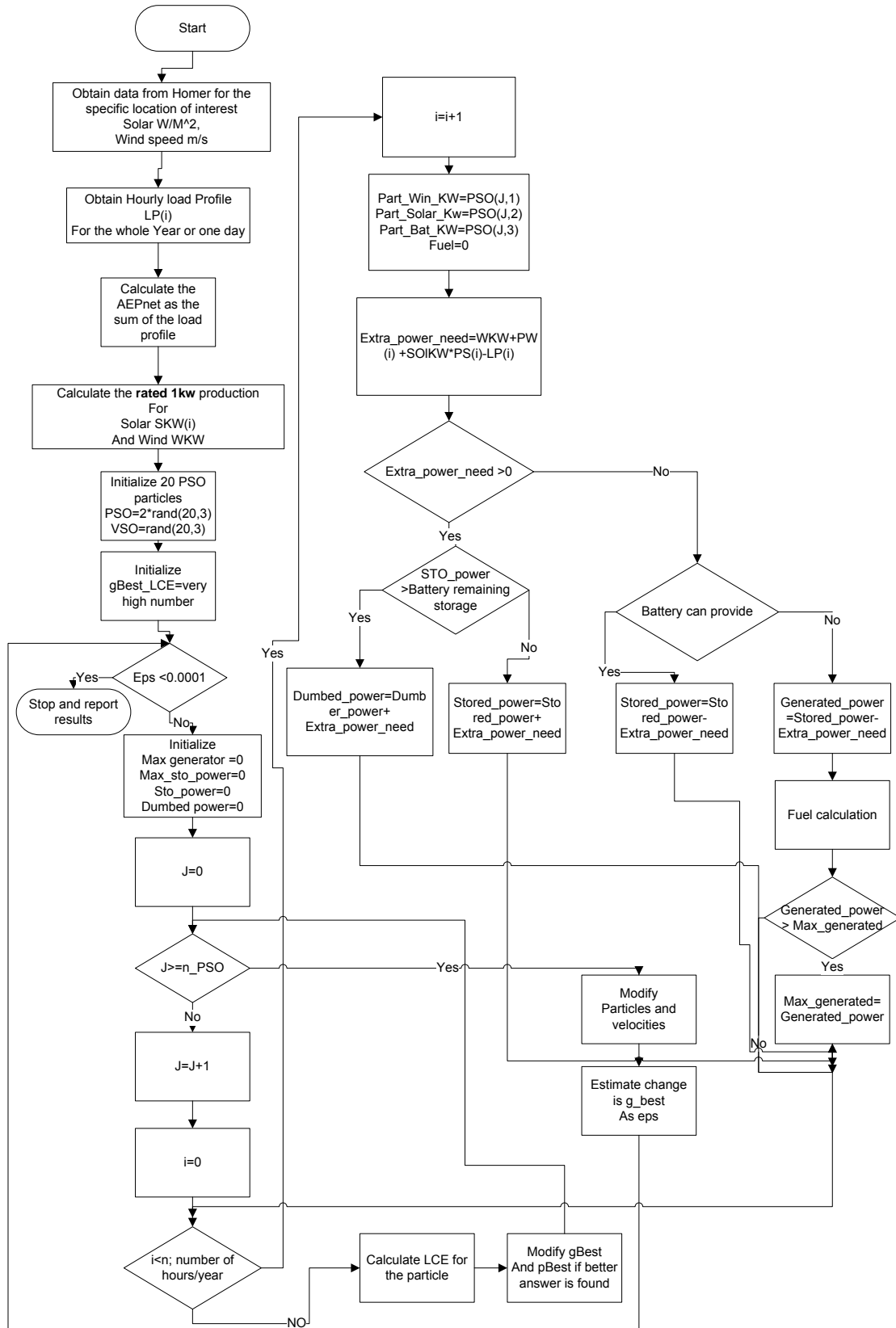


Figure 2. Hybrid system optimization Algorithm

The model of the fuel consumption as a function of the power generated is approximately:

$$F_c = 3.2 \times 10^{-6} P_F^3 + 1.0 \times 10^{-3} P_F^2 + 0.4 P_F + 2.2 \quad (6)$$

where F_c is the fuel consumption in liter/hour and P_F is the power generated by the diesel generator in kW [1].

The total required power is used to calculate the levelized cost of energy (LCE), by dividing the total sum of the cost by the net Annual Energy Produced (AEP_{net}) as follows for each solution, [6]:

$$LCE = \frac{(CRF \times TPI) + (O\&M) + (LO\&R)}{AEP_{net}} \quad (7)$$

where: TPI is the total plant investment and in this work it is defined as $TPI = (P_s \times C_s + P_w \times C_w + P_f \times C_f + Bat \times C_B)$; where C_s is the cost of solar power \$/kW, C_w is the cost of wind power \$/kW, C_f is the cost of diesel generated power (Fuel) \$/kW, and C_B is the cost of Battery energy \$/kWh, CRF is the Capital Recovery Factor given as:

$$CRF = \frac{i(1+i)^n}{(1+i)^n - 1} \quad (8)$$

where i is the interest rate (7.5%) and n is the operational life (25 years), and $CFR=0.09$. $O\&M$ is the annual Operating and Maintenance cost, and $LO\&R$ is the periodic Levelized Overhaul and Replacement cost.

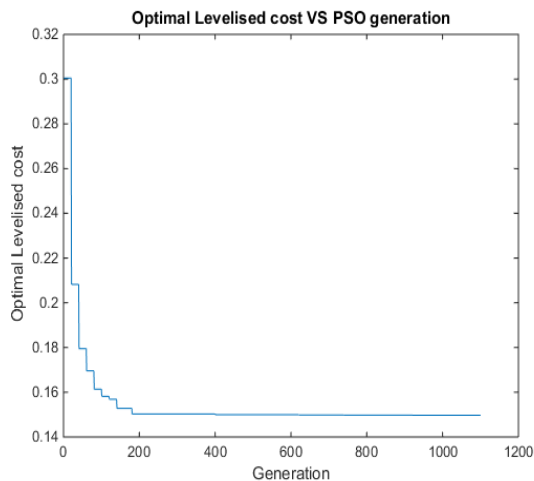


Figure 4. Optimal LCE

The g_{best} and the P_{best} is modified and the PSO particles and velocities are modified according to Equations 1 and 2. In case the modifications of the g_{best} is less than the eps ; which is the convergence criteria; then we have an optimal solution and the algorithm is stopped as shown in Figure 4.

4. Results and Discussion

Due to the variability in prices of solar panels, wind turbines and battery units; we have run the PSO algorithm for several probable prices of these items. Consequently, different solutions are obtained for these different actual or hypothetical situations. Table 1 shows the optimal results.

Table 1. Different optimal solutions with different assumptions

Prices \$/kWh				Solution kWh				Optimal LCE
Solar	Wind	Battery	Generator	Solar	Wind	Battery	Generator	
550	550	500	100	6	0.8	0.3	0.77	0.148
550	550	100	100	3	1.78	0.63	0.32	0.087
550	550	45	100	2.75	1.76	0.70	0.34	0.071
300	550	45	100	3.82	0.28	0.85	1	0.057
300	550	100	100	5.54	0.47	0.44	0.95	0.07
300	300	100	100	5.02	1.26	0.41	0.65	0.068
300	300	45	100	3.65	0.90	0.75	0.81	0.056

From the table, we notice that the price of the batteries is the decisive factor in the optimal capacity of the HRES system. If we reduce battery prices from 500 to 45, we can reduce the capacity of the needed system from (6 kW solar, 0.8 kW wind) to (3.82 kW solar, 0.28 kW wind). Furthermore, reducing the prices of solar and wind will likely increase their contribution to the optimal solution.

In Table 2, we compare our LCOE results to similar research reported in [32-36].

Table 2. Comparison of Obtained Results with Previous Similar Research

Reference Year	LCOE \$/kWh	Notes
[32] 2018	0.37	The annual average wind speed is 2.22 m/s, which is considered inadequate for wind energy production. The monthly average irradiance value is minimum in August, with the value of 3.90 kWh/m ² /day and maximum in March having a value of 6.05 kWh/m ² /day.
[33] 2017	0.25	The annual average solar irradiation and wind speed are 5.57 kWh/m ² /day and 7.29 m/s, respectively.
[34] 2019	0.22	The annual average global solar radiation (5.23-6.57 kWh/m ² /day) as well as substantial wind-speed (3.0-4.37 m/s)
[35] 2019	0.12	The annual average wind speed of 3.6 m/s Similarly, average value of daily solar radiations was estimated to be 4.13 kWh/m ² /day
[36] 2015	0.08	The annual average wind speed is 4.67 m/s scaled annual average radiations are 5.45704 kWh/m ² /day
Our work	0.057	(3.82 kW solar, 0.28 kW wind)

Comparing LCOEs as shown in Table 2 need to be considered with caution as the LCOE calculation depends heavily on the following assumptions which must be provided and justified [37]:

- Degradation rate of solar panels efficiency over their lifetime.
- Scale, size and cost, including cost breakdown (residential, commercial, and utility scale).
- Capacity factor, solar insolation, geographic location, and shading losses.
- Lifetime of project and financial terms: financing (interest rate, term, equity/debt ratio cost of capital), and discount rate.
- Additional terms: inflation, incentives, credits, taxes, depreciation, carbon credits etc.

Since the inputs for the algorithm are highly variable; there is a need for using sensitivity analysis to represent actual variable distributions so that overconfidence in a single set of assumptions may be avoided.

5. Conclusions

During the course of this crucial study presented in this paper; we observed that the *PSO* searching technique tends to converge well after a short period of time with an optimal solution. Also, when using a lower battery price, the optimal solution tends to use lower capacity for wind and solar. Furthermore, because of the variability in both solar and wind, the best solution will have both; but the amount of each in the optimal solution will depend on its cost.

References

- [1] L. Gan, J. Shek, M. Mueller. Hybrid wind–photovoltaic–diesel–battery system sizing tool development using empirical approach, life-cycle cost and performance analysis: A case study in Scotland. *Energy Conversion and Management* 2015; 106:479–494, <https://doi.org/10.1016/j.enconman.2015.09.029>.
- [2] Noguera, A.L.G., Castellanos, L.S.M., Lora, E.E.S. and Cobas, V.R.M. Optimum design of a hybrid diesel-ORC / photovoltaic system using PSO: Case study for the city of Cujubim, Brazil. *Energy* 2018, 142:33–45. <https://doi.org/10.1016/j.energy.2017.10.012>
- [3] Olatomiwa, L., Blanchard, R., Mekhilef, S. and Akinyele, D. Hybrid renewable energy supply for rural healthcare facilities: An approach to quality healthcare delivery. *Sustainable Energy Technologies and Assessments* 2018, 30:121–138. <https://doi.org/10.1016/j.seta.2018.09.007>
- [4] Keles, C., Alagoz, B.B and Kaygusuz, A. Multi-Source Energy Mixing for Renewable Energy Microgrids by Particle Swarm Optimization. *International Conference on Artificial Intelligence and Data Processing (IDAP17)*, Malatya, Turkey, 2017, 6 pages. <https://doi.org/10.1109/IDAP.2017.8090163>
- [5] Khare,V., Nema,S. and Baredar,P. Solar–wind hybrid renewable energy system: A review. *Renewable and Sustainable Energy Reviews* 2016, 58:23–33 <https://doi.org/10.1016/j.rser.2015.12.223>
- [6] A. Niez. Comparative study on rural electrification policies in emerging economies. Technical Report, IEA Energy Technology Policy Division 2010.
- [7] Celik, A. Techno-economic analysis of autonomous PV–wind hybrid energy systems using different sizing methods. *Energy Conversion and Management* 2003; 44:1951–1968, [https://doi.org/10.1016/S0196-8904\(02\)00223-6](https://doi.org/10.1016/S0196-8904(02)00223-6).
- [8] Bhattacharjee,S. and Acharya,S. PV–wind hybrid power option for a low wind topography. *Energy Conversion and Management* 2014; 89:942–954, <https://doi.org/10.1016/j.enconman.2014.10.065>.
- [9] Kumar,U. and Manoharan,P. Economic analysis of hybrid power systems (PV/diesel) in different climatic zones of Tamil Nadu. *Energy Conversion and Management* 2014; 80:469–476,<https://doi.org/10.1016/j.enconman.2014.01.046>.
- [10] Muselli,M., Notton,G. and Louche,A. Design of hybrid-photovoltaic power generator, with optimization of energy management. *Solar Energy* 1999; 65(3): 143–157, [https://doi.org/10.1016/S0038-092X\(98\)00139-X](https://doi.org/10.1016/S0038-092X(98)00139-X).
- [11] Bagen,B. and Billinton,R. Evaluation of different operating strategies in small standalone power systems. *IEEE Transaction on Energy Conversion*. 2005; 20(3):654–660, DOI: 10.1109/TEC.2005.847996.
- [12] Mohammadi,M., Hosseinian,S. and Gharehpetian,G. Optimization of hybrid solar energy sources/wind turbine systems integrated to utility grids as microgrid (MG) under pool/bilateral/hybrid electricity market using PSO. *Solar Energy* 2012; 86:112–125, DOI:10.1016/j.solener.2011.09.011.
- [13] Elhadidy,M. and Shaahid,S. Parametric study of hybrid (wind + solar + diesel) power generating systems. *Renewable Energy* 2000; 21(2):129–139, [https://doi.org/10.1016/S0960-1481\(00\)00040-9](https://doi.org/10.1016/S0960-1481(00)00040-9).
- [14] Vera,J.G.. Options for rural electrification in Mexico. *IEEE Transaction on Energy Conversion* 1992; 7(3):426–430, DOI: 10.1109/60.148562.
- [15] Bekele,G. and Tadesse,G. Feasibility study of small Hydro/PV/Wind hybrid system for off-grid rural electrification in Ethiopia. *Applied Energy* 2012; 97: 5–15, <https://doi.org/10.1016/j.apenergy.2011.11.059>.
- [16] Wichert,B. PV–Diesel hybrid energy systems for remote area power generation-A review of current practice and future developments. *Renewable and Sustainable Energy Reviews* 1997; 1(3):209–228, [https://doi.org/10.1016/S1364-0321\(97\)00006-3](https://doi.org/10.1016/S1364-0321(97)00006-3).
- [17] Acakpovi, A. Performance Analysis of Particle Swarm Optimization Approach for Optimizing Electricity Cost from a Hybrid Solar, Wind and Hydropower Plant. *International Journal Of Renewable Energy Research A* 2016, 6(1): 12 pages.
- [18] Laura Tribioli, L and Cozzolino, R. Techno-economic analysis of a stand-alone microgrid for a commercial building in eight different climate zones. *Energy Conversion and Management* 2019, 179:58–71. <https://doi.org/10.1016/j.enconman.2018.10.061>
- [19] Shaahid,S. and Elhadidy,M. Opportunities for utilization of stand-alone hybrid (photovoltaic + diesel + battery) power systems in hot climates. *Renewable Energy* 2003; 28(11):1741–1753, [https://doi.org/10.1016/S0960-1481\(03\)00013-2](https://doi.org/10.1016/S0960-1481(03)00013-2)
- [20] Adaramola,M., Paul,S. and Oyewola,O. Assessment of decentralized hybrid PV solar–diesel power system for applications in Northern part of Nigeria. *Energy for Sustainable Development* 2014; 19:72–82, <https://doi.org/10.1016/j.esd.2013.12.007>.
- [21] Gobinath, T.T, Rajarathnam, P. and Vassallo, A.M. Optimization of a stand-alone photovoltaic-wind-diesel-battery system with multi-layered demand scheduling. *Renewable Energy* 2019, 131:333–347. <https://doi.org/10.1016/j.renene.2018.07.029>
- [22] A. Niez. Comparative study on rural electrification policies in emerging economies. Technical Report, IEA Energy Technology Policy Division 2010.
- [23] Kaldellis,J.K., Kondili,E. and Filios,A. Sizing a hybrid wind–diesel stand-alone system on the basis of minimum long-term electricity production cost. *Applied Energy* 2006; 83:1384–1403, <https://doi.org/10.1016/j.apenergy.2006.01.006>.
- [24] Das, G.S. Forecasting the energy demand of Turkey with a NN based on an improved Particle Swarm Optimization. *Neural Comput & Applic* 2017, 28: S539–S549. <https://doi.org/10.1007/s00521-016-2367-8>
- [25] Saha,T. and Kastha,D. Design optimization and dynamic performance analysis of a stand-alone hybrid wind–diesel electrical power generation system. *IEEE Transaction on Energy Conversion* 2010; 25:1209–1217, doi: 10.1109/TEC.2010.2055870.
- [26] Deshmukh,M. and Deshmukh,S. Modelling of hybrid renewable energy systems. *Renewable Sustainable Energy Reviews* 2008; 12:235–249, <https://doi.org/10.1016/j.rser.2006.07.011>.

- [27] Chen,H. Optimum capacity determination of stand-alone hybrid generation system considering cost and reliability. *Applied Energy* 2013; 103:155–164, <https://doi.org/10.1016/j.apenergy.2012.09.022>.
- [28] Luo,Y., Shi,L. and Tu,G. Optimal sizing and control strategy of isolated grid with wind power and energy storage system. *Energy Conversion and Management* 2014; 80:407–415, <https://doi.org/10.1016/j.enconman.2014.01.061>.
- [29] Huneke,F., Henkel,J., González,J. and Erdmann,G. Optimisation of hybrid off-grid energy systems by linear programming. *Energy Sustainability and Society* 2012; 2-7, <https://doi.org/10.1186/2192-0567-2-7>.
- [30] Eberhart,R. and Kennedy,J. A new optimizer using particle swarm theory. In *Proc. Sixth International Symposium on Micro Machine and Human Science* 1995; 39-43, DOI: 10.1109/MHS.1995.494215.
- [31] HOMER[®] hybrid power system optimization software. Available online: <https://www.homerenergy.com/>
- [32] Ariyo, B.O., Akorede, M.F., Omeiza, I.O.A., Amuda, S.A.Y. and Oladeji, S.A. Optimisation analysis of a stand-alone hybrid energy system for the senate building, university of Ilorin, Nigeria. *Journal of Building Engineering* 2018, 19:285–294, <https://doi.org/10.1016/j.jobee.2018.05.015>
- [33] Lu,J., Wang,W., Zhang,Y. and Song Cheng,S. Multi-Objective Optimal Design of Stand-Alone Hybrid Energy System Using Entropy Weight Method Based on HOMER, *Energies* 2017, 10, 1664;doi:10.3390/en10101664
- [34] Gebrehiwot,K., Mondal,M.A.H., Claudia Ringler,C. and Gebremeskel,A.G. Optimization and cost-benefit assessment of hybrid power systems for off-grid rural electrification in Ethiopia. *Energy* 2019, 177: 234-246. <https://doi.org/10.1016/j.energy.2019.04.095>
- [35] Ali,S. and Jang,C-M. Ali and Choon-Man Jang Evaluation of PV-Wind Hybrid Energy System for a Small Island, Chapter In book: *Wind Solar Hybrid Renewable Energy System*, IntechOpen 2019 <http://dx.doi.org/10.5772/intechopen.85221>
- [36] Niazi,I.K., Khan,M.B. and Wazir,R. Techno-economic analysis of hybrid system (PV/wind/diesel generator/grid) for domestic consumers in balochistan (nokkundi &ormara).*World Journal of Engineering* 2015, 12(1): 29-36. DOI: 10.1260/1708-5284.12.1.29
- [37] Branker, K., Pathak, M. J.M. and Pearce, J. M. “A Review of Solar Photovoltaic Levelized Cost of Electricity”, *Renewable & Sustainable Energy Reviews* 2011, 15: 4470-4482. <http://dx.doi.org/10.1016/j.rser.2011.07.104>

Using Renewable Energy Criteria for Construction Method Selection in Syrian Buildings

Bassam Hassan^a, Madonna Beshara^{b*}

^a Professor, department of Construction Management and Engineering, Faculty of Civil Engineering, Tishreen University, Lattakia, Syria.

^b PHD student, department of Construction Management and Engineering, Faculty of Civil Engineering, Tishreen University, Lattakia, Syria

Received 7 May, 2019

Abstract

Renewable energy criteria can be considered as the first step in the development of the IBS construction industry. They illustrate global criteria that define direct design and construction processes. IBS (Industrialized Building System) has many advantages and benefits that are closely related to renewable energy requirements. The construction sector in Syria - especially in the field of building - is characterized by the domination of traditional methods of building systems. The introduction of modern IBS construction technologies that are compatible with the requirements of renewable is not accompanied by a proven scientific fit and consistent with the administrative decision-making programs for construction and project operations in general. Syria is currently suffering from the great needs of construction imposed by reality, and the need for reconstruction within the possibilities of benefiting from the concept of renewable energy. It has become imperative for everyone working in the field of engineering to keep pace with this development to get the best performance of the work. The research aim is to prioritize the selection of construction methods used in Syria, and to determine how the renewable energy criteria affects the selection within the reconstruction scheme by using the AHP method. The results were as following: The technology advanced prefabrication system had the winning percentage of 37.9% (39.4% in part1). The technical composite system (cast-in-place, pre-cast) came second with 26.5% (21.8% in part1); followed in third place by a low difference developed technology the cast-in-place system gaining 19.9% (20.8%, in part 1); and the last place for conventional building system with 15.6% (18.1% in part 1). Taking renewable energy criteria into consideration will modify the ranking of technological alternatives for construction according to the adaptation of these methods, with the possibility of using renewable energies to replace the traditional ones used to meet the requirements of reconstruction in Syria.

© 2019 Jordan Journal of Mechanical and Industrial Engineering. All rights reserved

Keywords: Industrialized Building System in Syria, Industrialized Building System (IBS), Renewable Energy criteria, Priority of Construction Methods;

1. Introduction

Construction industry forms an evolutionary orientation for construction sector, which is considered one of the important economic sectors, in terms of its role in the formation of fixed capital, gross national product, and the magnitude of its employees [1]. This industry is currently facing unprecedented developmental pressures in our country as a result of the lack of resources and the rising prices of raw material and the instability of environmental factors surrounding it [2]. This encourages us to introduce the new construction, industrial technologies of industrialized building systems (IBS), which are symmetrical with the necessities of renewable energy. Industrialized building systems must keep up with the global trend towards reducing and rationalizing energy consumption in all its forms, and depending on the renewable natural resources in procuring energy which

Commensurate with the necessity of introducing the concept of renewable energy in Building techniques.

Due to the size and magnitude of engineering projects in Syria, it is imperative that everyone working in the field of engineering keeps pace with this development to get the best performance of the work. Hence the need to find a clear approach that enables the project owner to choose the best technical building system, the success of the selection process will be an important tool for project success in general, and management of obstacles that may encounter work environment, and therefore achieve goals of reconstruction in Syria within the possibilities of taking advantage of the concept of renewable energy.

Determining the best technical building system is complicated because each has its own advantages and disadvantages. One of the best decision-making methods in engineering management is the AHP method, where different choices are arranged according to different criteria.

* Corresponding author e-mail: madonnabeshara@hotmail.com

1.1. Research methodology

- Review of previous studies about the construction industry and modern techniques used.
- Determine of the priority to choose one of the technical systems used for construction in Syria using the Expert Choice program.
- And then introduce the criteria of renewable energy in choosing the method of construction and comparing the results with each other.

1.2. Benefits of adopting IBS

The Questionnaire and field survey showed that despite the promotion of benefits in IBS adoption, the industry stakeholders and contractors are still skeptical about the IBS usage since issues such as technical difficulties, enormous capital cost, design conflicts and skill shortages during the construction phase represent the barriers. Accordingly, in addressing a knowledge gap in the construction level, this paper has tried to explain the benefits of using IBS components. The numerous benefits of adopting IBS had been reported by academicians around the world and became the driving force to the construction industry players in deciding whether to use IBS or not [3]. The benefits of IBS adoption are summarized in Table 1.

1.3. Previous studies

The terminology used in the construction industry could hardly be defined, and definitions rely heavily on user experience and the amount of understanding, which vary from one country to another, but also there are several definitions developed by some researchers in this field, [7] defined IBS as the component manufacturing, assembling, transporting, and placement construction using minimum additional work possible inside or outside the site. While the Construction Industry Development Board (CIDB) in Malaysia defined IBS as a building system where components being manufactured in the factory or off-site, then developed and assembled into a structure with a minimum of extra work at the site [9]. [11] Defined the IBS as an integrated manufacturing and building process, organized and planned well to achieve efficiency in the management, setup and control of resources used and support the activities and results using sophisticated components. There are different classifications of IBS according to [4] depends on: materials, processes and systems. It is important to develop a clear vision for different types of construction systems and modern techniques used that contribute to getting the IBS and are an integral part of it. Generally, there are four types of building regulations in accordance with the Badir-Razali Building System Classification which are: traditional building systems, cast in place, pre-made, and composite [12]. Each of the construction systems is represented in accordance with their own construction methodology, its advantages in addition to construction technology, and the engineering and functional composition [5] as shown in Figure 1.

The different template systems offer a wide range of concrete construction solutions that can be selected to suit the required development needs [13]. In Syria,

reconstruction requirements impose significant challenges on this sector in terms of the need for the introduction of modern technology systems and following the designing solutions and management decisions that fit these challenges, in addition to the production of buildings within time and economic constraints.

Table 1. Summary of IBS benefits resource (author and Izatul Iaili Jabar [8] et al Idrus, [6] 2013)

Benefits	Explanation
Cost and financial	IBS offers cost saving through:
Advantages	- Earlier completion time (Kamar et al., 2011; Pan et al., 2007). Repetitive use of system formwork made of steel, aluminum, etc. (Thanoon et al., 2003; Besharah et al., 2015). - Less wastage (Idrus et al., 2008). - Reducing site infrastructure and overhead (Kamar et al., 2011). - Increased certainty less risk (Pan et al., 2007).
Construction speed	IBS construction process is governed by the speed of production and controlled environment of manufacturing facilities (Aburas, 2011), thus the need for fast delivery can easily be met by increasing the production capacity (Abdullah et al., 2009).
Reducing labor	The using of foreign labor (Jabar, 2013). The using of IBS component, which is manufactured in centralized factory, automatically will reduce labor requirements at construction site (CIDB, 2010).
Better quality	Better quality products can be produced with the adoption of IBS as it uses good quality components and involved numerous expertise throughout the process starting with manufacturing, installer, engineers, contractors and others (Kamar et al., 2011; Thanoon et al., (2003).
Health and safety measures	IBS application will improve site safety by providing cleaner and tidier site environment (Pan et al., 2007; Rahman & Omar, 2006) as the site activities become minimum (Besharah., 2015).
Flexibility	IBS allows flexibility in architectural design, in order to minimize uniformity of repetitive facades. Simultaneously, the flexibility of different system used in IBS construction process produced own unique prefabrication method (Thanoon et al., 2003).
Waste minimization	All IBS components are manufactured from the factory, resulted in less wastage (Kamar et al., 2011).
Improving productivity	Productivity (CIDB, 2010; Kadir et al., 2006). At the same time, it enhances productivity by removing difficult operation off-site and less site disruption (Arif & Egbu, 2010) [10].

2. Factors affecting the consumption of renewable energy during the construction phase of the building

There are a number of factors affecting the consumption of renewable energy in the construction phase of the building. It is noted that these factors control the modality and the amount of energy consumption at this stage, as their characteristics affect the method of energy consumption through its impact on the various consumption elements, namely equipment, Construction and mismanagement of project implementation [14]. It is noted that these elements are collectively governed by a combination of factors as shown in Figure 2: building materials used, building systems followed, methods of implementation used, design process and time control, noting that the characteristics of each of these factors have a direct impact on consumption in the construction phase of the building.

With regard to our research, it is important to clarify the impact of building systems and methods of implementation used to consume renewable energy during the construction phase of the building.

2.1. The effect of building system followed on the energy consumption in the construction phase of the building

The structure of the building system reflects the energy type used in the construction process, whether human or mechanical, or both, specifying the ratio of each of them. It also determines the nature of each of these energies according to this ratio.

For example, the human energy varies between the unskilled labor force and the trained labor force, the percentage of their use varies according to the construction system used, as well as for equipment, the equipment capacity used is determined according to the ratio of equipment and labor, which is also determined by the building system used.

The effect of the building system on the amount of energy consumption in the construction phase of the building is reflected in: [15]

- The ratio of equipment use to labor, on the basis of which the effort to accomplish a task is determined by

specifying the capacity used in the implementation of each of them. It is necessary to access through the equipment and labor to the optimum time of achievement and thus access to optimal energy. For example, it is not preferable to use many labors in the case of large projects. In addition, it is not preferable to use full mechanization in the case of small projects. The impact of the construction system on the percentage of equipment to labor is not limited to the capacity used, but rather to the time of implementation.

- The quality of employment used; According to the type of construction system used, different levels of employment are shown, from skilled labor to regular labor. Thus, the amount of energy used by these workers varies, as does the amount of energy spent.
- The degree of accuracy and proficiency depends on the quality of elements implemented in the building, the proportion of labor and equipment. The degree of the possibility increases in introducing electronic control methods on the proportion of equipment used in the project, which helps the speed, accuracy and quality of work while reducing equipment capacity and mortality rate, and it improves the management of project implementation in the construction, storage, finishing and petty operations. [16],[18]

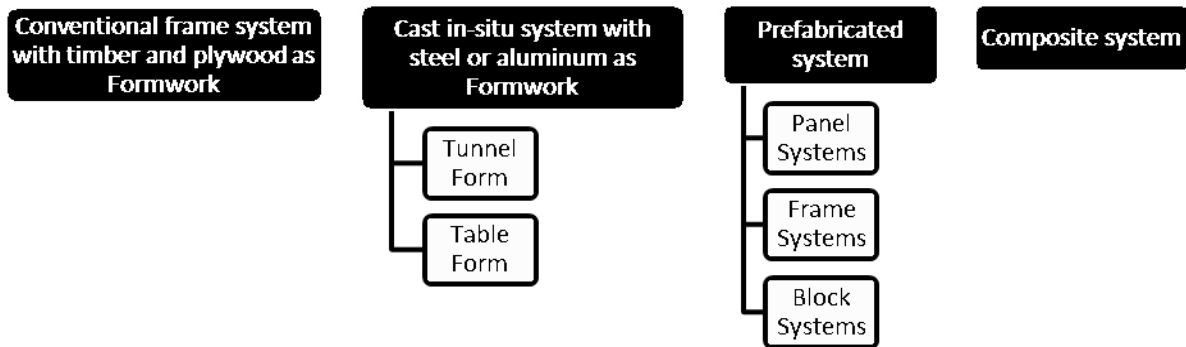


Figure 1. Types of Building Systems (Source: author by using [5])

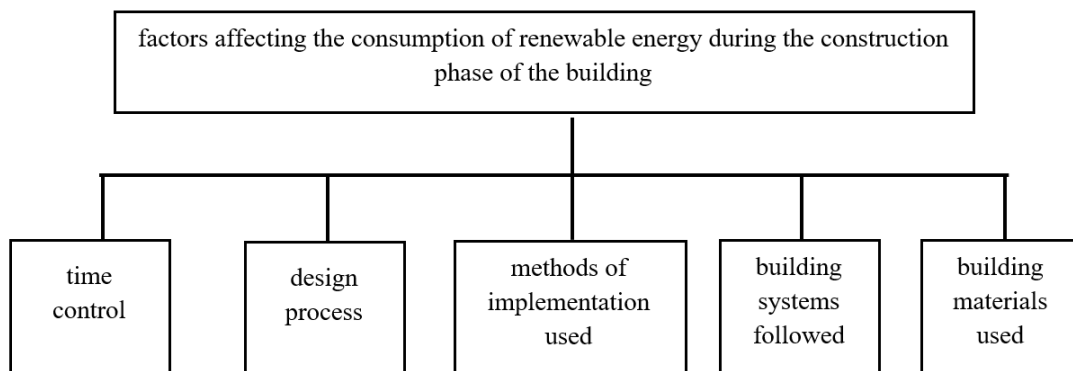


Figure 2. Factors affecting the consumption of renewable energy during the construction phase of the building [14]

2.2. The impact of the implementation method used on energy consumption in the construction phase of the building

The implementation method is the main control of the executive power. Therefore, it controls the energy of the labor and the implementation equipment. It is important to ensure good control and prevent waste, especially when most of the work is carried out at the construction site, which may cause material waste. The effect of the choice of implementation methods used on energy consumption in the construction phase of the building is illustrated by: [19]

- Transportation capacity; where, for example, using precast or Pre-processing items leads to the initial transfer from raw material sites to the factory and transfer elements to the site. While using traditional methods leads to transfer raw materials directly to the site. Therefore, transport capacity depends heavily on the method of implementation used.
- Energy equipment and labor; where the least energy spending method of implementation is chosen for both the labor and equipment, which does not conflict with the quality of the product, and commensurate with the time of implementation required.
- The materials used in the implementation methods; some methods specify that certain materials should be used such as clamps, and these methods determine the type of these materials. For example, the implementation method specifies the use of wooden or metal clamps or others, thus controlling the manufacturing capacity of some materials used in the implementation.
- Materials waste, as the choice of implementation method affects the amount of waste in building materials.
- Finishing capacity, where the method of implementation used determines the shape of the final surface of the building as well as the properties of the building material used, and thus affects the amount of

finishing the building needs and determines the energy of manufacturing finishing materials as well as the energy of finishing work. [17]

3. Prioritizing the selection of construction methods and how the renewable energy criteria affect the selection within the reconstruction scheme in Syria

The final decision about implementation options associated with factors that have been identified through a large questionnaire that can affect this decision, and therefore it is important to make the order of priorities for the use of one of the technical systems, for decision-making about the technology that must be followed using one of the decision-making tools, hierarchical analysis method AHP.

The decision will be divided into two parts:

Part 1: prioritize the use of one of the construction methods used in Syria using the AHP method.

Part 2: introduce the criteria of renewable energy in choosing the method of construction and comparing the results with each other.

3.1. Steps to implement the AHP

The process of the AHP includes three basic steps: the first step is to build a model of hierarchical analysis, which consists of the primary goal, alternatives and the main and sub- criteria, the second step is to demand from decision makers to individually express their opinions regarding the relative importance of the criteria and preferences between alternatives using paired comparisons, the third step is to prioritize the decision.

Part 1: After preparing the overall shape of the model (as shown in Fig.3), and introducing the preference values to the program (expert choice) for comparison of the alternatives (technical systems) according to the criteria, the result of the final paired comparisons of alternatives according to figure4 was obtained.

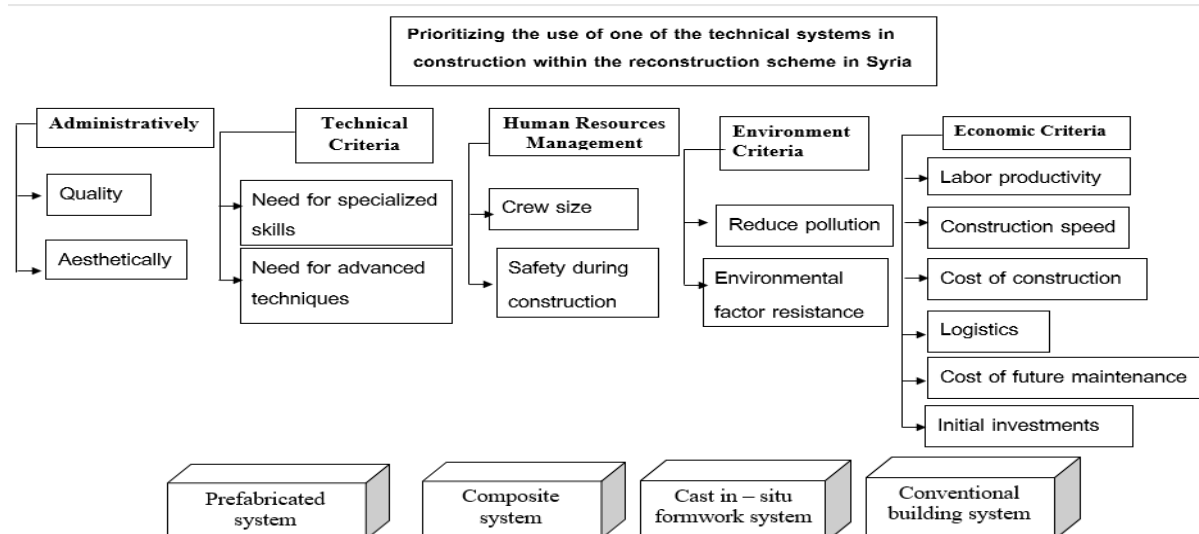


Figure 3. Hierarchical Analysis Model for Priority Determination

As shown in figure 4, the technical system which received the highest importance is the technologically advanced prefabrication system which had the winning percentage of 39.4%. The researcher referred that to the extent of the actual importance of the advanced prefabrication technology, which stems not only from its large contribution in the rapid construction, but also in its ability to fill a large proportion of housing needs of the Syrian citizens, especially in light of destruction risks of Syria and the pressures of development and the great need of reconstruction. The technical composite system (cast-in-place, pre-cast) came second with 21.8%; followed in third

place by a low difference developed technology the cast-in-place system gaining 20.8%; stated in the last ranking: traditional methods and tools with 18.1%.

Part2: preparing the overall shape of the hierarchical analysis model (as shown in Fig.5) With the use of renewable energy criteria obtained from previous studies and advanced research in this field, and introduction of the preference values to the program (expert choice) for comparison of the alternatives (technical systems) according to the criteria, the result of the final paired comparisons of alternatives according to figure 6 was obtained.

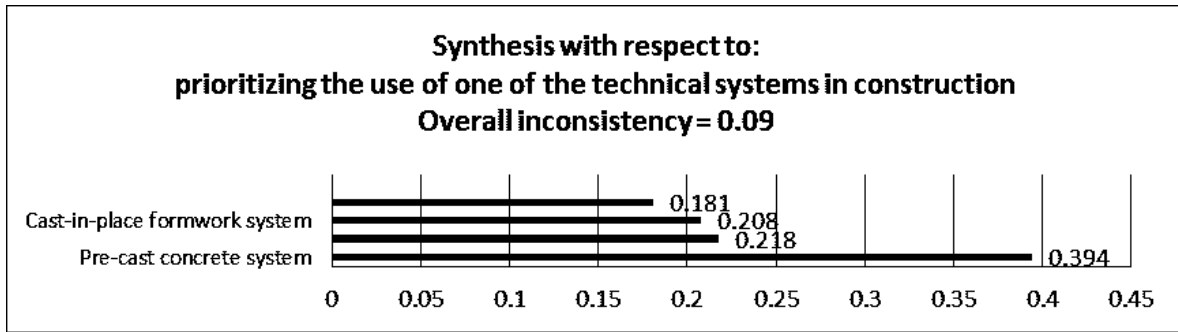


Figure 4. order of technical building systems after a paired comparison using expert choice.

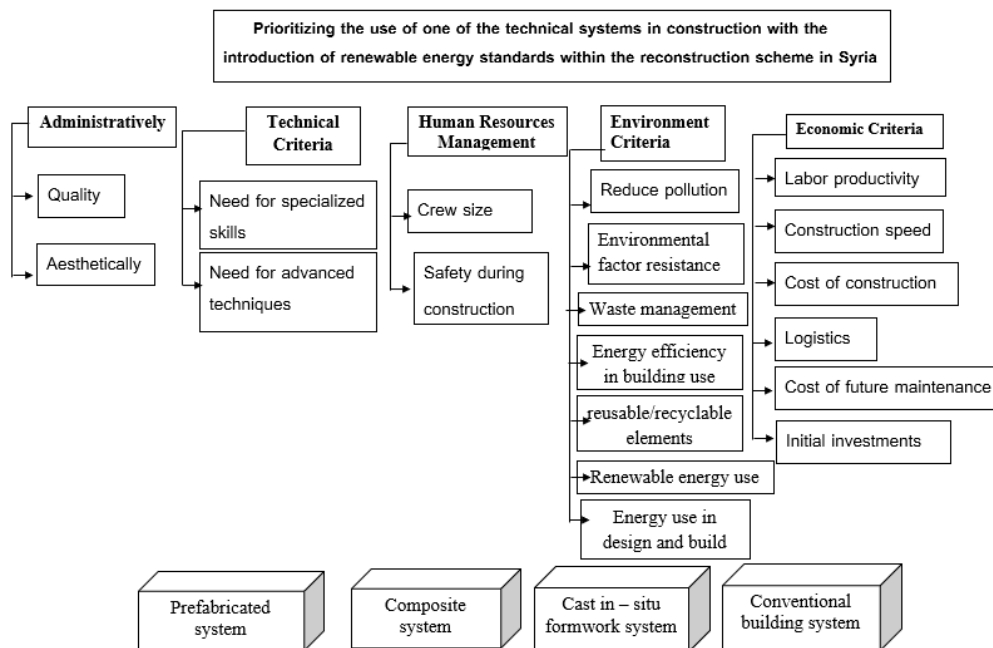


Figure 5. hierarchical analysis model for priority determination with the use of renewable energy criteria

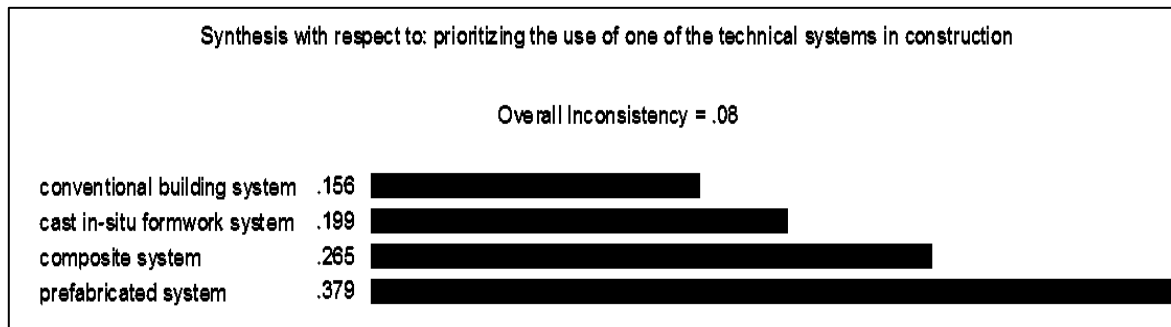


Figure 6. order of technical building systems after a paired comparison using expert choice with the use of renewable energy criteria

3.2. comparing the results with each other

The use of renewable energy criteria modified the ranking of technological alternatives for construction, according to the adaptation of these methods. The technology advanced prefabrication system had the winning percentage of 37.9% (39.4%, in part1). The technical composite system (cast-in-place, pre-cast) came second with 26.5% (21.8%, in part1); followed in third place by a low difference developed technology the cast-in-place system gaining 19.9% (20.8%, in part 1); and the last place for conventional building system with 15.6% (18.1%, in part 1). Therefore, the renewable energy criteria have emphasized the importance of industrialization and mechanization with the possibility of using renewable energies which meet the requirements of reconstruction in Syria to replace the traditional ones

This relative convergence of alternatives can set the direction of development in accordance with all of these alternatives and not toward a single so that they form with each other a technological package appropriate and in accordance with the conditions and factors existing and emerging.

4. Conclusions and Recommendations

This paper looked at the definition and classification of IBS, and characterization of their own construction techniques. As this paper discussed factors affecting the consumption of renewable energy during the construction phase of the building. Given the importance of having a comprehensive methodology in Syria to adopt strategic issues for the Syrian construction industry (the IBS), we have identified priorities for choosing the right technical system for building within the reconstruction system in Syria, and introduce the criteria of renewable energy in choosing the method of construction and comparing the results with each other, we reached the following conclusions and recommendations:

- The use of the building industry systems (IBS) in Syria can offer the benefits of speed, quality and safety for construction projects, and achieve the construction requirements.
- Obtaining a high level in IBS requires a move towards industrialization.
- IBS is facing significant challenges in Syria.
- Using the method of AHP, the advanced technology, prefabricated system was in first place with 39.4%, followed by the composite technical system (cast-in-place + pre-cast) with 21.8%, in third place advanced cast-in-place technology with 20.8%, as stated in last rank were traditional methods and tools.
- The use of renewable energy criteria modified the ranking of technological alternatives for construction methods which emphasized the importance of industrialization and mechanization with the possibility of using renewable energies which meet the requirements of reconstruction in Syria to replace the traditional ones.

References

[1] Beshara, M., Hassan, B. Construction Industry as a Requirement for Reconstruction Phase in Syria. 2015. The 1st Engineering Conference on Reconstruction and Development Priorities. In Arabic.

- [2] Mohee, M., Bayati, H. Study of the Efficiency Performance of Precast Building: Practical Research on Civil Engineering Department of Building - University of Tikrit. Diyala Journal of Engineering Sciences, 2011, pp. 1-22. ISSN 1999 – 8716. In Arabic.
- [3] Pan, W., Gibb, A. G. F., & Dainty, A. R. J. (2007). Strategies for Integrating the Use of Off-site Production Technologies in Housebuilding. Journal of Construction Engineering and Management.
- [4] Mohd Kamar, KA., Abd Hamid, Z., Azman, MNA., Ahamad, MSS. Industrialised Building System (IBS): Revisiting the Issues on Definition, Classification and the Degree of Industrialisation. International Journal of Emerging Sciences, 2011. 1: 120-132.
- [5] Thanoon, W.A, Kadir, M. R. A., Jaafar, M. S., & Salit, M. (2003). The essential characteristics of industrialised building system. International Conference on Industrialised Building System KL. Malaysia.
- [6] Idrus, A., Hui, N. F. K., & Utomo, C. (2008). Perception of Industrialized Building System (IBS) Within the Malaysian Market. International Conference on Construction and Building Technology, ICCBT2008, (07), 75-92.
- [7] Abdullah, MR., Mohd Kamar, KA., Mohd Nawi, MN., Haron, AT., Arif, M. Industrialised Building System: A Definition and Concept. ARCOM Conference. 2009, Nottingham, United Kingdom.
- [8] Jabar, L, I., Ismail, F., Mustafa, A., A. (2013). Issues in Managing Construction Phase of IBS Projects. Procedia - Social and Behavioral Sciences 101 (2013) 81 – 89. Available online at www.sciencedirect.com.
- [9] Construction Industry Development Board (CIDB). Manual for IBS Content Scoring System (IBS SCORE). 2010, CIDB, Kuala Lumpur, Malaysia.
- [10] Arif, M., & Egbu, C. (2010). Making a case for offsite construction in China. Engineering, Construction and Architectural Management, 17(6), 536-548. doi:10.1108/09699981011090170
- [11] Lessing, J., Stehn, L., Ekholm A. Industrialised Housing: Definition and Categorization of the Concept. IGLC-13 Sydney, Australia. 2005.
- [12] Badir, YF., Kadir MRA, Ali AAA. Theory of Classification on Badir-Razali Building System Classification. Bulletin of Institute of Engineer. 1998.
- [13] Baxi, CK. Formwork – A Concrete Quality Tool. 36th Conference on Our World in Concrete & Structures. 2011. Singapore, August 14-16.
- [14] Shams al din, A. Energy conservation in the building construction phase. 2003, Master Thesis in Ain Shams University, Egypt.
- [15] Youssef, O. Building Technology - The Foundations and Criteria that Control Construction in the Modular Unit (Self-Building Method and Methods of Evaluation), PhD Thesis, Cairo University, 1996.
- [16] Arnold, B. Philippe, M. High energy performing buildings: Support for innovation and market uptake under Horizon 2020 Energy Efficiency, Publications of the European Union, Project number 2018.4202. 2018.
- [17] Thapa, S, Kr. Panda, G. Energy Conservation in Buildings – a Review, International Journal of Energy Engineering, India, 2015, Vol. 5 Iss. 4, PP. 95-112.
- [18] Stephan, André & Stephan, Laurent, 2016. "Life cycle energy and cost analysis of embodied, operational and user-transport energy reduction measures for residential buildings," Applied Energy, Elsevier, vol. 161(C), pages 445-464.
- [19] Dixit, Manish K., 2017. "Life cycle embodied energy analysis of residential buildings: A review of literature to investigate embodied energy parameters," Renewable and Sustainable Energy Reviews, Elsevier, vol. 79(C), pages 390-413.

Impact of Decentralized PV Systems Installation on Transmission Lines During Peak Load Situations – Case Study Amman, Jordan

Daniel Christ*, Martin Kaltschmitt

Hamburg University of Technology (TUHH), Institute of Environmental Technology and Energy Economics (IUE)

Received 15 May, 2019

Abstract

An increased installation of decentralized small scale photovoltaic (PV) and/or photovoltaic-thermal (PVT) systems for electricity generation within growing urban areas might influence the need of a grid extension because electricity is provided close to the place where it is needed. Thus, for the metropolitan area of Amman / Jordan characterized by a strong increase in electrical energy demand, the effects of selected variants of such an installation strategy of decentralized PV / PVT systems is assessed in detail. Additionally, for the various PV / PVT installation variants a DC power flow analysis focused on the degree of capacity utilization of the most important transmission lines providing electricity for the metropolitan area of Amman / Jordan is carried out. The results show a positive impact for higher installed electrical capacities of decentralized PV / PVT systems related to the capacity utilization of the existing lines. In this context, PVT systems lead to more efficient overload reductions than PV for the investigated case.

© 2019 Jordan Journal of Mechanical and Industrial Engineering. All rights reserved

Keywords: ;

1. Introduction

Jordan is characterized by a strongly increasing demand for electricity due to a growing population as well as an ongoing industrialization. In order to cover this increasing demand for electrical energy in a more sustainable way in the years to come, renewable energy should be used in a clearly expanded manner. In addition, it is important not to endanger the security of electricity supply. For example, during a heat wave and a correspondingly strong increase in the demand for electrical energy due to additionally used cooling devices, the transmission grid characterized by already widely used transportation capacities is subjected to very high loads. This has been the case for example in 2015. On August 4th, 2015, the highest load to date occurred in Jordan causing substantial overloads in the transmission lines South of Amman. Thus, various measures must be taken to ensure a high degree of supply security during such days with high ambient temperatures and thus high electricity demand. One measure could be the increased decentralized installation of PV systems within Amman metropolitan area in order to reduce the residual load which will also result in reducing load flows to Amman region. [1, 2]

Against this background, the overall aim of this paper is to assess potential effects of the installation of photovoltaic (PV) and photovoltaic-thermal (PVT) systems to reduce electrical overloads in the transmission grid of Jordan related to the Amman metropolitan area

exemplarily for the day with the highest load situation. For this purpose, August 4th, 2015, is taken into consideration. Especially for such high load situations, a decentralized electricity generation from photovoltaic systems might be beneficial to reduce the load to be covered by conventional power plants.

Typically, for Jordan as well as other MENA-countries the highest yearly electrical load usually correlates directly with the highest daily mean temperature [3, 4]. Additionally, at days with high ambient temperatures, the load peak shifts from the evening to noon due to the significantly increased usage of air conditioning systems operated by electrical energy; this will make the increased integration of electricity from PV / PVT systems even more promising. Therefore, an increase in decentralized installations of PV or PVT systems might be beneficial for the overall load situation on such high load days; one positive effect might be a relief of the degree of the capacity utilization of the existing transmission lines.

2. Background

Below some background information are provided. This is true for PV / PVT-systems as well as the overall electricity system of Jordan.

2.1. PV / PVT-systems

Photovoltaic (PV) modules can convert solar irradiation directly into electrical energy [5]. The main parameters

* Corresponding author e-mail: daniel.christ@tuhh.de.

determining the conversion efficiency related to the influencing meteorological parameters are irradiation on the module surface and the modules' temperature [6, 7]. An increase in module temperature has a negative effect on the electrical efficiency of the PV modules. For silicon based PV modules this value reaches approximately $-0.4\%/K$ [6].

One way to overcome this disadvantage and to improve the overall performance and thus the electrical power output of a PV system is to reduce actively its modules' temperature [8]. This is possible based on different technological approaches. Air- and fluid-based cooling systems are under discussion and partly offered on the market [9, 10]. The main factors for the module temperature are the ambient temperature, the wind speed and the solar irradiation [11]. With these cooling approaches, reduced temperatures of modules can be achieved while efficiency increases are well documented, where fluid-based cooling systems always lead to higher efficiencies [12–14].

For a fluid-based cooling system, a cooling fluid is pumped through pipes attached at the rear side of a regular market mature PV module while functioning as a heat sink. Such a PVT-system is operated with a mixture of Glycol and water to allow for a certain frost resistance. The dominant variables here are the flow rate through the cooling system and the inlet temperature of the cooling fluid [10, 13]. Different operating strategies can be used to generate either an increased output of electrical or thermal power [15]. This paper focuses on maximum electrical output to estimate the potential effects on the characteristic curves of PV/PVT systems.

In addition to an increase in electrical conversion efficiency due to lower module temperatures, low-temperature heat can be gained and used for numerous down-stream processes; this could be the provision of hot water e.g. provided by heat pump systems where the low temperature heat from such PVT cooling systems is used as a heat source [16–18]. Thus, if there is a demand for low temperature heat, PVT systems can contribute towards a better integration of the electricity and the heat sector, and thus better interlink renewable energy systems in general [12, 13, 17, 19].

For countries like Jordan, characterized by high ambient temperatures and high solar irradiation in average, and especially during summer time, PVT-systems can reduce the efficiency drop of PV-systems during hot and sunny days.

2.2. Jordanian electricity system

The Kingdom on Jordan has been characterized by an overall electricity demand of ca. 16.2 TWh in 2015. This electricity demand is increasingly growing especially due the fact that the population is increasing and industrialization is progressing. [3, 20, 21]

Electricity generation in Jordan is realized almost exclusively by power plants operated by fossil fuel energy. The electricity generation units under operation in 2015 are characterized by a total installed electrical capacity of 4,266 MW. Units with 2,526 MW realize direct combustion of natural gas, and plants with 814 MW are operated by diesel fuel. Units with a conventional steam

cycle contribute with an installed electricity capacity of 787 MW. Conversion units using renewable sources of energy are limited to systems based on hydroelectricity, wind and biogas as well as to a very minor extend PV. Altogether, these options do not exceed an electrical capacity of 139 MW related to the year 2015 [20].

The high voltage electrical grid in Jordan covers the overall Hashemite Kingdom. It mainly consists of overhead lines with voltage levels of 132 and 400 kV, shown in figure 1 [20]. While there is a strong accumulation of transmission lines in the metropolitan area of Amman, the rural areas of Jordan are supplied by very few lines only.

One crucial point of the transmission system in Jordan is the connection between the two substations "Queen Alia International Airport" (QAIA) and "Qatrana". This transmission system's bottleneck is located between these substations and overloads in these lines could cause a serious blackout in the Amman metropolitan area. These lines are critical as they connect the main demand area of Amman with the South of Jordan and the interconnector with Egypt. Because Egypt is responsible for controlling Jordan's grid frequency, an overload on these lines could lead to a blackout in the Amman metropolitan area. Relatively small percentages of overload can be tolerated for a short amount of time, but with frequently repeated overloads problems can occur [22].

The integration of large PV capacities into an existing electricity grid has already been investigated many times, where the focus was often on the distribution network plane or focused on studying the changing load curves due to additionally installed PV systems. The challenges integrated here by the fluctuating behavior of the PV systems can be eliminated with well-designed and technologically adapted planning. Especially for Germany there are several studies to integrate much larger shares of PV feed-in than in Jordan, and at the same time even provide system services. [23–25]

Figure 1 shows also that the majority of Jordan's conventional power plants are located in the wider Amman area and supply the metropolitan area directly [14].

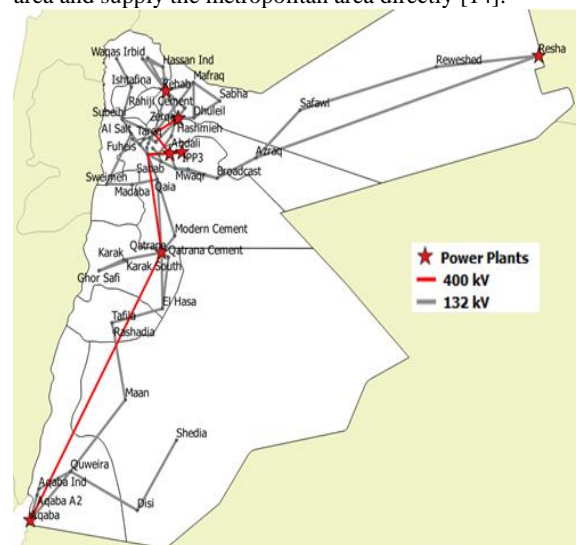


Figure 1. Transmission lines and Power Plant Park of Jordan

2.3. Peak load day

In figure 2 exemplarily Jordan's highest load day during the year 2015 (i.e., 4th of August) is shown being also the hottest days in 2015 [3, 4, 26]. The peak power at this day sums up to 3,205 MW. The curve shows that the daily demand peaks between 12:00 and 18:00; this peak is typically during the evening hours at days where there is not such a high demand for cooling devices. The highest share of Jordan's load on that day was demanded within the metropolitan area of Amman with a share of 37.7 % related to the rest of the country [3].

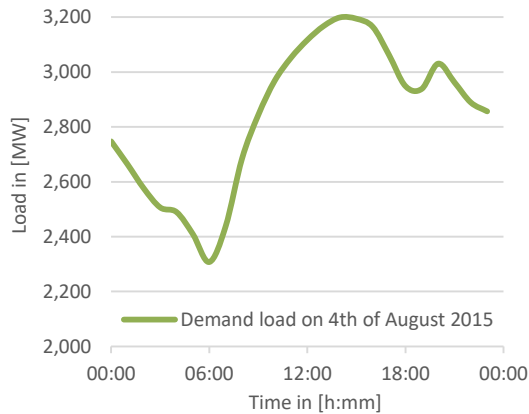


Figure 2. Peak load day in 2015 for Jordan

3. Assessment approach

With an increased installation of decentralized PV / PVT-systems in the metropolitan area of Amman, an electricity conversion shift towards Amman as major area of demand could occur. The electrical energy coming from solar irradiation is used directly, mainly by households, at the place of provision. This results in a decreased residual load to be covered by the conventional electricity provision system (i.e., power plants operated by fossil fuel energy). A consequence of such a strategy could be reduced capacity utilization of the transmission lines surrounding and supplying the Amman metropolitan area. Such an approach could decrease possibly occurring overloads within parts of the existing transmission lines especially during high load situations and reduce additionally necessary grid extensions due to a strongly growing demand. To investigate and quantify the impact of the integration of such PV / PVT-systems on Jordan's transmission system related to the Amman metropolitan area, simulated PV and PVT characteristic curves are combined with a direct current (DC) power flow analysis, whereby the focus of this paper lies on the shifting loads of the transmission lines.

Thus, this effect of a decentralized installation strategy of PV and PVT-systems on the transmission grid is assessed. First, a load analysis of the investigated load situation is realized. Then, characteristic curves of PV and PVT-systems are modelled for various installation variants. This is realized based on a physical model allowing for the simulation of the theoretical differences between PV and PVT-systems. Based on the simulated PV and PVT generation curves the residual load for the

investigated day is calculated for the various variants. The resulting residual load is then used to carry out a DC power flow analysis with the aim of quantifying the maximum load situation at the investigated day. Based on these results, conclusions are drawn whether a decentralized installation of PV / PVT-systems could contribute to reduce potential overloads within the transmission grid. This overall procedure is shown in figure 3 and outlined in detail below.

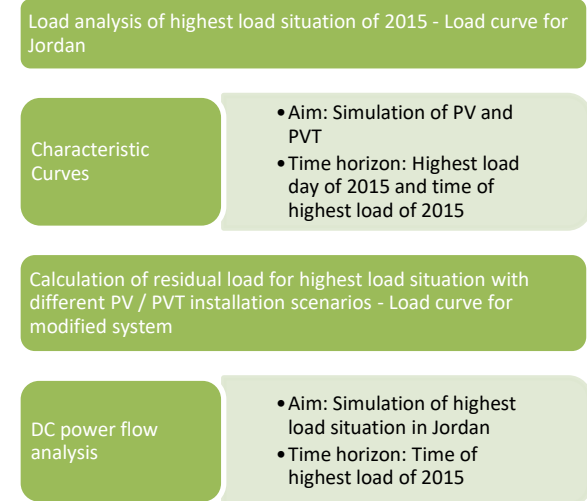


Figure 3. Schematic description of procedure

3.1. PV power provision

PV and PVT-systems show different characteristic electricity provision curves due to the cooling device used for PVT-systems. This results in higher efficiencies in general and especially during high temperature situations (e.g. around noon) if the cooling temperature is kept constant. Therefore, such PVT-systems are typically operated with a constant cooling-fluid inlet temperature (e.g. groundwater as a possible cooling fluid source shows basically the same temperature throughout the overall year) [27]. To simulate such effects a quasi-stationary (hourly based) simulation model of PV and PVT-systems has been developed based on the physical characteristics of these systems. The simulated system is shown in figure 4. In order to calculate the electrical yield, the following aspects were modelled.

- Mixed convection heat transfer is assumed at the surface of the PVT-system, consisting of natural and forced convection with heat transfer coefficients dependent on the actual wind speed and its direction. The driving temperature gradient occurs between the module temperature and the ambient temperature.
- On the back of the PVT-system natural convection heat transfer is assumed depending on the module characteristics and the temperature gradient between the module and the ambient temperature.
- Forced convection heat transfer is assumed by fluid cooling in the tubes as a function of a fluid velocity dependent heat transfer coefficient as well as the temperature gradient between fluid and module temperatures. A constant cooling-fluid inlet temperature is assumed.

- The remaining irradiation energy minus the mentioned heat losses is responsible for heating up of the modules. This heating up of the PV-module depends on material properties, the modules' mass and module temperature.
- The electrical power of a regular market-mature PV cell is finally simulated as a function of irradiation and temperature-dependent electrical efficiency. Increasing module temperatures reduce the efficiency and increase the heat to be dissipated by convection in the system under consideration.

By drawing up the balance of incident radiation, electrical conversion and the resulting calculated heat flows, an equation system was created being the basis for the simulations realized here. Since both the electrical conversion and the heat flows within the balance limits are directly dependent on the unknown module temperature, the latter can be calculated iteratively under the assumption that an equilibrium can be maintained. After calculating the module temperature, all heat flows of the system can be calculated.

Due to the temperature dependence of the electrical efficiency of the PVT-system, the module temperature strongly influences the electrical yield of the overall system. Thus, based on the calculated module temperature, the electrical yield of the PVT-system can be quantified. The aim of the simulated characteristic curves is to make a statement about the possible additional yield of PVT modules under their ideal conditions (high radiation and high temperatures). These theoretical differences between PV and PVT systems are used in this paper to estimate the bandwidth of the effect on the transmission lines.

3.2. DC power flow analysis

The PV / PVT power generation reduces the residual power demand to be covered by the grid and thus by the fossil fuel-based power plants providing electricity for the Amman metropolitan area. To investigate the effect of this reduction exemplarily for different expansion variants for PV / PVT-systems related to the free capacity of the transmission lines around the Amman metropolitan area a DC power flow analysis is carried out [28, 29].

Within such a DC power flow analysis, demand and generation side are connected and the electrical load on

each transmission line is simulated. Three main assumptions have been made to enable such a simulation [30].

- The line impedance is significantly greater than the resistance of the line. Based on this assumption, transmission losses within the system are neglected.
- All voltages within the system are equal, implemented through a "per Unit" system within the calculation. As a result, reactive power is no longer calculated.
- The phase angle differences are assumed to be very small for a linearization of the sine term. These assumptions lead to equation 1 [31].

$$P_1 = Y_{bus} \Delta\delta \tag{1}$$

P_1 is the power flow between every substation, Y_{bus} is the admittance matrix of the system (including all impedances and resistances) and $\Delta\delta$ are the phase angle differences. After inverting the admittance matrix, equation 2 follows.

$$\Delta\delta = Y_{bus}^{-1} P_2 \tag{2}$$

P_2 is the net performance of every substation. All phase angle differences are calculated in relation to a neutral point. The result of the phase angle differences is inserted in equation 1 and the load flow between all substations is calculated.

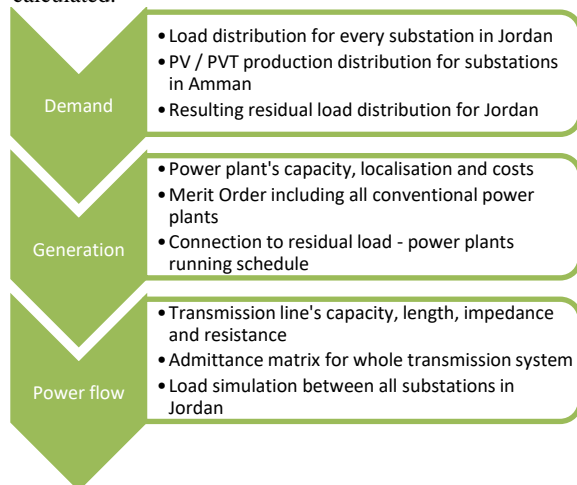


Figure 5. DC power flow methodology

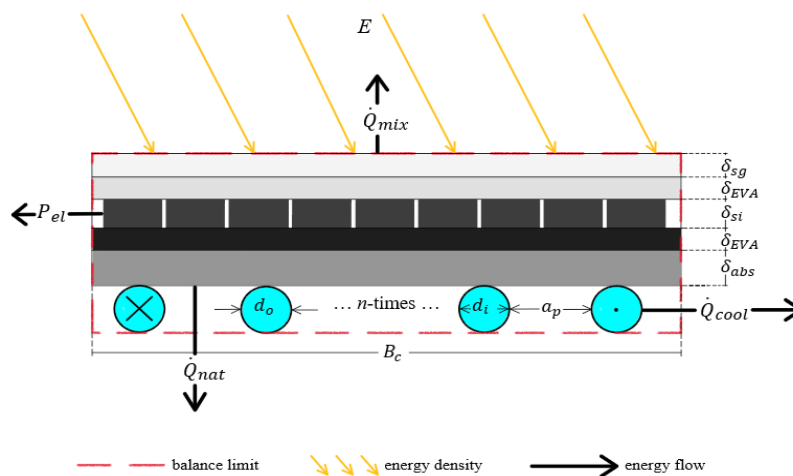


Figure 4. Balance limits of simulated PVT-module

Figure 5 shows the DC power flow methodology applied here. Thus, the methodological procedure is divided into three main steps:

- determination of the overall and distributed demand of a system,
- determination of the overall and distributed generation of a system and
- calculation of the resulting power flows between all substation within a system.

A spatial breakdown of the load demand at the investigated time of maximum load was used to calculate a base variant (i.e., current situation) with no additional decentralized installed PV / PVT-systems. Based on this spatial distribution, the decentralized installed PV / PVT-capacity is then divided among the various substations already under operation within the Amman metropolitan area. This results in spatially differentiated residual loads.

Data on the power plant park, its spatial connection to the transmission grid (feed-in points) and the costs of the individual power plants are the basis for determining the generation side. Based on this, a merit order is created for all conventional power plants under operation related to the time frame of this assessment. The combination with the previously defined residual loads makes it possible to calculate different power plant loads and their spatial distribution at the time of peak load.

By summarizing the properties of the transmission lines (capacitance, length, impedance, resistance) the admittance matrix of the transmission grid is created. Based on the equations described above, the load flow between the substations in Jordan can be calculated. To compare each line's load with its possible capacity, a percentage for the load situation for all lines in Jordan can be quantified and overloaded lines can easily be detected.

4. Case Study

Within this assessment in total four variants with different amounts of decentralized installed capacities are investigated related to the situation given in 2015 (figure 6). This base variant with no additional decentralized installation of PV / PVT-systems was defined first. Based on this, four variants with 500 MW and 1,000 MW either as PV or PVT-systems were fixed.

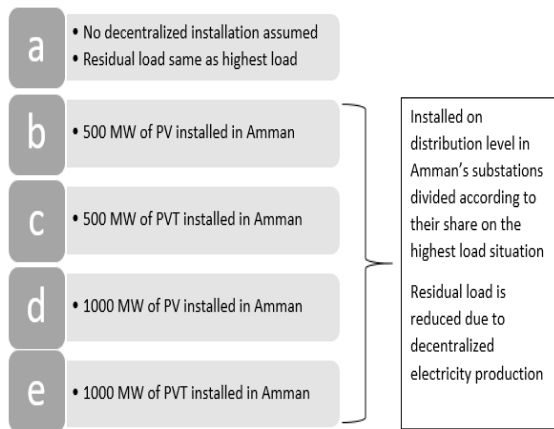


Figure 6. Description of investigated variants a to e (Amman means the overall Amman metropolitan area)

For the assessment of the variants (a to e) defined in figure 6 both methodological steps outlined in section 3

need to be realized separately. The necessary input parameters taken into consideration to realize such an assessment are discussed below. While the input parameters for the first part of the methodology outlined in section 3 are primarily compiled from data sheets of the PV-modules assumed to be installed here, the input parameters of the DC power flow analysis are taken from data resulting from Jordan's National Electric Power Company (NEPCO).

4.1. PV power provision

The input parameters used for the model approach discussed in section 3.1 are shown in table 1. Thus a combination of two 280 W modules with a combined 560 W capacity is assumed to be installed here [32]. All PV / PVT-systems are modular and therefore linearly scalable. Thus, the results of a single system can be scaled up to the required capacities of the defined variants. Losses due to shading as well as due to pollution are not taken into consideration even due the fact that these effects might lower the electrical yield slightly.

Table 1. Input parameters for PV / PVT model

Description	Formula symbols	Input value	Unit
Width of collector [32]	B_K	1.984	m
Length of collector [32]	L_K	1.640	m
Total area of silicon cells [32]	A_Z	2.920	m ²
Electrical nominal efficiency of PV-collector [32]	η_{NK}	17.21	%
Angle of installation with regard to vertical	γ_K	60	°
Critical Rayleigh-number [33]	Ra_c	900,000	-
Coolant volume flow	V_K	60	l/h
Inner pipe diameter	d_{iR}	6	mm
Outer pipe diameter	d_{aR}	8	mm
Number of cooling pipes per module	n	24	-
Standard test temperature [32]	T_S	25	°C
Temperature coefficient for electrical collector efficiency [32]	$m_{T,K}$	-0.41	%/K
Mass of aluminum frame [34]	M_R	2	kg
Material thickness of solar glass [32]	δ_{SG}	3.2	mm
Material thickness of EVA-film	δ_{EVA}	1	mm
Material thickness of silicon cells [6]	δ_Z	200	µm
Material thickness of absorber plate [34]	δ_{Abs}	0.5	mm

Additionally, the following data are used.

- Direct and diffuse irradiation, air density, ambient temperature and wind speed from historic data from Amman on the 4th of August 2015 with a time resolution of one hour [4].

- Cooling-fluid properties of the Glycol-water-mixture (i.e. temperature dependent thermal conductivity, heat storage capacity, density and dynamic viscosity) [10, 35].

4.2. DC power flow analysis

For the DC power flow analysis the following data for the year 2015 are used [20]. This is true for the different data categories.

- Demand data of the individual substations in Jordan, divided temporally and spatially (data for all 62 substations with a time resolution of 15 min throughout the year 2015). From this, the residual loads were calculated in combination with the variants already presented by assuming that the additional decentralized PV / PVT capacities were installed in the Amman metropolitan area as a percentage of their share related to the maximum load [3].
- Generation data of the power plant park, the costs incurred and the spatial distribution of the individual power plants, from which both the merit order used and the power plant schedule depending on the assumed variants were calculated [36].
- Transmission network data for all existing transmission lines in Jordan in 2015 (data for 80 transmission lines), including capacities, lengths, impedances and resistances as well as the respective connections to existing substations, distributed locally throughout the country [3, 22].

5. Results

Below the results of the various variants defined in section 4 based on the methodological approach presented in section 3 are discussed.

5.1. PV power provision

Results. Figure 7 shows the simulation results for the different PV and PVT efficiencies for different cooling-fluid inlet temperatures and the uncooled PV case. The graphic makes it obvious that the electrical efficiency strongly depends on the cooling-fluid's inlet temperature. Because for the (uncooled) PV system the module temperature increases over the first part of the day a lower electrical efficiency occurs related to the cooled PVT system. This decrease in efficiency also occurs for the

cooled PVT systems, but to a significantly lesser extent. Typically, the lower the cooling-fluids inlet temperature is the higher the overall efficiency is in general.

Figure 7 makes it obvious that while the average efficiency of the (uncooled) PV-system for August 4th, 2015, was calculated as 14.9 %, the efficiency of the PVT-system ranged from 16.9 % for 30 °C inlet temperature up to 17.9 % for 15 °C inlet temperature of the cooling fluid. This resulted in an average relative efficiency increase of up to roughly 20 % due to these cooling efforts for the simplified model used under these extreme external conditions.

Figure 8 shows the electrical power output for the module defined in table 1 simulated also for August 4th, 2015. An increased additional yield of the cooled PV systems can be seen above all during the midday hours. The variations in the electrical output of the cooled systems vary considerably less than in the uncooled system. The electrical yield for this investigated day for the PV-system is calculated with 3.0 kWh while PVT-systems show a simulated yield ranging from 3.7 kWh for 30 °C inlet temperature up to 3.9 kWh for 15 °C inlet temperature. This represents a daily electrical yield increase of close to 30 % caused by the higher average efficiencies due to the cooling activities.

For the subsequent combination of the simulated characteristic curves for PV and PVT-systems (the latter with 15 °C as inlet temperature for all following results in order to be able to make a simplified statement about the theoretically maximal effect possible) with the DC power flow analysis, all electrical power outputs for the four variants defined in section 4 have been calculated. For realizing this with the historical weather data of August 4th, 2015, the respective electrical power output has been simulated. The results show that while an installed capacity of 500 MW PV results in a maximum power output of 341.7 MW on this day, 500 MW PVT sum up to 461.2 MW (i.e., an increase of ca. 35 %). For the variant with an installed capacity of 1,000 MW, PV reached a maximum power output of 683.5 MW while PVT showed a power output of 922.3 MW. Compared to the first two variants here the values are roughly doubled as it has been expected.

The simulated characteristic curves for PV and PVT-systems are then combined with the load curve for the same day (i.e., August 4th, 2015). This has been realized for all variants defined in section 3.

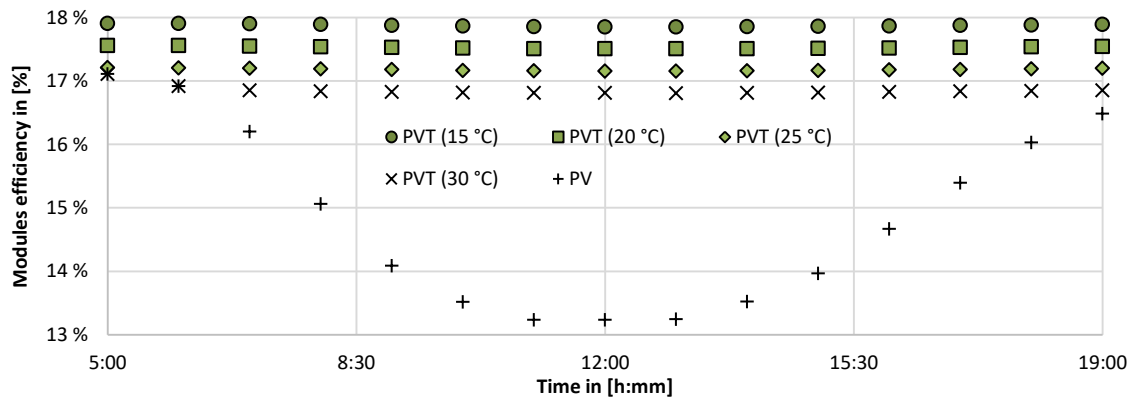


Figure 7. Simulated modules efficiency

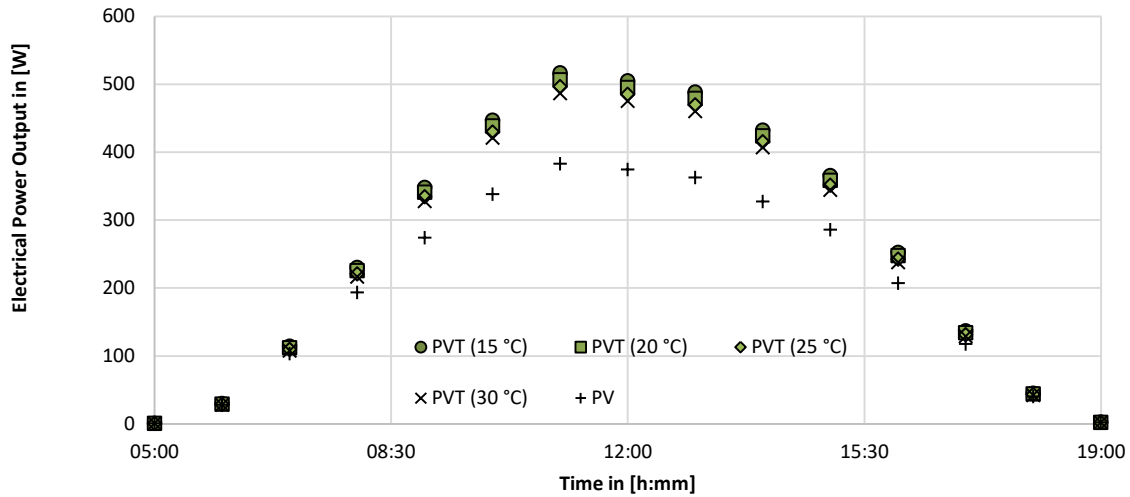


Figure 8. Simulated electrical power output

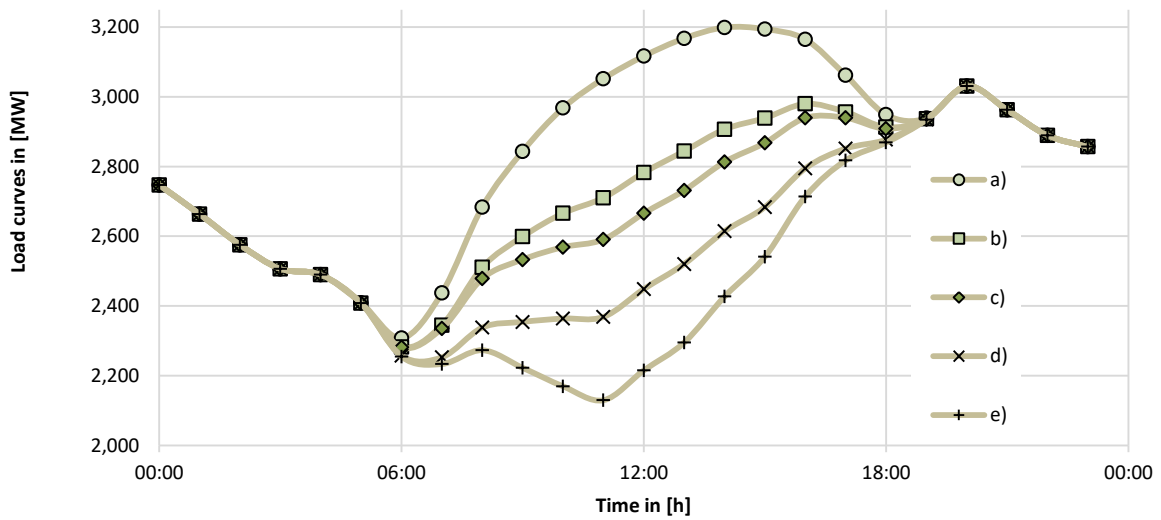


Figure 9. Resulted theoretical load curves for August 4th, 2015

Figure 9 shows the resulting theoretical residual load curves; these are the load curves that are still to be covered by energy coming from the conventional power plant park. The graphic makes it obvious that due to higher efficiencies – PVT-systems showing higher electrical power outputs at noon – these systems result in lower resulting load demands at these hours of the day. The extent to which this effect can occur is only estimated theoretically and would have to be validated by real measurements. Nevertheless, a peak shaving effect for the noon peak was detected in all variants in a different intensity due to the additional installed PV / PVT-capacities. Thus, regardless of the assessed variant, a positive effect in the form of a reduction of the noon peak was clearly observed. However, the evening peak was not changed regardless of the installed capacity (i.e., no PV / PVT energy provision during night hours).

Discussion. The simulation results for the assumed PV and PVT-systems show a strong theoretical increase in module efficiency if the system is cooled. A small variation occurs due to different cooling-fluid inlet temperatures; generally, it can be stated that the cooler the inlet temperature is the higher the overall efficiencies are. During sunrise and sunset, the effect shrinks to zero,

whereas during noon with high irradiation, the cooling effect leads to clearly higher efficiencies compared to “classical” PV-systems without a cooling device (i.e. only natural cooling due to convection). This cooling effect results in higher noon peaks for the PVT electricity provision; and considerably higher electrical yields throughout the overall day are the consequence. Even in low irradiation cases, like in the early morning of the investigated day, a cooled system leads to higher efficiencies. In this simplified model, the theoretical improvements become clear.

For the integration of the four variants of PV and PVT-system installation and the resulting effects on the highest load day of Jordan in 2015, the electrical power output varies considerably. Comparing PV with PVT-systems, a strong increase was detected for the maximal electrical power output. This results in a theoretical higher peak shaving potential for PVT-systems due to their more effective electrical conversion when irradiation and temperatures are peaking within the course of a day. Comparing the two 500 MW and the two 1,000 MW variants, PVT-systems show a clear advantage for peak shaving. How large this effect can be under real conditions must be validated with measurements.

5.2. DC power flow analysis

Results. Results for the DC power flow analysis are shown below for the five previous defined variants. These results show for the base variant overloads between QAIA and Qatrana as well as overloads within Amman metropolitan area. Table 2 lists all lines and their percentage overload for all five variants.

For the base variant five different overloaded lines are identified (table 2). The overload between Amman North and Tareq occurs due to the high demand within the central Amman area. All power plants in the Amman metropolitan area are located in the surrounding area so high loads need to be transmitted. The same applies to the overloaded lines around Hashmieh where electricity from the Samra power plant is transmitted to central Amman. Problematic are the overloads on both transmission lines starting in Qatrana.

Table 2. Overloaded lines in all variants

Line between	Capacity	Calculated load	Ratio
-	[MW]	[MW]	%
Base variant (a)			
Amman North - Tareq	264.0	379.1	143.6
Samra - Hashmieh	105.6	142.8	135.2
Hashmieh - Zerqa	105.6	142.8	135.2
Modern Cement - Qatrana	105.6	106.2	100.6
Qatrana - QAIA	105.6	121.3	114.8
500 MW PV variant (b)			
Amman North - Tareq	264.0	307.1	116.3
Samra - Hashmieh	105.6	126.3	119.6
Hashmieh - Zerqa	105.6	126.3	119.6
Qatrana - QAIA	105.6	111.1	105.2
500 MW PVT variant (c)			
Amman North - Tareq	264.0	287.1	108.7
Samra - Hashmieh	105.6	121.9	115.5
Hashmieh - Zerqa	105.6	121.9	115.5
1,000 MW PV variant (d)			
Samra - Hashmieh	105.6	112.7	106.7
Hashmieh - Zerqa	105.6	112.7	106.7
1,000 MW PVT variant (e)			
Samra - Amman North	800.0	815.7	102.0

- The 500 MW PV variant reduces the total number of overloaded lines from five to four. This occurs due to a higher electricity production from PV, leading to a lower residual load in the Amman metropolitan area. Also, the remaining overloaded lines show a decrease

in their overload percentage and a reduction of the risk of system failure.

- For the 500 MW PVT variant a reduction of the total number of overloaded lines down to three is counted. Most importantly, the line between Qatrana and QAIA is not overloaded anymore. The overload percentage for the three remaining lines decreases even more, with additional positive aspects for the grid stability within the overall Amman area.
- The 1,000 MW PV variant only shows two remaining overloaded lines connected to Hashmieh and the total overload percentage decreases in comparison to the previously described variants.
- The variant for 1,000 MW of PVT installed in Amman area show that all five overloads from the base variant are reduced and are now below the line-specific maximum capacities. Nevertheless, one new line shows an overload between the power plant in Samra and the substation of Amman North. With only 2 % of overload on this line just minor changes are necessary.

To visualize these overloads and the resulting effects of Jordan's transmission system, figure 10 shows the loads on every transmission line for the highest total load situation for Jordan in ratio to the specific capacities of each line.

Discussion. The results of the DC power flow analysis show a clear effect within the transmission system of Jordan. As expected with a higher share of decentralized electricity production by PV or PVT-systems fewer overloads occur.

Most of the investigated variants show a relaxed situation for the previously overloaded transmission lines between Qatrana and QAIA. The variant with 1,000 MW PVT installed causes a new overload within Amman area. Following this, an installation of too high capacities can lead to subsequent challenges; i.e. different transmission lines can get overloaded. An optimum, especially designed regarding the investigated system needs to be detected. Additional interactions with the transmission grid could result from the decentralized installation of PV systems. Further studies would have to be carried out to determine which effects could occur and which measures would have to be taken to maintain grid stability. The grid loads found in this paper apply only to the considered highest load situation.

All simulations for the load situations within Jordan's transmission system support the statement that the decentralized installation of PV or PVT-systems in the Amman metropolitan area could be beneficial for the overall grid stability by avoiding overloads.

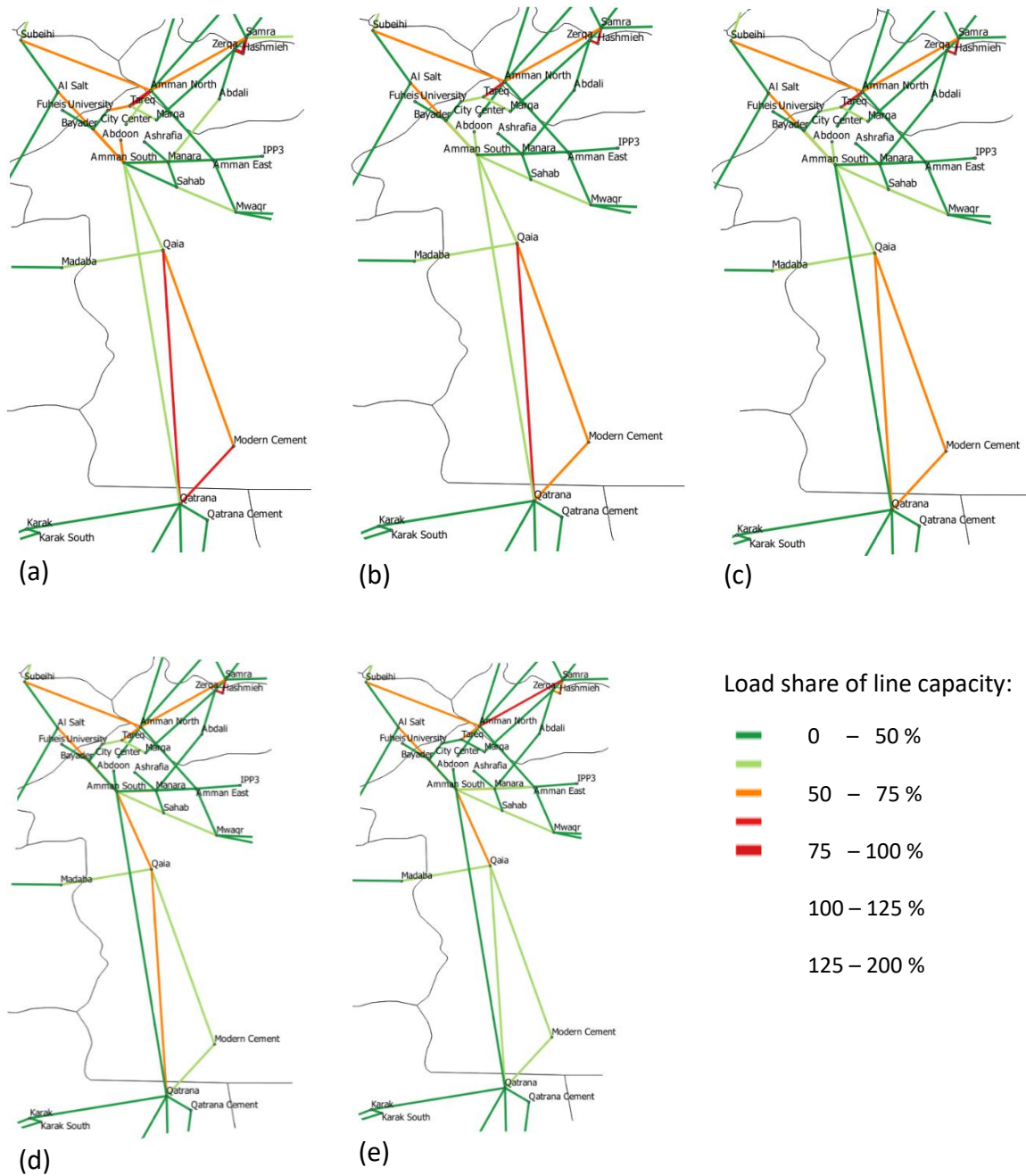


Figure 10. Load situations in Amman's transmission lines for (a) base variant, (b) 500 MW PV variant, (c) 500 MW PVT variant, (d) 1,000 MW PV variant and (e) 1,000 MW PVT variant

6. Conclusion

In this paper, the potential effect of a decentralized installation of PV / PVT-systems in the metropolitan region of Amman on the transmission grid is investigated. The scope of the study is the 2015 peak load case in which overloaded lines occurred. The aim is to assess whether a decentralized installation of PV / PVT-systems would have prevented the overloaded lines.

The following results were achieved:

- PVT-systems are more efficient than PV-systems at shaving the noon peak, leading to a more homogenized residual load curve over the peak load day in 2015.

- A decentralized installation of 500 MW PV in the metropolitan region of Amman still leads to overloaded transmission lines in the main investigated lines for the day of the highest demand. For the investigated variants with 500 MW PVT and 1,000 MW PV these lines show no more overloads. However, a decentralized installation of 1,000 MW PVT leads to new occurring overloads within the system.
- For the aim of reducing the overloads in the focused transmission lines, PVT-systems show a more efficient reduction compared to PV-systems, if the same capacity is installed.

Validating these results by the real implementation of PV / PVT-systems in a larger scale can help to improve the overall integration of renewable energy sources and especially of PV / PVT-systems in countries with a high supply of solar irradiation and compatible load curves in high load / high temperature situations. In order to investigate how the transmission grids behaves in low load situations due to the additional installation of PV systems, further studies would have to be carried out.

References

- Department of Statistics - Jordan: Statistical Yearbook 2012. http://www.dos.gov.jo/dos_home_e/main/Demograghy/2012/2-1.pdf (2012)
- M. A. A. Zarour: Renewable Energy Transition in Jordan and MENA Region, Amman, Jordan, 6 May 2015
- National Electric Power Company: Substations Load Data Sheets for Jordan. Excel, Amman, Jordan (2015)
- S. Pfenninger, I. Staffell: Renewables.ninja. <https://www.renewables.ninja>. Accessed 20 February 2019
- P. Viebahn, O. Zelt, M. Fischedick, J. Hildebrand, S. Heib, D. Becker, J. Horst, M. Wietschel, S. Hirzel: Technologien fuer die Energiewende, 14, Wuppertal (2018)
- A. Wagner: Photovoltaik Engineering. Handbuch für Planung, Entwicklung und Anwendung. Springer Berlin Heidelberg, Berlin, Heidelberg (2019)
- M. Kaltschmitt, W. Streicher, A. Wiese: Renewable Energy. Technology, Economics and Environment. Springer Berlin Heidelberg, Berlin, Heidelberg (2007)
- S. P. Philipps, A. W. Bett, B. Rau, R. Schlatmann: Technologiebericht 1.3 Photovoltaik (2017)
- T. T. Chow: A review on photovoltaic/thermal hybrid solar technology. Applied Energy (2010). <https://doi.org/10.1016/j.apenergy.2009.06.037>
- J. Cremers, U. Eicker, N. Palla, X. Jobard, F. Klotz, I. Mitina: Forschungsbericht PVTintegral. Multivalente photovoltaisch-termische Kollektoren zur Kälte-, Wärme- und Stromerzeugung und Szenarien für die Gebäudeintegration, Stuttgart (2016)
- Skoplaki, E., Palyvos, J.A.: Operating temperature of photovoltaic modules: A survey of pertinent correlations. Renewable Energy (2009). <https://doi.org/10.1016/j.renene.2008.04.009>
- Bertram, E., Glembin, J., Rockendorf, G.: Unglazed PVT collectors as additional heat source in heat pump systems with borehole heat exchanger. Energy Procedia (2012). <https://doi.org/10.1016/j.egypro.2012.11.049>
- Fudholi, A., Sopian, K., Yazdi, M.H., Ruslan, M.H., Ibrahim, A., Kazem, H.A.: Performance analysis of photovoltaic thermal (PVT) water collectors. Energy Conversion and Management (2014). <https://doi.org/10.1016/j.enconman.2013.11.017>
- Bojanampati, S., Rodgers, P., Evely, V.: Experimental assessment of flat-type photovoltaic module thermal behavior. In: 13th International Conference on Thermal, Mechanical and Multi-Physics Simulation and Experiments in Microelectronics and Microsystems (EuroSimE), 2012. 16 - 18 April 2012, Cascais, [near Lisbon], Portugal. 2012 13th Intl. Conf. on Thermal, Mechanical & Multi-Physics Simulation and Experiments in Microelectronics and Microsystems (EuroSimE), Cascais, Portugal, 16.04.2012 - 18.04.2012, 1/4-4/4. IEEE, Piscataway, NJ (2012). <https://doi.org/10.1109/ESimE.2012.6191695>
- M. Lämmle: Thermisches Management für PVT Kollektoren
- N. Palla, R. Braun, X. Jobard, I. Mitina, J. Cremers, U. Eicker: Entwicklung neuartiger PVT-Kollektoren - Leistungsfähigkeit und Potenzialanalyse für verschiedene Klimazonen (2015)
- Calise, F., d'Accadia, M.D., Vanoli, L.: Design and dynamic simulation of a novel solar trigeneration system based on hybrid photovoltaic/thermal collectors (PVT). Energy Conversion and Management (2012). <https://doi.org/10.1016/j.enconman.2012.01.025>
- M. Lämmle, A. Oliva, M. Hermann, K. Kramer, W. Kramer: PVT collector technologies in solar thermal systems: A systematic assessment of electrical and thermal yields with the novel characteristic temperature approach. Solar Energy (2017). <https://doi.org/10.1016/j.solener.2017.07.015>
- Forschungsprojekt PVTintegral. Multivalente photovoltaisch-termische Kollektoren zur Kälte-, Wärme- und Stromerzeugung und Szenarien für die Gebäudeintegration
- National Electric Power Company: Annual Report 2015. National Electric Power Company, Amman, Jordan (2015)
- M. Al-Omary, M. Kaltschmitt, C. Becker: Electricity System in Jordan: Status & Prospects. Renewable & Sustainable Energy Reviews, 2398-2409 (2018)
- National Electric Power Company: Transmission Systems Data Sheets for Jordan. Excel, Amman, Jordan (2015)
- Appen, J. von, Braun, M., Stetz, T., Diwold, K., Geibel, D.: Time in the Sun: The Challenge of High PV Penetration in the German Electric Grid. IEEE Power and Energy Mag. (2013). <https://doi.org/10.1109/MPE.2012.2234407>
- Marinopoulos, A., Papandrea, F., Reza, M., Norrga, S., Spertino, F., Napoli, R.: Grid integration aspects of large solar PV installations: LVRT capability and reactive power/voltage support requirements. In: Staff (Hg.) 2011 IEEE Trondheim PowerTech, pp. 1-8
- Lorenz, E., Scheidsteger, T., Hurka, J., Heinemann, D., Kurz, C.: Regional PV power prediction for improved grid integration. Prog. Photovolt: Res. Appl. (2011). <https://doi.org/10.1002/pip.1033>
- israelnetz: Hitzewelle in Nahost. www.israelnetz.com/nachrichten/detailansicht/aktuell/hitzewelle-in-nahost-92937/. Accessed 20 February 2019
- M. Bakker, H. A. Zondag, M. J. Elswijk, K. J. Strootman, M. J. M. Jong: Performance and costs of a roof-sized PV/thermal array combined with a ground coupled heat pump. Solar Energy (2005). <https://doi.org/10.1016/j.solener.2004.09.019>
- Mathworks: Matlab (2019)
- J. Kunath: Optimierung mit Matlab, BTU Cottbus (2015)
- D. Van Hertem, J. Verboomen, K. Purchala: Usefulness of DC power flow for active power flow analysis with flow controlling devices. The 8th IEE International Conference on AC and DC Power Transmission (2006)
- K. Van den Bergh, E. Delarue, W. D'haeseleer: DC power flow in unit commitment models (2014)
- EcoDelta: High Performance 60 Cell Polycrystalline Solar Photovoltaic Module. www.ecodeltapower.com (2019). Accessed 20 February 2019
- VDI e.V. (ed.): VDI-Wärmeatlas, 11th edn. Springer Vieweg, Berlin, Heidelberg (2013)
- F. Ostermann: Anwendungstechnologie Aluminium, 3rd edn. Springer Vieweg, Berlin, Heidelberg (2014)
- H. Grimm: Eigenschaften von Wasser in Tabellen. http://www.wissenschaft-technik-ethik.de/wasser_eigenschaften.html (2006). Accessed 20 February 2019
- National Electric Power Company: Power Plants of Jordan - Capacities and Merit Order. Excel, Amman, Jordan (2015)



الجامعة الهاشمية



المملكة الأردنية الهاشمية

المجلة الأردنية
للمهندسة الميكانيكية والصناعية

JJIMIE

مجلة علمية عالمية محكمة
تصدر بدعم من صندوق البحث العلمي

<http://jjmie.hu.edu.jo/>

ISSN 1995-6665

المجلة الأردنية للهندسة الميكانيكية والصناعية

المجلة الأردنية للهندسة الميكانيكية والصناعية: مجلة علمية عالمية محكمة تصدر عن الجامعة الهاشمية بالتعاون مع صندوق دعم البحث العلمي والابتكار - وزارة التعليم العالي والبحث العلمي في الأردن.

هيئة التحرير

رئيس التحرير

الأستاذ الدكتور محمد سامي الأشهب

مساعد رئيس التحرير

الدكتور احمد المقدادي

الدكتور مهند جريسات

الأعضاء

الأستاذ الدكتور طارق العزب

جامعة البلقاء التطبيقية

الاستاذ الدكتور محمد الوديان

جامعة العلوم والتكنولوجيا الاردنية

الاستاذ الدكتور جمال جابر

جامعة البلقاء التطبيقية

الاستاذ الدكتور محمد تيسير هياجنه

جامعة العلوم والتكنولوجيا الاردنية

الأستاذ الدكتور محمد الطاهات

الجامعة الاردنية

الدكتور علي جوارنه

الجامعة الهاشمية

فريق الدعم

المحرر اللغوي

الدكتور بكر محمد بني خير

تنفيذ وإخراج

م . علي أبو سليمة

ترسل البحوث إلى العنوان التالي

رئيس تحرير المجلة الأردنية للهندسة الميكانيكية والصناعية

الجامعة الهاشمية

كلية الهندسة

قسم الهندسة الميكانيكية

الزرقاء - الأردن

هاتف : 00962 5 3903333 فرعي 4147

Email: jjmie@hu.edu.jo

Website: www.jjmie.hu.edu.jo